TURBO CODING AND EQUALIZATION FOR WIRELESS COMMUNICATION SYSTEMS

Grace Ogheneruonano Oletu

A thesis submitted in partial fulfilment of the
requirements of the University of Greenwich
for the Degree of Doctor of Philosophy

2013

DECLARATION

I certify that this work has not been accepted in substance for any degree, and is not concurrently being submitted for any degree other than that of Doctor of Philosophy (PhD) being studied at the University of Greenwich. I also declare that this work is the result of my own investigations except where otherwise identified by references and that I have not plagiarized the work of others.

Signed ....., *Date* .....

Grace Ogheneruonano Oletu

(Student)

Signed ....., *Date* .....

Prof. Predrag Rapajic

(Ist supervisor)

Signed ....., *Date* .....

Dr. Ruiheng Wu

(2nd supervisor).

ACKNOWLEDGMENTS

I thank the Almighty God, my helper, for bringing me this far, the giver of wisdom and knowledge. Praises to Him according to his excellent greatness.

One could hardly hope for a better mentor than Professor Predrag B. Rapajic. I am deeply grateful and thankful to Professor Predrag B. Rapajic for his endless support, guidance, and encouragement. Professor Predrag B. Rapajic's dedication to research and the breadth and depth of his knowledge on all things scientific have greatly amazed me and others both in his research group. Researchers who followed this role model have become good researchers and engineers. Regardless of where I go, I have learned from Predrag that a true and genuine love and dedication to one's career is what it takes to excel in every environment.

I thank Dr. Ruiheng Wu for his support as my second supervisor. I must also acknowledge colleagues at the University of Greenwich, including Dr. Titus I. Eneh, Dr. Kwashie Anang, Dr Bello Lawal and fellow PhD students whose contributions made the years of graduate school enjoyable: Anousheh Tavakoli Dehkordi, Dr Shokrollah Karimian, Dr. Peter K. Bernasko, Dr. Kenny C. Otiaba and Mathias Ekpu.

My special thanks go to Dr Steve Woodhead, Director of Research, Medway School of Engineering and Dr Raj Bhatti for their support and assistance over the years. I'm also grateful to the supporting staff of the school of engineering at Medway for their friendly and skilled assistance. My gratitude also goes to the school of engineering, for the provision of financial assistance.

I also thank my brother and his wife, Mr and Mrs Joshua Oletu, for their financial support and their willingness to go the extra mile to get whatever I needed to make this dream come true. Special thanks go to my sisters, brothers, sister-in-laws, brother-in-laws,

nephews and nieces for their encouragement and support. I am grateful to the Pastors and members of King's Church Gillingham in the UK, for their prayers, encouragement, and support.

Finally, my most heartfelt gratitude goes to my beloved mother, Mrs Beatrice Oletu for her endless love and care. She also inspired me with the love of learning and dedication. I thank God for giving her to me.

ABSTRACT

Turbo coding, a forward error correcting coding (FEC) technique, has made near Shannon Limit performance possible when Iterative decoding algorithms are used. Intersymbol interference (ISI) is a major problem in communication systems when information is transmitted through a wireless channel. Conventional approaches implement an equalizer to remove the ISI, but significant performance gain can be achieved through joint equalization and decoding.

In this thesis, the suitability of turbo equalization as a means of achieving low bit error rate for high data communication systems over channels with intersymbol interference was investigated. A modified decision feedback equalizer algorithm (DFE) that provides significant improvement when compared with the conventional DFE is proposed. It estimates the data using the a priori information from the SISO channel decoder and also a priori detected data from previous iteration to minimize error propagation.

Investigation was also carried out with Iterative decoding with imperfect minimum mean square error (MMSE) decision feedback equalizer, assuming soft outputs from the channel decoder that are independent identically distributed Gaussian random variables. The prefiltering method is considered in this thesis, where an all-pass filter is employed at the receiver before equalization to create a minimum phase overall impulse response.

The band limited channel suffers performance degradation due to impulsive noise generated by electrical appliances. This thesis analysed a set of filter design criteria based on minimizing the bit error probability of impulse noise using digital smear filter.

LIST OF ABBREVIATIONS

3G	Third-generation
3GPP	Third-generation Generation Partnership Project
ADSL	Asynchronous Digital Subscriber Line
AMPS	Advanced Mobile Phone Systems
APP	A Posteriori Probability
AWGN	Additive White Gaussian Noise
BCJR	Bahl, Cocke, Jelinek and Raviv
BER	Bit Error Rate
BPSK	Binary Phase Shift Keying
BS	Base Station
BTS	Base Transceiver Station
CCI	Co-channel Interference
CDMA	Code Division Multiple Access
CIR	Channel Impulse Response
CMR	Cellular Mobile Radio
CNR	Carrier-to-Noise Ratio
CSI	Channel State Information
DFE	Decision Feedback Equalizer
ETSI	European Telecommunication Standards Institute
FDMA	Frequency Division Multiple Access
FEC	Forward Error Correction
FIR	Finite Impulse Response
FM	Frequency Modulation
GSM	Groupè Spècial Mobile
Eb/No	The energy per bit to noise power spectral density ratio

HIPERLAN	High Performance Radio Local Area Networks
HSDPA	High Speed Downlink Packet Access
IEEE	Institute of Electrical and Electronics Engineers
iid	Independent Identically Distributed
IMTS	Improved Mobile Telephone Services
IN	Impulse Noise
ISI	Inter Symbol Interference
LAN	Local Area Network
LE	Linear Equalizer
LMS	Least Mean Square
Log MAP	Logarithmic Maximum a Posteriori
LOS	Line-of-Sight
LPR	Log Probability Ratio
LTE	Long Term Evolution
MAC	Medium Access Control
MAI	Multiple Access Interference
MAP	Maximum a Posteriori
Mbps	Megabite per Second
MF	Matched Filter
MIMO	Multiple Input Multiple Output
ML	Maximum Likelihood
MLSD	Maximum Likelihood Sequence Detection
MLD	Maximum Likelihood Detection
MLSE	Maximum Likelihood Sequence Estimator
MMSE	Minimum Mean Square Error
MMSE DFE	Minimum Mean Square Decision Feedback Equalization

MS	Mobile Station
MSE	Mean Square Error
Non-Los	Non-Line-of-Sight
OFDM	Orthogonal Frequency Division Multiplexing
PER	Packet Error Rate
PIC	Picture Interference Cancellation
PSTN	Public Switched Telephone Network
PSK	Phase-shift keying
QAM	Quadrature Amplitude Modulation
RAN	Radio Access Network
RF	Radio Frequency
RLS	Recursive Least Square
RNC	Radio Network Controller
RSC	Recursive Systematic Convolution
SDT	Smear Desmear Technique
SIC	Successive Interference Cancellation
SINR	Signal to Interference Noise Ratio
SNR	Signal-to-Noise Ratio
SOVA	Soft Output Viterbi Algorithm
SISO	Soft Input Soft Output
SFEIC	Soft Feedback Equalizer Interference Canceller
TCM	Trellis Coded Modulation
TDMA	Time Division Multiple Access
UHF	Ultra High Frequency
VA	Viterbi Algorithm
VLSI	Very Large Scale Integration
WiMax	Worldwide Interoperability for Microwave Access
WLAN	Wireless Local Area Networks

LIST OF NOTATION SYMBOLS

W_k	Bandwidth allocated to the kth user
λ_{min}(A)	Smallest eigen value of Matrix
$tr\{\mathbf{A}\}$	trace of a Matrix **A**
$\mathbf{A} \otimes \mathbf{B}$	Kronecker product of Matrices **A**, **B**
$\mathbf{I}_n$	n x n identity matrix
$\mathbf{H}_{ij}$	Channel Frequency response
$\triangle_n$	Gradient
ε_{opt}	Optimum (Wienner solution) Linear and DFE
$\mathbf{H}(a/\beta)$	Entropy
$(\hat{a} - a)$	Mutually Independent and gaussian
σ^2	Average Noise Power
$(.)^\star$	Conjugate
K	Constraint lengths
R_c	Channel code rate
$\alpha_k(s)$	Probability of being at node *k* while moving forward
$\beta(s)$	Probability of being at node *s* while moving backward
$\gamma(k$	Transitional probability from node *k* while moving
$L_c(x)$	Log-likelihood ratio (LLR) on the code bit c_k
L_e	Extrinsic LLR
$\lambda^E(c_k)$	LLR output from equalizer
$\lambda^D(c_k)$	LLR output from decoder

$\bigwedge$	a posteriori LLR of the coded bits
$\hat{u}$	Estimated value
$(.)^T$	Transpose operator
Φ	Estimated covariance matrix
ϵ	shorthand for belong to
$\mid \mathbf{A} \mid$	Determinant of a matrix **A**
$\mathcal{E}[\mathbf{A}]$	Probabilistic expectation of a Matrix **A**
λ_{min}(A)	Smallest eigen value of Matrix **A**
λ_{max}(A)	Largest eigen value of matrix **A**
$tr\{\mathbf{A}\}$	trace of a Matrix **A**
$\mathbf{A} \otimes \mathbf{B}$	Kronecker product of Matrices **A**, **B**
$\mathbf{I}_n$	n x n identity matrix
σ_1^2	Unit Variance
μ	Threshold level
$\mathbf{H}_{ij}$	Channel Frequency response
R	Correlation Matrix
$\triangle_n$	Gradient
ε_{opt}	Optimum (Wiener solution) Linear and DFE
H	Toeplitz Matrix
$\mathbf{H}(a/\beta)$	Entropy
$(\hat{a} - a)$	Mutually Independent and gaussian
$(.;.)$	Mutual Information
$(.)^H$	Hermittian Transpose

Contents

List of Figures

List of Tables

LIST OF PhD CANDIDATE'S PUBLICATIONS RELATED TO PhD THESIS

Journal Papers:

1. **Grace Oletu**, Predrag Rapajic and Kwashie Anang "Minimization of Channel Impulse Noise using Digital Smear filter," *Journal of Communications (JCM): Regular Issue: Advances in wireless comm. and networks*.ISSN: 1796-2021, vol. 8, no. 2, pp. 82-90 , Feb. 2013.

2. **Grace Oletu**, P. Rapajic, T. Eneh, and K. Anang "Turbo Equalization Enhanced high data rate in wireless communication systems,". *International Journal of Multimedia Technology (IJMT)* SSN: 2225-1456, vol. 2, no. 1, pp. 1-4 , Oct. 2012.

3. T. I. Eneh, **G. Oletu**, P. B. Rapajic, K. A. Anang, and L. Bello. "Adaptive multiuser receivers scheme for MIMO OFDM over iterative-equalization for single-carrier transmission," *Journal of emerging trends in engineering and applied sciences (JETEAS)*. ISSN: 2141-7016, vol. 2, no. 2, pp. 282-288, April, 20011.

Conference Papers:

1. **G. Oletu** and P. Rapajic. "The Performance of Turbo codes for Wireless Communication Systems" in Proc. of 3rd International Conference on Computer Research and Development (ICCRD 2011). Shanghai, China, pp. 346-349, Mar. 2011.

2. **G. Oletu**, P. Rapajic,T. Eneh and K. Anang. "Turbo Equalization Enhanced high data rate in wireless communication Networks" in Proc. of International Symposium on Modeling and Optimization in Mobile, Ad Hoc and Wireless Networks (WiOpt 2011). New Jersey, USA, pp. 373, May 2012.

3. **G. Oletu**, P. Rapajic,T. Eneh and K. Anang. "The Performance of Iterative decoding with Imperfect MMSE DFE" in Proc. of 4th Wireless Days (WD 2011 IFIP). Ontario, Canada, pp. 1-3, Oct. 2011.

4. **G. Oletu**, P. B. Rapajic, T. I. Eneh and K. A. Anang. "Enhanced Equalization for Mobile Communication Systems" 5th IEEE European Modelling Symposium on Mathematical modelling and Computer Simulation (5th IEEE EMS 2011), Madrid, Spain, pp. 446 - 450, Nov. 2011.

5. **G. Oletu**, P. Rapajic, T. Eneh and K. Anang. "Interference Cancellation Using Iterative Equalization for Communication System" in Proc. of 14th International Conference on Computer Modelling and Simulation (UKSim 2012). Cambridge, UK, pp. 608-612, March 2011.

6. **G. Oletu**, P. Rapajic, K. Anang, R. Wu and T. Eneh. "The Smearing Filter Design Techniques for Data Transmission" in Proc. of 76th International Conference on IEEE Vehicular Technology Conference (VTC Fall 2012). Quebec city, Canada, pp. 1-5, Sept. 2012.

7. **G. Oletu**, P. Rapajic, K. Anang and R. Wu. "Channel impulse noise minimization using digital smear and desmear filter" in Proc. of 31st International Conference on IEEE Performance Computing and Communications Conference (IPCCC 2012). Austin, USA, pp. 456-462, Dec. 2012.

8. **G. Oletu** and P. Rapajic. "Modified Iterative Decision Feedback Equalization for Communication Systems" in Proc. of 8th EUROSIM Congress on Modelling and Simulation. Cardiff, Wales, United Kingdom, 10-13 September 2013.(Accepted).

9. T. I. Eneh, **G. Oletu**, P. B. Rapajic, K. A. Anang, and B. Lawal. "Adaptive MMSE Multiuser Detection for MIMO OFDM over Turbo-Equalization for Single-Carrier

Transmission Wireless Channel". In Proc. of 7th IEEE International Wireless Communications and Mobile Computing Conference (IEEE - IWCMC 2011). Istanbul, Turkey, pp. 1408-1412, July 2011.

10. T. I. Eneh, **G. Oletu**, P. B. Rapajic, K. A. Anang, and B. Lawal. "Adaptive vector precoding for Multiuser MIMO OFDM". International conference on ICT for Africa (ICT4Africa 2011). Covenant University, Canaan Land, Nigeria.

11. K. A. Anang, P. B. Rapajic, R. Wu, **G. Oletu** and L. Bello. "Minimum cell size for information capacity increase in a shadowed environment of land mobile cellular system" 7th International Conference on Broadband and Wireless Computing, Communication and Applications (BWCCA 2012). (Accepted)

12. K. A. Anang, P. B. Rapajic, T. I. Eneh, L. Bello and **G. Oletu**. "Impact of Vehicular Traffic on Information Capacity of Cellular Wireless Network at Carrier Frequencies Greater Than 3 GHz" 5th IEEE European Modelling Symposium on Mathematical modelling and Computer Simulation (5th IEEE EMS 2011), Madrid, Spain, pp. 430 - 434, Nov. 2011.

13. K. A. Anang, P. B. Rapajic, T. I. Eneh and **G. Oletu**. "Sensitivity of Information Capacity of Land Mobile Cellular System to the Base Station Antenna Height at Higher Microwave Frequencies," in Proc. of 3rd International Conference on Computer Research and Development (IEEE- ICCRD 2011). Shanghai, China, pp. 167-172, Mar. 2011.

Chapter 1

Introduction

1.1 Research Aims and Outline of the Thesis

In recent years, there has been an increasing demand for efficient and reliable digital data transmission. This demand has been accelerated by emergence of large-scale, high-speed data networks for the exchange, processing, and storage of digital information in the commercial, governmental, and military spheres [1]. A major concern of system designers is the control of errors so that the data can be reliably reproduced [2].

In 1948, Shannon [3] demonstrated in a landmark paper that, by proper encoding of the information, errors induced by a noisy channel can be reduced to any desired level without sacrificing the rate of information transmission as long as the information rate is less than the capacity of the channel. Since Shannon's work much effort has been expanded on this problem by devising efficient encoding and decoding methods for error control in a noisy environment. Recent developments have contributed toward achieving the reliability required by today's high-speed digital systems, and the use of coding for error control has become an integral part in the design of communication systems [2].

This has led to Turbo coding being regarded as one of the most promising emerging wireless techniques. This principle is used in error control and equalization systems. Error correction techniques make wireless communications more efficient and reliable. Data transmission over ISI channels is a major problem in communication systems. Conventional approaches implement an equalizer to remove ISI or use MAP or maximum likelihood (ML) detection [4] [5]. But significant performance gains can be achieved through joint equalization and decoding at the cost of added complexity.

The remainder of this chapter is organized as follows. The next section gives a definition and a description of wireless communication systems. Section 1.3, focuses on the future of wireless communications. Section 1.5, explains motivations that led to this work and states the thesis contribution. Finally, Section 1.6, provides an outline of the thesis.

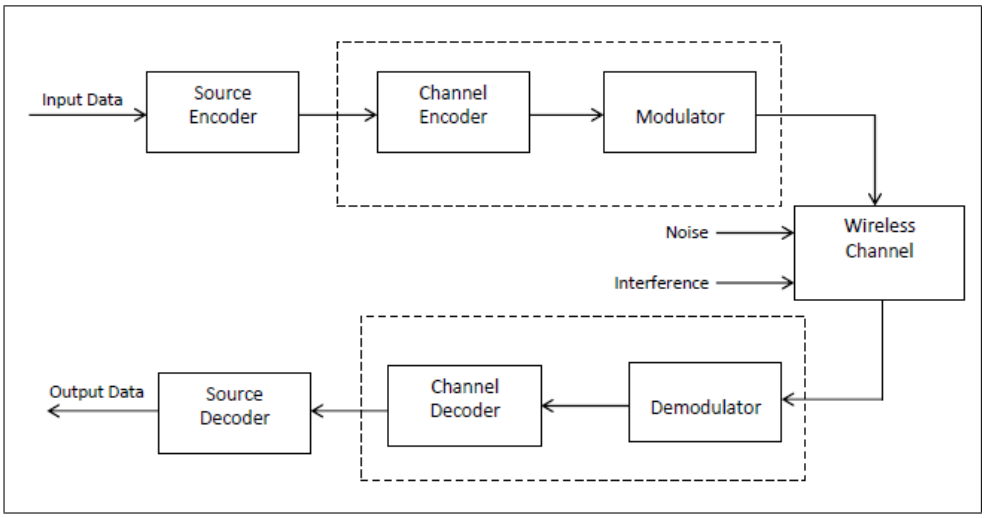

Figure 1.1: A basic wireless communication system showing a transmitter and a receiver.

1.2 Description of Basic Wireless Communication System Related to this Thesis

The Figure 1.1 illustrates the basic block elements of a digital wireless communication system. The information input is converted into a sequence of binary digits. The process of efficiently converting the output of the digital information into a sequence of binary digits is called source encoding. The sequence of the binary digits from the source encoder is passed to the channel encoder [6, 7].

The purpose of the channel encoder is to introduce, in a controlled manner, some redundancy in the binary information sequence that can be used at the receiver to overcome the effects of noise and interference encountered in the transmission of the signal through the wireless channel [6, 7].

The added redundancy serves to increase the reliability of the received data and improves the fidelity of the received signal. In effect, redundancy in the information sequence aids the receiver in the decoding of the desired information sequence. The binary sequence at the output of the channel encoder is passed to the digital modulator, which serves as the interface to the wireless communication channel.

The purpose of the digital modulator is to map the binary information sequence

into signal waveforms. The wireless communication channel is the physical medium that is used to send the signal from the transmitter to the receiver. In wireless transmission, the channel may be the atmosphere (free space) and microwave radio. The transmitted signal is corrupted by additive thermal noise generated by electronic devices, and atmospheric noise such as electrical lightning discharges during thunderstorms [6, 7].

At the receiver, the digital demodulator processes the channel corrupted transmitted waveform and reduces the waveforms to a sequence of numbers that represent estimates of the transmitted data symbols. This sequence of numbers is passed to the channel decoder, which attempts to reconstruct the original information sequence from the knowledge of the code used by the channel encoder and the redundancy contained in the received data [7].

A measure of how well the demodulator and decoder perform is the frequency with which errors occur in the decoder sequence. The probability of error is a function of the code characteristics, the types of waveforms used to transmit the information over the channel, the transmitted power, the characteristics of the channel and the method of demodulation and decoding [7].

Finally the source decoder accepts the output sequence from the channel decoder and from the knowledge of the source encoding method used, the original signal is reconstructed. Because of channel decoding errors and possible distortion introduced by the source encoder and source decoder, the signal at the output of the receiver is an approximation of the original source input [7]. In this Thesis we focus only on the area represented as a dash line in Figure 1.1.

1.3 Future Evolution of Wireless Communication Related to this Thesis

The introduction of mobile wireless and cordless telephone systems in the early 1980s caused wireless communication systems and services to have undergone a remarkable development and growth [8]. The vision of wireless communication providing faster, high-speed, high-quality and real time information exchange between two portable devices located anywhere in the world is now the communications frontier of the next century [9].

During the last decade it has emerged from wireless communication research and development activity, that the future wireless is based on three trends: a broader range of wireless communication products, high data-rate wireless communication systems and higher user density [10]. The vision of wireless communications supporting information exchange between people or devices is the communications frontier of the next few decades, and much of it already exists in some form.

This vision will allow multimedia communication from anywhere in the world using a small handheld device or laptop. Wireless networks will connect palmtop, laptop, and desktop computers anywhere within an office building or campus, as well as from the corner cafe.

In the home these networks will enable a new class of intelligent electronic devices that can interact with each other and with the Internet in addition to providing connectivity between computers, phones, and security/monitoring systems. Such "smart" homes can also help the elderly and disabled with assisted living, patient monitoring, and emergency response. Wireless entertainment will permeate the home and any place that people congregate [11].

Video teleconferencing will take place between buildings that are blocks or continents apart, and these conferences can include travellers as well from the salesman who missed his plane connection to the chief executive officer who went sailing in the Caribbean. Wireless video will enable remote classrooms, remote training facilities, and remote hospitals anywhere in the world [12]. Finally, wireless networks enable distributed control systems with remote devices, sensors, and actuators linked together via wireless communication channels. Such systems in turn enable automated highways, mobile robots, and easily reconfigurable industrial automation.

Wireless applications include voice, Internet access, Web browsing, paging and short messaging, subscriber information services, file transfer, video teleconferencing, entertainment, sensing, and distributed control. One reason for this fragmentation is that different wireless applications have different requirements. Voice systems have relatively low data-rate requirements (around 20 kbps) and can tolerate a fairly high probability of bit error (bit error rates, or BERs, of around 10^{-3}), but the total delay must be less than about 100 ms or else it becomes noticeable to the end user [11].

On the other hand, data systems typically require much higher data rates (1–100 Mbps) and very small BERs (a BER of 10^{-8} or less, and all bits received in error must be retransmitted) but do not have a fixed delay requirement. Real-time video systems have high data-rate requirements coupled with the same delay constraints as voice systems, while paging and short messaging have very low data-rate requirements and no hard delay constraints [11].

These diverse requirements for different applications make it difficult to build one wireless system that can efficiently satisfy all these requirements simultaneously. It is impossible to predict what wireless failures and triumphs lie on the horizon [11]. Moreover, there must be sufficient flexibility and creativity among both engineers and regulators to allow for accidental successes. It is clear, however, that the current and emerging wireless systems of today coupled with the vision of applications that wireless can ensure a bright future for wireless technology [11].

These trends motivate the direction of the research in this thesis. The next section gives an overview of the technical issues involved in the implementation of the wireless communication. A number of these technical issues will be examined in the thesis, where new methods are proposed, evaluated and compared with other existing techniques that are currently being implemented.

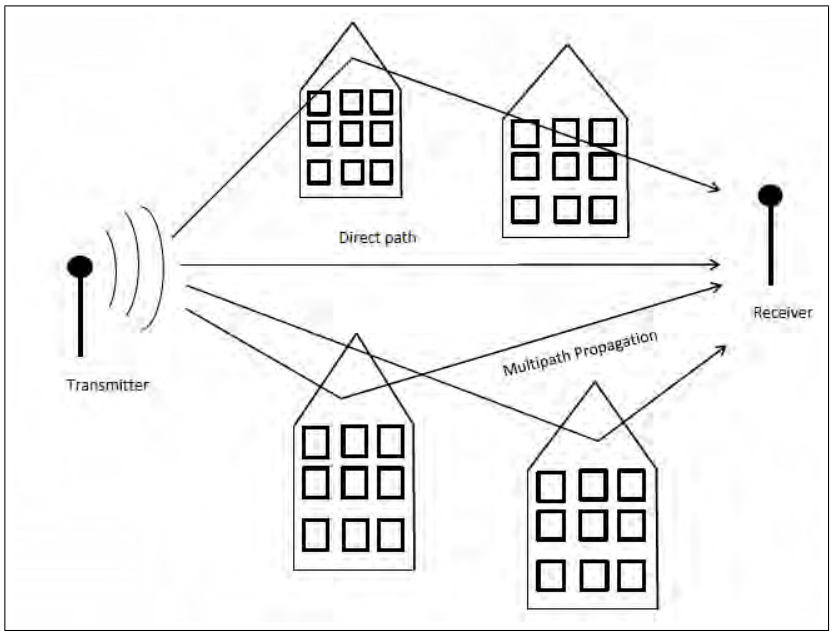

Figure 1.2: A wireless communication channel showing a direct path, and multi path from transmitter to receiver.

1.4 Technical Problems Related to Future Wireless Systems

Technical issues related to wireless communication cover limitations which arise from the technology chosen for the wireless system implementation. A lot of these technical challenges needs to be addressed to enable the implementation of future wireless communication. This thesis only addressed the challenges related to this research study and are as follows:

- Multipath propagation
- Spectrum limitations

1.4.1 Multipath propagation

The fundamental technical challenges of future wireless systems arise from physical laws. It is therefore necessary to understand the fundamental technical issues for determining the feasibility of a given wireless technology with respect to the absolute physical limits. The wireless communication channel is susceptible to noise, interference, multipath

propagation and users movement, which causes the wireless communication channel to change over time in an unpredictable manner [13].

A wireless communication channel is illustrated in Figure 1.2, showing noise, interference and multipath. Multipath propagation occurs, when a radio signal transmitted from a Transmitter to a receiver experiences variation in amplitude and phase, which arises when the transmitted signal is reflected, diffracted or scattered by an object.

These reflected, diffracted or scattered signals create additional copies of the transmitted signal which can be attenuated in power, delayed in time, and shifted in phase and/or frequency from the line-of-sight (LOS) signal path, where LOS signal path is the straight line path between the transmitter and receiver. Multipaths cause the received signal amplitude to vary, whilst the time delay of each path causes intersymbol interference if the signal bandwidth is larger than the inverse of the delay spread [13].

1.4.2 Spectrum limitations

Wireless mobile multimedia communication which has captured the attention of the media and the imaginations of the public because it allows connectivity between users without sacrificing mobility, are fundamentally limited by the information capacity of the wireless communications channel. The wireless communication channel information capacity can be defined as the highest rate at which information can be sent over the wireless communication channel with a negligible probability of error.

The information capacity of the wireless communication channel is determined by the channel information transmission resources, which include: time, bandwidth and power (signal-to-noise ratio) [14]. Transmitting more power to increase the channel capacity or data rate of the wireless communication system is costly, because of the logarithmic relationship between the channel capacity of the wireless communication link and the signal-to-noise ratio (SNR) at the receiver. This logarithmic relationship was first developed by Shannon in his landmark 1948 paper "mathematical theory of communications" [15]. By Shannon's result, the channel capacity is given by:

$$\mathcal{C} = B \log(1 + SNR) \tag{1.1}$$

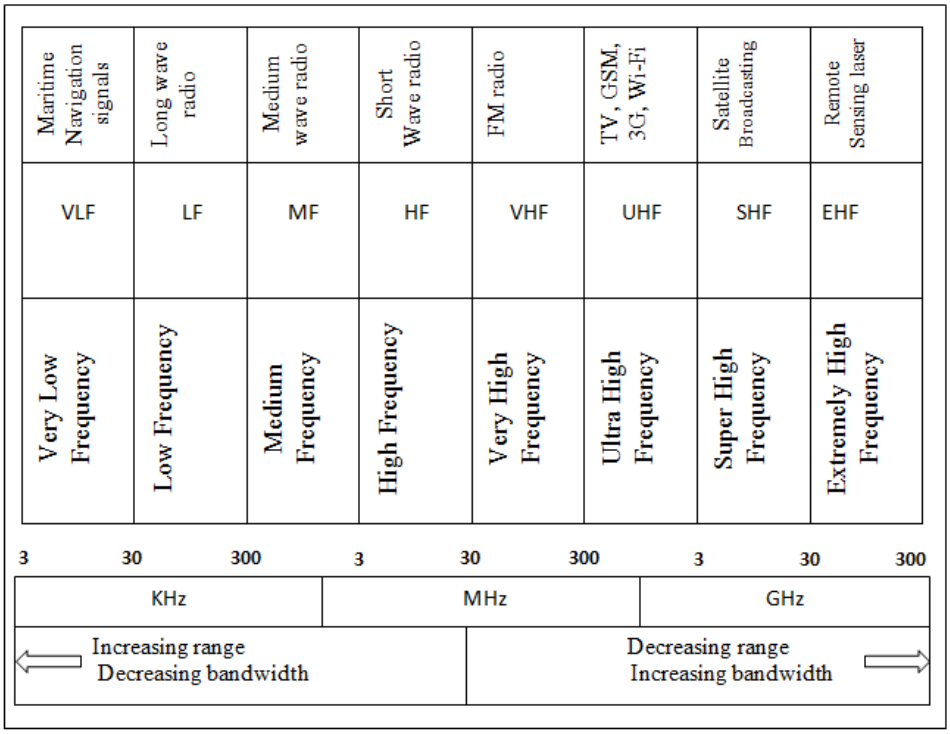

Figure 1.3: Wireless communications radio spectrum allocation and usage.

Where B is the signal bandwidth. Thus, asymptotically error-free communication at rates below $log(1 + SNR)$ is possible, while transmission at any rate larger than $log(1 + SNR)$ is guaranteed to have errors. Another effective method of increasing data rate in wireless communication system is to increase the signal bandwidth, in addition to the transmitted power. However the radio spectrum available for wireless communication systems is expensive and limited [16]; therefore it is regulated by international agreements [17], especially the frequencies of interest, where propagation conditions are favorable.

Therefore efficient utilization of the limited spectrum is important in the design of wireless systems. With the recent increase in spectrum allocation for wireless applications, this limited radio spectrum will be stretched to its capacity to accommodated the various wireless services. The allocation of the limited radio spectrum is illustrated in Figure 1.3, where the description of the bandwidth and wavelength are specified in Hertz and meters.

The spectrum efficiency of a wireless communication system is defined as the information rate that can be transmitted over a given bandwidth in a specific wireless communication system and it is measured in bits/s/Hz. The system capacity of a wireless com-

munication systems is directly related to the spectrum efficiency, hence it is an important parameter to be considered in the design of wireless communication systems [16, 18, 19].

Efficient utilization of the congested radio spectrum is partly achieved by the cellular networks [20]. Other techniques to increase spectral efficiency include; methods such as combination of bandwidth efficient coding/modulation techniques at the communication link level and the use of sophisticated channel allocation schemes that minimize the overall carried traffic at the network or systems levels [21]. Techniques to utilize the radio spectrum efficiently and effectively have been a major design concern for emerging wireless communication systems.

1.5 Motivation of this Thesis

The ever-growing demand for higher data rates transmission in wireless communication systems has triggered the design and techniques by which system capacity can be increased, and at the same time maintaining high quality of service [22]. Several wireless networks have almost reached their limits, hence the allocation spectrum is not sufficient to support the growing demand for mobile communications. There are many challenges facing a system designer to ensure reliable high quality communications in severe error prone environments.

First, to receive multimedia at digital Tv quality, high bandwidth is necessary which is an expensive resource in wireless communication. The transmission rates are limited by channel noise, interference, fading, multipath, pathloss and shadowing in the wireless links.

This has led to the development of a novel coding scheme called Turbo codes introduced in [23, 24], that was near to Shannon's limit. In 1993 Berrou showed that it was possible to transmit data with a code rate above the channel cutoff rate. He even achieved an exceptionally low BER with a signal SNR per information bit close to Shannon's theoretical limit on a Gaussian channel.

This coding scheme [23, 24] consists of two recursive systematic convolutional codes concatenated in parallel and which are decoded using iterative maximum-likelihood decoding (MLD) (or soft decoding) of the component codes. For the decoding of the

component codes, Berrou used a maximum a posteriori (MAP) algorithm [25] which performs maximum-likelihood (ML) bit estimation and thus yields reliability information (soft-output) for each bit.

This algorithm can be viewed as a soft-input/soft-output decoder. Due to the tremendous performance gains of turbo codes and the turbo decoding algorithm, a concept introduced in [26] combines equalization with channel decoding called turbo equalization. It is an iterative equalization and decoding technique that can achieve equally impressive performance gains for communication systems that send digital data over channels that require equalization, hence, those that suffer from ISI [5].

This work was motivated by the desire to achieve reliable communications by making efficient use of limited resources and increase the data rates at a reasonable cost over channels affected by severe disturbance. To Specially, focus on the class of frequency-selective channels, which are subject to intersymbol interference.

Intersymbol interference arises when successive transmitted symbols are smeared together in time by the communication channel to the extent that they overlap at the receiver side. Such a phenomenon is commonly encountered over radio links, where the signal at the receiving end is formed by the superposition of multiple propagation paths affected by different delays of arrival.

Previous works leave the following unanswered fundamental questions:

- How can higher data transmission rates over channels with intersymbol interference be achieved with low error probability?
- Why is the receiver using MMSE LE which provides a better performance improvement than MMSE DFE at higher iteration and higher Modulation scheme?
- How can error propagation of decision feedback equalizer be solved?
- Is there any counter measure against impulse noise over band limited channels?

Motivated by the preceding questions, this thesis seeks to address and find answers to them.

1.5.1 Contributions of this Thesis

The main contribution of this thesis is based on the key papers of the author [27–33]. The thesis is based on the key paper of the author. The main contribution of this thesis is summarized as follows:

- The suitability of Turbo equalization as a means of achieving low bit error rate in high data communication systems over channels with intersymbol interference.
- Mathematical analysis supported by computer simulation is used to show that at a higher modulation scheme using iterative decoding, a high data rate can be achieved.
- A modified approach which estimates the data using the a priori information from the SISO channel decoder and uses the a priori detected data from previous iteration to minimize error propagation.
- Iterative decoding using imperfect MMSE decision feedback equalizer for time-invariant communication channels, that exhibit severe ISI with a different modulation scheme.
- The capacity of the dispersive multipath propagation channel was enhanced by using a prefilter at the receiver before equalization.
- A set of filter design criteria based on minimizing the bit error probability of impulse noise using a digital smear filter is analysed.

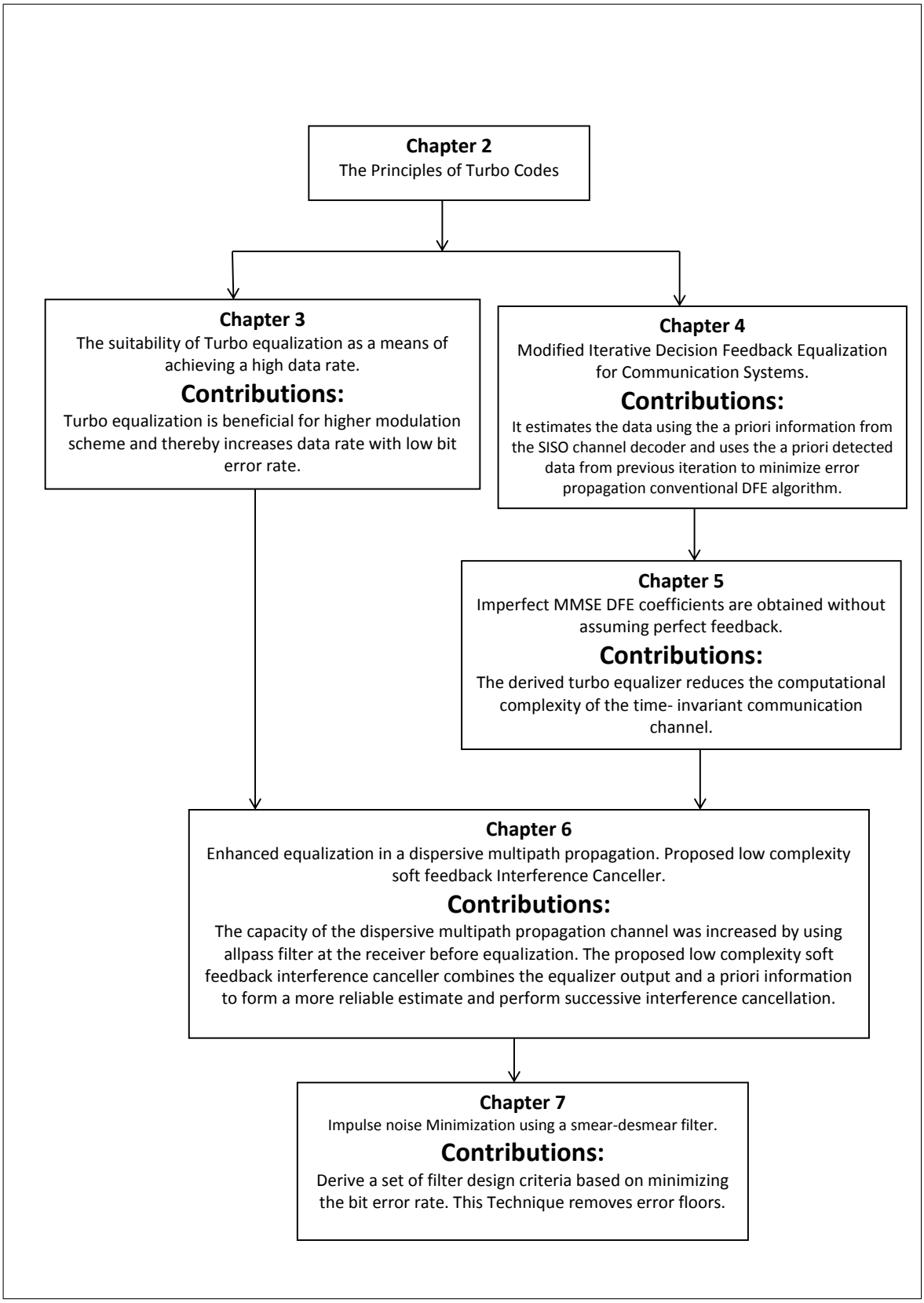

Figure 1.4: Flowchart of thesis and thesis contribution.

1.6 Organization of the Thesis

This thesis has been written and structured in a way that will hopefully make it accessible and interesting to a broad range of readers, including researchers, communication engineers and academics. It aims at finding how to achieve a low bit error rate for future high data communication systems using joint equalization and decoding. For time-invariant communication channels, that exhibit severe ISI with different modulation schemes, the proposed imperfect MMSE DFE provides performance improvement.

Also it aims at trying to minimize impulse noise using smear and desmear filter. Chapter 2, provides a brief Literature survey of the turbo coding concept for wireless channel. The research contributions are presented in chapters 3 - 7. Chapter 8, presents conclusions and outlines future work. Figure 1.4, is a flowchart of the routes that one might decide to follow through the chapters.

Outlined are the chapters of this thesis:

- Chapter 2: Gives the performance of Turbo coding for wireless channels and their useful coding gain at higher values of Eb/No and bit error rate. This chapter also studies two turbo decoding algorithms, soft-output viterbi algorithm (SOVA) and Logarithmic maximum a posteriori (Log MAP).

- Chapter 3: Investigates the suitability of Turbo equalization as a means of achieving low bit error rate in the future high data communication systems.

- Chapter 4: A modified approach is proposed to mitigate the error propagation in the DFE algorithm when used in turbo equalization while retaining low computational complexity. It estimates the data using the a priori information from the SISO channel decoder and also the a priori detected data from previous iteration to minimize error propagation.

- Chapter 5: Studies the iterative decoding with imperfect MMSE decision feedback equalizer using different modulation schemes assuming, that soft outputs from the channel decoder are independent identically distributed Gaussian random variables with known mean and variance.

- Chapter 6: A prefiltering method where an All-pass Filter is employed at the receiver before equalization is considered. A low complexity soft feedback Equalizer Interference canceller (SFEIC) that combines the equalizer outputs and a priori information to form more reliable estimates that perform successive interference cancellation is proposed.

- Chapter 7: Describes a digital smear-desmear technique (SDT) based on polyphase sequences with good autocorrelation properties in [33]. These sequences are applied to the design of digital smear/desmear filters and combined with Trellis-coded modulation (TCM) codes.

- Chapter 8: Summarizes the conclusion drawn from the preceding chapters and points to future directions of this thesis.

Chapter 2

The Principles of Turbo Codes

2.1 Introduction

In 1949 Claude Shannon published a paper that established a mathematical basis for the consideration of the noisy communications channel [34]. In his analysis he quantified the maximum theoretical capacity for a communications channel, the Shannon limit and indicated that error-correcting channel codes must exist that allowed this maximum capacity to be achieved. In the intervening years, many well-considered channel codes are inched towards the Shannon limit, but all contenders have required large block lengths to perform close to the limit.

The complexity of these codes have made them impractical within 3 to 5 dB of the limit, but they provide a useful coding gain at higher values of Eb/No and bit error rate. Turbo coding was proposed in 1993 by Berrou, Glavieux and Thitimajashima, who reported excellent coding gain results [24], approaching Shannon predictions. The objective of this chapter is to provide background material regarding turbo coding relevant to this thesis.

The information sequence is encoded, with an interleaver between the two encoders serving to make the two encoded data sequences approximately statistically independent of each other [35]. Often half rate Recursive Systematic Convolutional (RSC) encoders are used, with each RSC encoder producing a systematic output which is equivalent to the original information sequence, as well as a stream of parity information [35].

The two parity sequences can then be punctured before being transmitted along with the original information sequence to the decoder [35]. This puncturing of the parity information allows a wide range of coding rates to be realised, and often half the parity information from each encoder is sent with the original data sequence together, this results in an overall coding rate of 1/2 [35]. At the decoder two RSC decoders are used. Special decoding algorithms must be used which accept soft inputs and give soft outputs for the decoded sequence.

These soft inputs and outputs provide not only an indication of whether a particular bit was a 0 or a 1, but also a likelihood ratio which gives the probability that the bit has been correctly decoded. The turbo decoder operates iteratively. In the first iteration the first RSC decoder provides a soft output giving an estimation of the original data sequence

based on the soft channel inputs alone. It also provides an extrinsic output.

The extrinsic output for a given bit is based not on the channel input for that bit, but on the information for surrounding bits and the constraints imposed by the code being used. This extrinsic output from the first decoder is used by the second RSC decoder as a-priori information, and this information together with the channel inputs is used by the second RSC decoder to give its soft output and extrinsic information.

In the second iteration the extrinsic information from the second decoder in the first iteration is used as the a-priori information for the first decoder, and using this a-priori information the decoder can hopefully decode more bits correctly than it did in the first iteration. This cycle continues, with at each iteration both RSC decoders producing a soft output and extrinsic information based on the channel inputs and a-priori information obtained from the extrinsic information provided by the previous decoder.

After each iteration the Bit Error Rate (BER) in the decoded sequence drops, but the improvements obtained with each iteration falls as the number iterations increases so that for complexity reasons usually only between 4 and 12 iterations are used. In their original proposal Berrou et al. [24] invoked a modified version of the classic minimum bit error rate maximum aposteriory algorithm (MAP) due to Bahl et al [25] in the above iterative structure for decoding the constituent codes.

Since the conception of turbo codes a large body of work has been carried out in the area, aiming for example to reduce the decoder complexity, as suggested by Robertson, Villebrun and Hoeher [36] and [37] as well as by Berrou et al. [38]. Le Goff, Glavieux and Berrou [39], Wachsmann and Huber [40] as well as Robertson and Worz [41] suggested using the codes in conjunction with bandwidth efficient modulation schemes.

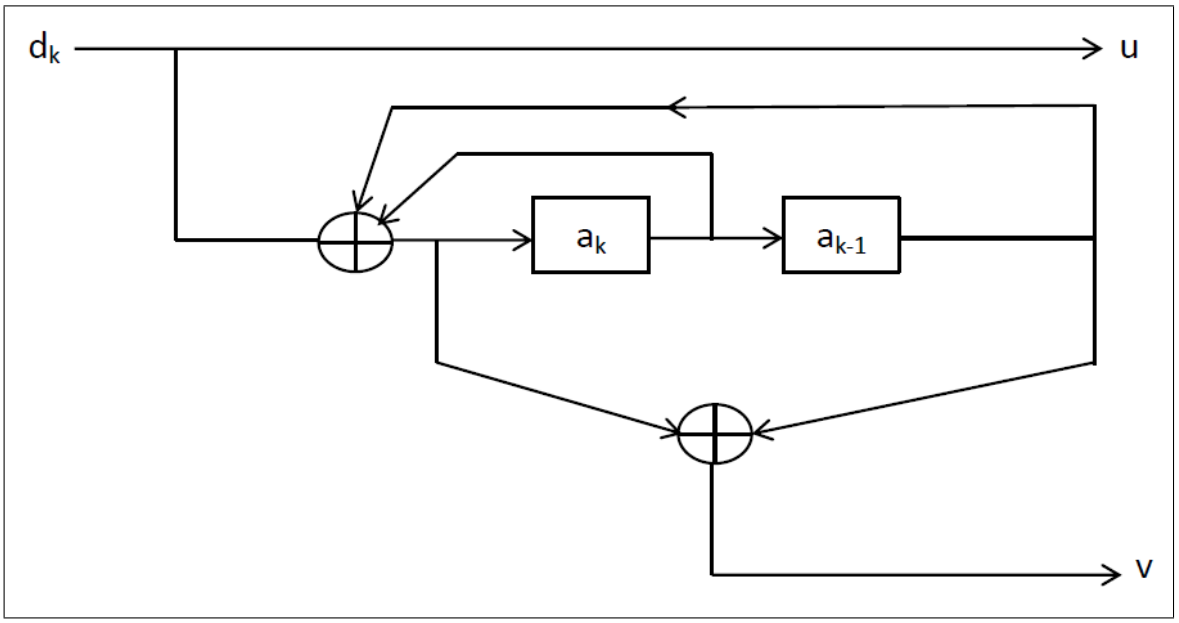

Figure 2.1: Recursive systematic convolutional Encoder with rate R = 1/2 and generator G = [7 5].

Further advances in understanding the excellent performance of the codes are due, for example, to Benedetto and Montorsi [42, 43] as well as to Perez, Seghers and Costello [44]. A number of authors, including Hagenauer, Offer and Papke, as well as Pyndiah [45, 46], extended the turbo concept to parallel concatenated block codes. Jung and Nasshan [47] characterised the coded performance under the constraints of short transmission frame length, which is characteristic of speech systems.

In collaboration with Blanz they also applied turbo codes to a CDMA system using joint detection and antenna diversity [48]. Barbulescu and Pietrobon [49] as well as a number of other authors addressed the equally important issues of interlever design. Due to space limitations here we have to curtail listing the range of further contributors in the field, without whose advances this treatise could not have been written [50]. It is particularly important to note the tutorial paper authored by Sklar [51].

This chapter examines the principles of turbo coding and decoding, focussing on the coding and decoding algorithms. Specifically, in Section 2.2 details of turbo encoder, while in Section 2.3 the decoder is portrayed and section 2.4 details the principle of Turbo decoding. Then Section 2.5 shows the performance results of two turbo coding algorithms.

2.2 Turbo Encoding

It is theoretically possible to approach the Shannon limit by using a block code with large block length or a convolutional code with a large constraint length. The processing power required to decode such long codes makes this approach impractical [24]. Turbo codes overcome this limitation by using recursive coders and iterative soft decoders. The recursive coder makes convolutional codes with short constraint length appear to be block codes with a large block length, and the iterative soft decoder progressively improves the estimate of the received message [24, 34].

The basic idea of turbo codes is to use two convolutional codes in parallel with some kind of interleaving in between. Convolutional codes can be used to encode a continuous stream of data, but in this case the data is configured in finite blocks corresponding to the interleaver size. The frames can be terminated; hence the encoders are forced to a known state after the information block. The termination tail is then appended to the encoded information and used in the decoder [52]. A basic turbo encoder shown in Figure 2.1,and is a recursive systematic encoder that employs two recursive systematic convolutional encoders in parallel, where the second encoder is preceded by an interleaver.

The two recursive systematic convolutional encoders may be identical or different. The channel code rate at the output of the turbo encoder is $R_c = 1/3$. However, puncturing the parity check bits at the output of the binary convolutional encoders, may achieve higher rates, such as 1/2. The use of the interleaver in conjunction with encoders results in codewords that have relatively few nearest neighbours, that is to say the codewords are relatively sparse. Hence, the coding gain achieved by a turbo code is due to the reduction in the number of nearest neighbouring codewords that result from interleaving [52, 53].

2.3 Turbo Decoding

Turbo codes play an important role in making communications systems more efficient and reliable. The near Shannon limit error correction performance of Turbo codes [24] and parallel concatenated convolutional codes [42] have raised a lot of interest in the research community to find practical decoding algorithms for implementation of these codes. The

implementation of turbo codes for wireless communication systems has been increasing since they were first introduced by Berrou et al. in the early 1990s [24].

Various systems such as 3GPP, HSDPA and WiMAX have already adopted turbo codes in their standards due to their large coding gain. In [54], it has also been shown that turbo codes can be applied to other wireless communication systems used for satellite and deep space applications. The MAP decoding also known as the BCJR [25] algorithm is not a practical algorithm for implementation in real systems [55]. The MAP algorithm is computationally complex and sensitive to SNR mismatch and inaccurate estimation of the noise variance [55]. The MAP algorithm is not practical to implement in a chip.

The logarithmic version of the MAP algorithm [36, 56, 57] and the Soft Output Viterbi Algorithm (SOVA) [58, 59] are the practical decoding algorithms for implementation. This section provides a description of two turbo codes decoding algorithms. Soft-output Viterbi algorithm and logarithmic-maximum a posteriori turbo decoding algorithms are the two candidates for decoding turbo codes. Soft-input soft-output (SISO) turbo decoder based on SOVA and the logarithmic versions of the MAP algorithm, called Log-MAP decoding algorithm. The BER performances of these algorithms are compared. Simulation results are provided for bit error rate performance using constraint lengths of K=3, over AWGN channel, and show improvements of 0.4 dB for log-MAP over SOVA at BER 10^4.

2.3.1 Soft Output Viterbi Decoding Algorithm (SOVA)

Let the binary logical elements 1 and 0 be represented electronically by voltages +1 and -1, respectively. The variable d in Figure 2.1 is used to represent the transmitted data bit, whether it appears as a voltage or as a logical element. Sometimes one format is more convenient than the other. Let the binary 0 (or the voltage value - 1) be the null element under addition. [51]

For signal transmission over an AWGN channel, a well-known hard-decision rule, known as maximum likelihood, is to choose the data d_k = +1 or d_k = -1 associated with the larger of the two intercept values. For each data bit at time k, this is tantamount to deciding that d_k = +1 if x_k, which is the intercept between the two points falls on the right

side of the decision line, otherwise deciding that d_k = -1. A similar decision rule, known as maximum a posteriori (MAP), which can be shown to be a minimum probability of error rule, takes into account the a priori probabilities of the data. The general expression for the MAP rule in terms of APPs is as follows:

$$P(d=+1|x) > P(d=-1|x) \quad or \quad when \quad P(d=+1|x) < P(d=-1|x) \tag{2.1}$$

Equation(2.1) states that one should choose the hypothesis $(d=+1)$, if the APP $P(d=+1|x)$is greater than the APP $P(d=-1|x)$. Otherwise, choose hypothesis $(d=-1)$. Using the Bayes' theorem, the APPs in (2.1) can be replaced by their equivalent expressions, yielding the following: [51]

$$P(x|d)=+1)P(d=+1) > P(x|d=-1)P(d=-1) \tag{2.2}$$

Equation(2.2) is generally expressed in terms of a ratio, yielding the so called likelihood ratio test, as follows:

$$\frac{P(x|d=+1)P(d=+1)}{P(x|d=-1)|P(d=-1)} > 1 \tag{2.3}$$

By taking the logarithm of the likelihood ratio, a useful metric called the log-likelihood ratio (LLR) is obtained. It is a real number representing a soft decision output of a detector, designated as follows: [51]

$$L(d|x) = \log \frac{P(x|d=+1)P(d=+1)}{P(x|d=-1)|P(d=-1)} \tag{2.4}$$

$$L(d|x) = \log \frac{P(x|d=+1)}{P(x|d=-1)} + \log \frac{P(d=+1)}{P(d=-1)} \tag{2.5}$$

$$L(d|x) = L(x|d) + L(d) \tag{2.6}$$

To simplify the notation, Equation(2.6) is rewritten as follows:

$$L^{'}(\hat{d}) = L_c(x) + L(d) \tag{2.7}$$

where the notation $L_c(x)$ emphasizes that this LLR term is the result of a channel measurement made at the receiver. The equations above were developed with only a data detector in mind. Next, the introduction of a decoder will typically yield decision-making

benefits. For a systematic code, it can be shown that the LLR (soft output) $L(d)$ out of the decoder is equal to Equation(2.8): [51]

$$L(\hat{d}) = L^{'}(\hat{d}) + L_e(\hat{d}) \tag{2.8}$$

Where $L^{'}(d)$ is the LLR of a data bit out of the demodulator (input to the decoder), and $L_e(\hat{d})$ is called the extrinsic LLR, represents extra knowledge gleaned from the decoding process. The output sequence of a systematic decoder is made up of values representing data bits and parity bits. From Equations(2.7) and (2.8), the output LLR $L(d)$ of the decoder is now written as follows: [51]

$$L(\hat{d}) = L_c(x) + L(d) + L_e(d) \tag{2.9}$$

Equation(2.9) show that the output LLR of a systematic decoder can be represented as having three LLR Elements: a channel measurement, a priori knowledge of the data, and an extrinsic LLR stemming solely from the decoder. To yield the final $L(\hat{d})$, each of the individual LLRs can be added as shown in Equation(2.9) because the three terms are statistically independent. This soft decoder output $L(d)$ is a real number that provides a hard decision as well as the reliability of that decision. The sign of $L(d)$ denotes the hard decision; that is, for positive values $L(d)$ of decide that d = +1, and for negative values decide that d =-1. The magnitude denotes the reliability of that decision. Often, the value L(d), due to the decoding has the same sign as $L_c(x) + L(d)$, and therefore acts to improve the reliability of $L(\hat{d})$ [51].

2.4 Turbo Decoding Principles

In a typical communications receiver, a demodulator is often designed to produce soft decisions, which are then transferred to a decoder [60]. The improvement in error performance of systems utilizing such soft decisions is typically approximated as 2dB, as compared to hard decisions in AWGN. Such a decoder could be called a soft input/ hard output decoder, because the final decoding process out of the decoder must terminate in bits (hard decisions). With turbo codes, where two or more component codes are used, and decoding involves feeding outputs from one decoder to the inputs of other decoders in an iterative fashion, a hard-output decoder would not be suitable [60].

That is because a hard decision into a decoder degrades system performance (compared to soft decisions). Hence, what is needed for the decoding of turbo codes is a soft input/ soft output decoder. For the first decoding iteration of such a soft input/soft output decoder, illustrated in Figure 2.2, we generally assume the binary data to be equally likely, yielding an initial a priori LLR value of $L(d) = 0$.

The channel LLR value, $L_c(x)$, is measured by forming the logarithm of the ratio of the values for a particular observation which appears as the second term in Equation(2.5).The output $L(d)$ of the decoder in Figure 2.2, is made up of the LLR from the detector, $L'(d)$, and the extrinsic LLR output, $L_e(d)$, representing knowledge gleaned from the decoding process. As for iterative decoding, the extrinsic likelihood is fed back to the decoder input, to serve as a refinement of the a priori probability of the data for the next iteration [60].

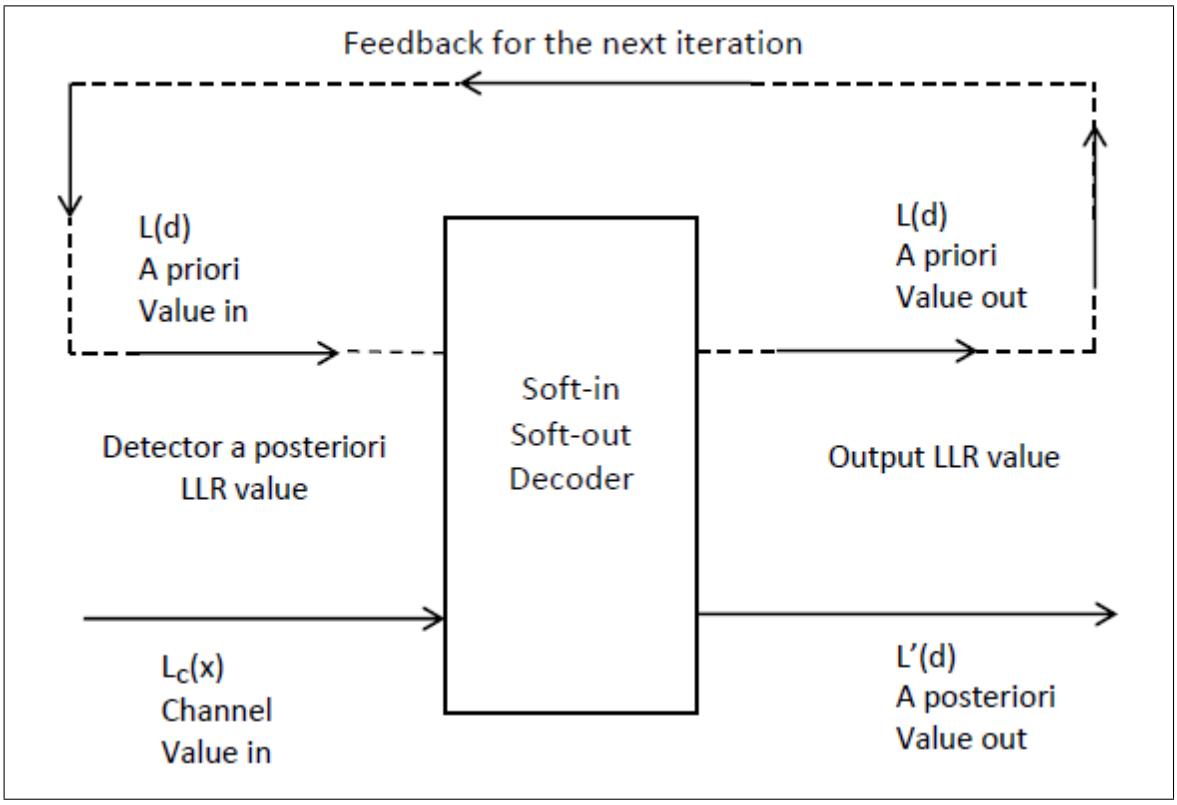

Figure 2.2: soft input soft output decoder.

2.5 Simulation Results of Turbo Decoding Algorithm

The simulation curves presented show the influence of iteration number, Block length, code rate and code generator. Rate $\frac{1}{2}$ codes are obtained from their rate $\frac{1}{3}$ counterparts by alternately puncturing the parity bits of the constituent encoders. The constraint length is 3 using generators polynomials [7, 5]. The BER has been computed after each decoding as a function of signal to noise ratio Eb/No.

Figure 2.3 shows the performance BER for Log MAP with block length of 1024. The performance of BER as a function of Eb/No for SOVA and Log MAP with block length of 4096 is shown in Figures 2.4 and 2.5. The comparison of the BER as a function of Eb/No for SOVA and LOG MAP is shown in Figure 2.6. Eight decoding iterations were performed for Block length of 1024 and 4096. From these figures it can be observed that a large block length corresponds to a lower BER. Also the improvement achieved when the block length is increased from 1024 to 4096 for both algorithms. Log MAP shows better performance than SOVA for the same constraint length.

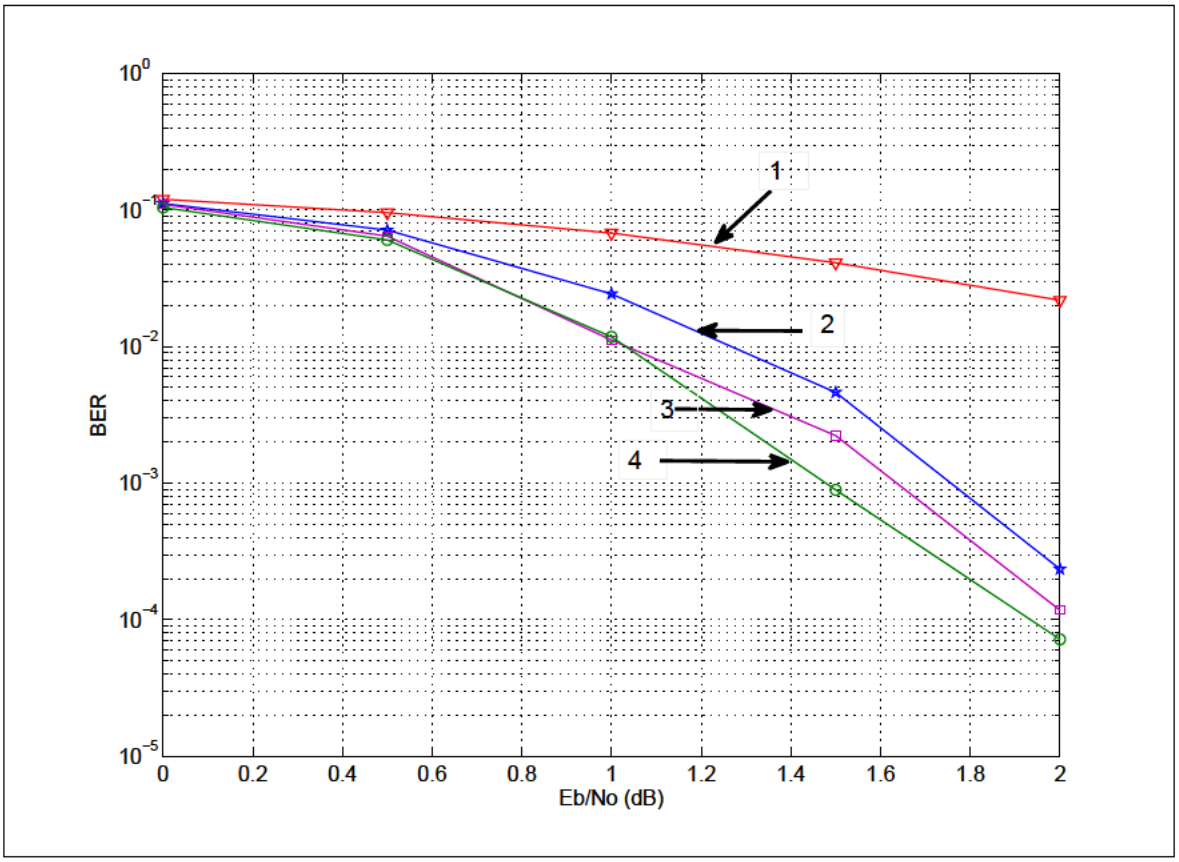

Figure 2.3: BER of K = 1024 Turbo code with Log MAP decoding in AWGN channel with various number of iteration.

1. Bit Error rate after 1 Iteration with Log MAP decoding

2. Bit Error rate after 3 Iterations with Log MAP decoding

3. Bit Error rate after 6 Iterations with Log MAP decoding

4. Bit Error rate after 8 Iterations with Log MAP decoding

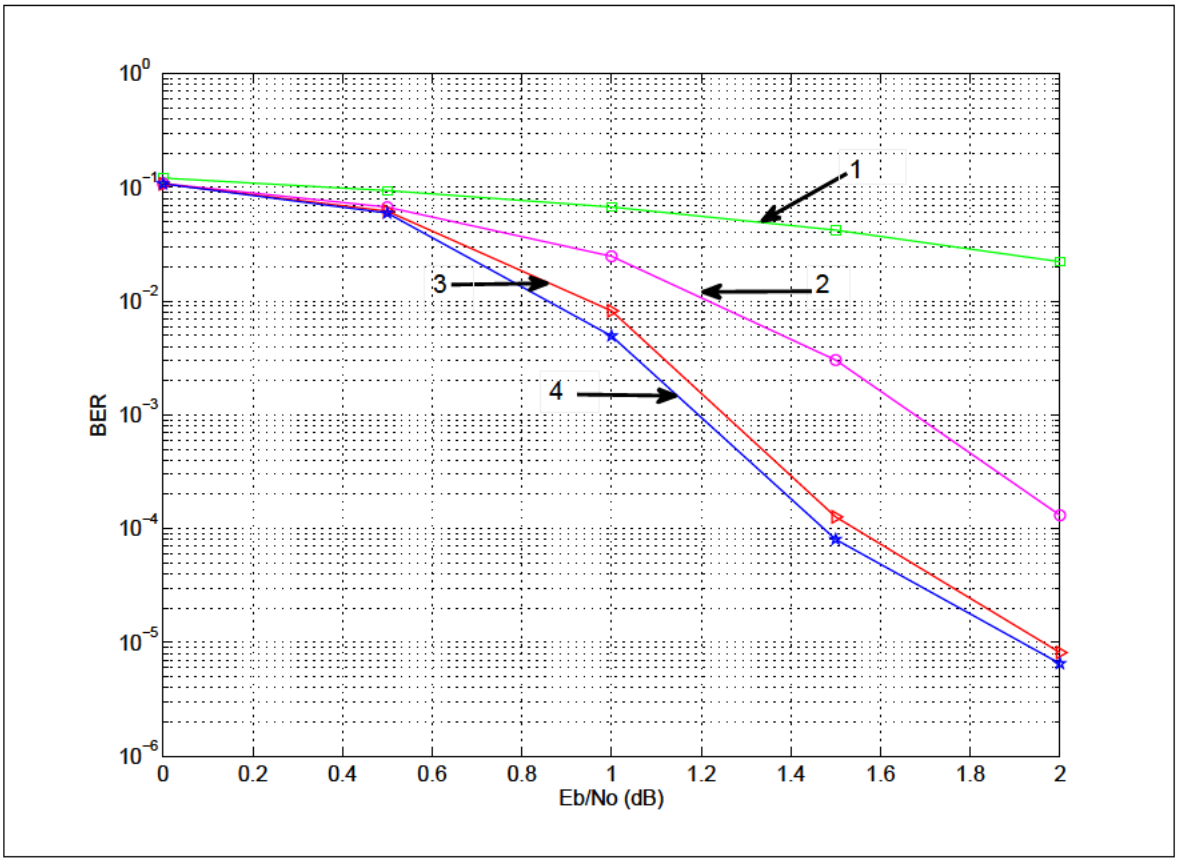

Figure 2.4: BER of K = 4096 Turbo code with SOVA decoding in AWGN channel with various number of iterations.

1. Bit Error rate after 1 Iteration with SOVA decoding

2. Bit Error rate after 3 Iterations with SOVA decoding

3. Bit Error rate after 6 Iterations with SOVA decoding

4. Bit Error rate after 8 Iterations with SOVA decoding

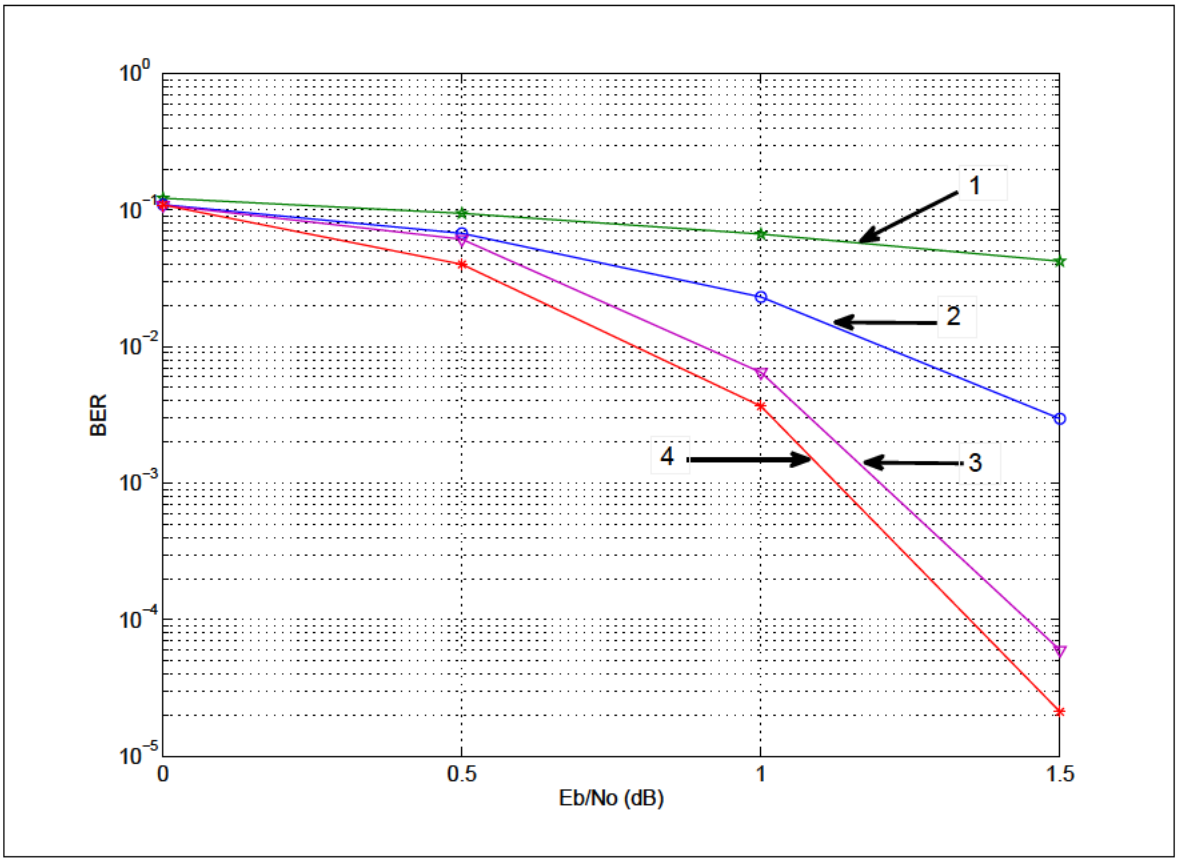

Figure 2.5: BER of K = 4096 Turbo code with Log MAP decoding in AWGN channel with various number of iteration.

1. Bit Error rate after 1 Iteration with Log MAP decoding

2. Bit Error rate after 3 Iterations with Log MAP decoding

3. Bit Error rate after 6 Iterations with Log MAP decoding

4. Bit Error rate after 8 Iterations with Log MAP decoding

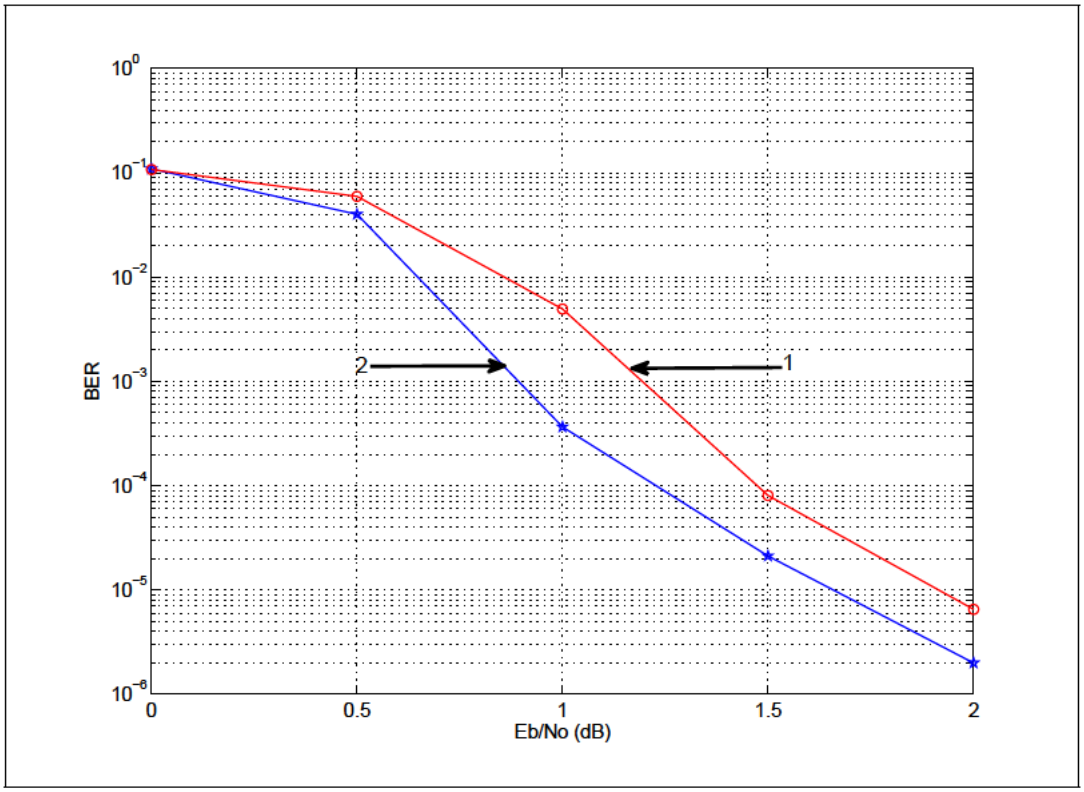

Figure 2.6: BER of K = 4096 Turbo code of Log MAP and SOVA after 8 decoder iteration in AWGN channel.

1. Bit Error rate after 8 Iterations with SOVA decoding

2. Bit Error rate after 8 Iterations with LOG-MAP decoding

2.6 Summary

In this chapter, a review have been carried out on turbo coding for wireless channels and it is shown that Log-MAP performs better in terms of block length compared to SOVA. The Log-MAP algorithm is more suitable for wireless communication applications. The Log-MAP parameters are approximations of the MAP parameters and therefore, the Log-MAP BER performance is close to that of the MAP algorithm. In the next chapter, Turbo Equalization and how this technique can increase data rate over wireless communication systems is examined.

Chapter 3

Iterative Equalization Enhanced Future High Data Rate

3.1 Introduction

In the previous chapter, a review of turbo coding for wireless channels has been carried out, and how turbo codes play an important role in making communication systems more efficient and reliable. Then two turbo codes algorithms, soft-output viterbi algorithm (SOVA) and Logarithmic maximum a posteriori (Log MAP) turbo decoding, were compared. In this chapter, the suitability of Turbo equalization as a means of achieving low bit error rate for future high data broadband wireless systems is investigated.

Turbo equalization is an iterative equalization and decoding technique that can achieve equally impressive performance gains for communication systems that send digital data over channels that require equalization, hence, those that suffer from intersymbol interference (ISI) [5]. Turbo equalization is an approach to coded data transmission over channels with ISI which can yield additional improvement in bit error rate.

Conventional approaches implement an equalizer to remove ISI or use MAP or maximum likelihood (ML) detection. Data reliability can be enhanced using coding, where the data is encoded in the transmitter prior to transmission [4] [5]. For reasons of complexity, the receiver then typically performs separate equalization and decoding of the data. But significant performance gains can be achieved through joint equalization and decoding at the cost of added complexity [4].

The iterative equalization approach can significantly reduce the complexity of joint equalization and decoding by passing soft information, the use of interleaving, and the controlled feedback of soft information to achieve performance gains [61]. Various algorithms similar to Turbo Equalization have been proposed to overcome the complexity of the MAP/ML algorithms, especially in the detector, where complexity is exponential in the channel delay spread [62, 63].

Since the initial proposal of 'Turbo Codes' by Berrou et al. in 1993 [24], the iterative principle has been extended to encompass single carrier Equalization techniques. This allows single carrier systems to combine the operations of Equalization and channel coding to operate in a wideband channel with performance that could not previously be achieved with traditional Equalization and forward error correcting (FEC) techniques [26]. Iterative Equalization techniques have been shown to give excellent error rate performance

for both fixed and fast fading channels [64].

For most time-invariant discrete channels, the turbo-equalizer performance is close to the coded Gaussian channel performance, even for low signal-to-noise ratios [65]. Conventional solutions generally involve both equalization and channel coding which are done separately [65]. In order to achieve high data rates for broadband wireless systems the symbol rate and the bandwidth have to be increased. This can also be combined with the use of M-ary modulation techniques. But the proposed approach makes the resulting transmissions more susceptible to delay dispersion in the radio channel. This manifests as increased ISI at the receiver. ISI in turn results in an irreducible BER. [66]

This has led to the investigation of Iterative equalization technique as a means of increasing data rate. The channel decoder used in this study is a Soft-Input Soft-Output (SISO) which is an approximated version of the MAP algorithm [65]. This algorithm is suboptimum but gives good performance.

The main contribution in this chapter is summarized as follows:

- Higher data transmission rates over channels with Intersymbol Interference are achieved with low error probability when using Iterative equalization.
- Turbo equalization is beneficial for higher modulation scheme and thereby increase data rate with reasonable complexity.

The rest of this chapter is organized as follows: in Section 3.2, the system model for the proposed technique is described. Section 3.3 describes the principle of Iterative Equalization and in section 3.4 the Daterate performance is analyzed. The Iterative equalization performance results are shown in section 3.5. The work presented in this chapter is published in [28, 29].

3.2 Description of the Proposed System Model

The system model is shown in Figure 3.1. In the transmitter side, a block of data bits $\boldsymbol{u}$ is protected by a convolutional encoder and interleaved to overcome fast fading phenomenon. The encoded bits $a = (a_0, a_1, ..a_{k-1})^T$ are modulated. The symbols are denoted by $b = (b_0, b_1, \ldots b_{k-1})^T$.

The modulated signal is transmitted over a frequency selective fading channel. In this work a block fading channel characteristics is assumed; hence the channel is time-invariant during one transmission burst. Thermal noise at the receiver is modelled as additive white Gaussian noise (AWGN). The received signal ***r*** that is sampled at the symbol rate can be given by the equation

$$\mathbf{r} = \mathbf{Ah} + \mathbf{w} \tag{3.1}$$

where **A** is the matrix containing symbols. The channel impulse response is described by the vector $\mathbf{h} = (h_0, h_1, \ldots h_L)^T$, which consists of symbol spaced complex-valued channel taps. The white noise samples are denoted by **w**; the noise variance is $\sigma^2 = N_0/2$

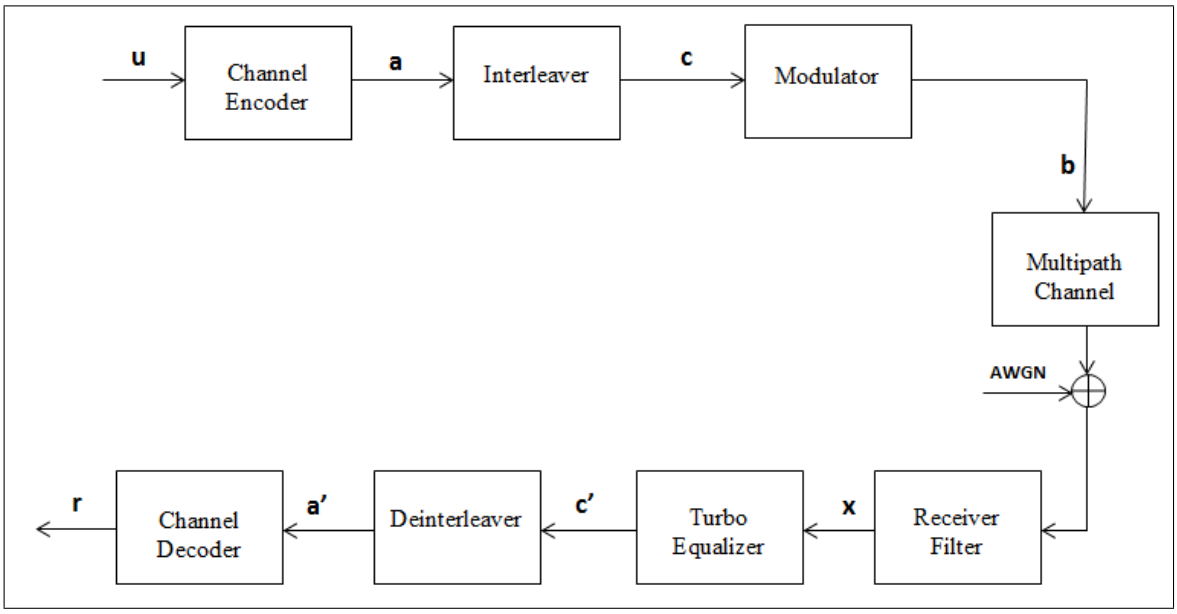

Figure 3.1: Proposed System Model

3.3 Principles of Iterative Equalization Used

Figure 3.2, shows the iterative equalization receiver structure used in this study. Both the equalizer and the decoder employ the optimal symbol by symbol Maximum A-Posteriori (MAP) soft input soft output (SISO) algorithm in [65]. Soft input symbols are fed into the decoder from a sampled receive filter stream $\mathbf{r}(t)$ and bit-wise hard decisions are produced as the final output. The equalizer provides soft outputs, hence, reliability information on the coded bits for the channel decoder. The soft information on the bit c_k is usually given as a log-likelihood ratio (LLR) or L-value as

$$\lambda^E(c_k) = \log \frac{P(c_k = +1|r)}{P(c_k = -1|r)} \tag{3.2}$$

which is the ratio between the conditional bit probabilities in the logarithmic domain. These L-values are deinterleaved and given for the channel decoder, which uses them to recover the information bits **u**. At the first iteration round there is no feedback information from the channel decoder available, so the equalizer calculates the L-values $\lambda^E(c)$ that are just based on the received samples **r** from the channel.

The L-values are deinterleaved to break consecutive bits far apart and thus giving the channel decoder independent input values. The interleaving is an essential part in the iterative receiver scheme, since the extra information on an individual data bit is due to the

different neighbouring bits in the detection and decoding processes. The soft values $\lambda^E(c)$ are provided for the SISO channel decoder. The decoder has to calculate new L-values $\lambda^D(c)$ for the coded bits *c*, since they are needed in the feedback branch to the equalizer.

Therefore we need to use the more complex SISO decoder instead of the conventional hard output decoder. The equalizer is able to produce the L-values $\lambda^E(c)$ based on the received samples from the channel, so that information should not be repeated in the feedback. Hence, the feedback only contains the extra information that is obtained from the surrounding bits in the channel decoding. The input L-values and the obtained extra information are called intrinsic and extrinsic information. The extrinsic information from the channel decoder is given in [4, 25, 61] as

$$\lambda_e^D(c_k) = \lambda^D(c) - \lambda_e^E(c_k) \tag{3.3}$$

where $\lambda_e^E(c_k)$ denotes the extrinsic information from the equalizer. The turbo equalization technique is based on the utilization of this extrinsic information at the next iteration round [25]. So it is passed through the interleaver to the equalizer as a priori information on the bit reliabilities. By exploiting this side information in the detection, more reliable decisions are achieved. Also in the equalizer output the extrinsic information $\lambda_e^E(c_k)$ is extracted from the output as follows

$$\lambda_e^E(c_k) = \lambda^E(c) - \lambda_e^D(c_k) \tag{3.4}$$

This equalizer information is again used in the SISO decoder to produce new soft outputs and furthermore, the new extrinsic information according to equation(3.3). As soon as this feedback information becomes available, the new iteration round can be started. The number of iterations may depend on the processing power available or the achieved performance improvement. At the final stage, there is no need for the SISO decoder, since only hard decisions $\hat{u}$ on the information bits are needed. The Turbo Equalization receiver is able to improve the performance, but at the cost of higher complexity. The main burden is the complex SISO decoder, especially due to the coding schemes that are based on the constraint length of 4. Also, as the Equalization and decoding are performed several times, the receiver complexity grows respectively.

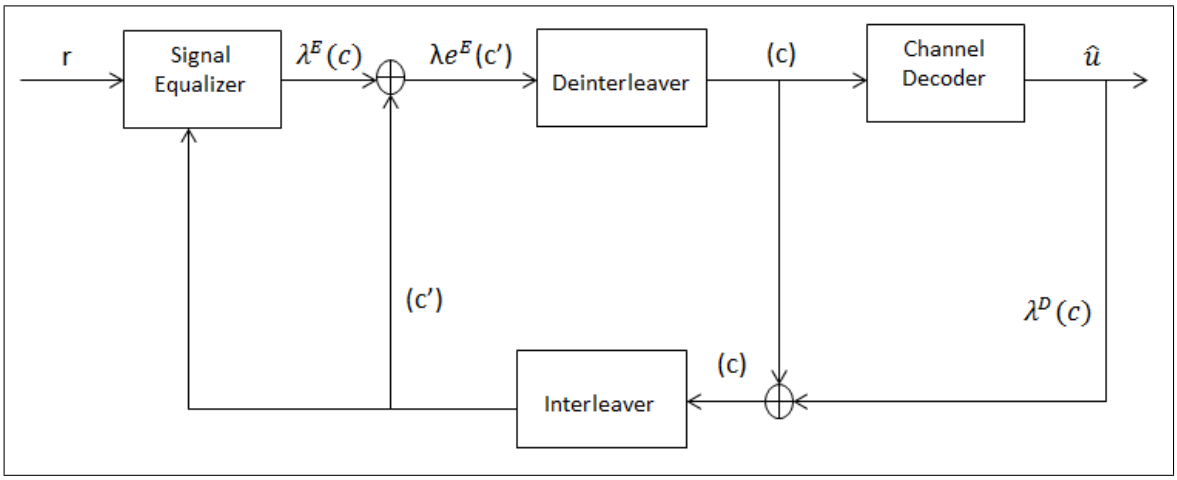

Figure 3.2: The Iterative structure of the System

3.4 Receiver Algorithm Used

The objective of the MAP algorithm is to minimize the bit error probability by estimating a posteriori probabilities (APP) of states and transitions of the Markov source from the received signal sequence. The MAP algorithm introduced by Chang and Hancock [67] uses the information of the whole received sequence to estimate a single bit probability. In other words, the MAP algorithm selects the bit $\hat{u} = [-1, +1]$ at time instant k, which maximizes the following APP

$$\hat{u} = \arg\max[p(u|\hat{c})] \tag{3.5}$$

The optimum MAP algorithm saves multiplicative transition probabilities in the trellis, which is computationally difficult. Therefore in practical implementations the path metric is calculated in the log-domain, which enables cumulative calculations [36, 68]. Since MAP requires both forward and backward recursions, it is around two times more complex than the soft output Viterbi algorithm (SOVA) [36]. The main advantage of the MAP algorithm is more reliable soft information, since it is optimised for symbol wise decoding. This is why MAP is very suitable for the SISO decoding algorithm in the Turbo Equalization scheme. The BCJR-log-MAP (BCJR stands for Bahl, Cocke, Jelinek and Raviv) provides the APP information for each bit as the L-value according to (3.2). The state probability for trellis state s at time k is denoted by

$$\alpha_k(s) = p(s, r_{j \leq k}) \tag{3.6}$$

in the forward direction and by

$$\beta(s) = p(r_{j>k|s}) \tag{3.7}$$

in the backward direction. The transition probability between states s' and s is given in log-domain as

$$\ln \gamma_k(s', s) = \sum_{i=0}^{N} \frac{1}{2} \lambda_e^E(c_k) c_{k,i} \tag{3.8}$$

where $c_{k,i}$ is the *ith* code bit for the information bit u_k and the coding rate is 1/N. Then the decoder output is given as in [36, 69]

$$\lambda(\hat{u}) = \ln \sum_{(s',s)} e^{\ln \alpha} k - 1^{(s')+\ln \gamma} k^{s',s)+\ln \beta k(s)} - \ln \sum (s', s)^{e^{\ln \alpha}} k - 1^{(s')+\ln \gamma} k^{(s',s)+\ln \beta k(s)} \tag{3.9}$$

where $u_k = +1 \quad or - 1$ and the state probabilities can be computed recursively

$$\ln \alpha_k(s) = \ln \sum s'^{e^{\ln \gamma k(s',s)+\ln \alpha}} k - 1^{(s')} \tag{3.10}$$

$$\ln \beta_k(s') = \ln \sum s^{e^{\ln \gamma}} k + 1^{(s',s)+\ln \beta} k + 1 \tag{3.11}$$

Finally, the soft information on the code bits $\lambda(c_k)$ needed for the feedback is obtained by re-encoding the achieved output.

3.5 Data Rate Performance Analysis for the Proposed System

The data rate Datarate against SNR_{dB} can be calculated from the packet error rate as follows:

$$Datarate = (S_R \times B_{eff}) \times (K) \times (1 - PER) \tag{3.12}$$

where S_R is the symbol rate in 20MHz channel, B_{eff} is the bandwidth efficiency, *K* is the packet code rate. It is assumed that no packets are discarded due to header errors. The PER is purely a function of the payload error rate. This quantitative measure allows us

to compare each of the modulation modes and channel scenarios in terms of the expected achievable data rates versus SNR.

$$SNR_{dB} = R_P - N \tag{3.13}$$

In order to examine the achievable data rates versus signal to noise ratio, a link budget must be established [53, 70] . To calculate the SNR, given by (3.12) at the receiver, the expressions for the noise power *N* must be considered and also the receiver power P_R in terms of the transmit power T_P and the path loss L_P given as

$$N = 10\log(K_B T) + 10\log_{10}(S_R \times (1+\alpha)) + NF \tag{3.14}$$

Where α is the filter roll-off factor, n is the total nunmber of bits per packet, KB is Boltzmann's constant $(1.38 \times 10_{-23} W - s/K)$ and T is the noise temperature in Kelvin. NF is the total noise power in signal bandwidth and $R_P = T_P + L_P$

$$L_P = G_T + G_R + 20\log 10\left(\frac{\lambda}{4\pi}\right) - n \times 10\log_{10}(d) \tag{3.15}$$

in [66].

Where G_T and G_R are the gains of the transmit and receiver antennas respectively relative to an isotropic source, λ is the wavelength of the carrier frequency and *d* the separation between the antennas, *n* is an empirical constant, the path loss exponent, which for line of sight (LOS) is 2 and greater than 2 for non-LOS conditions [66]. It is assumed that a path loss exponent of 6, represents a worst case scenario. The maximum actual data rates achievable for the different modulation modes are shown in Figure 3.5 calculated from (3.12) assuming a symbol rate of 20MHz. The transmission parameters are shown in Table 3.1 and are assumed in the link budget analysis.

3.6 Proposed Iterative Equalization Performance Results

The BER performance of an iterative equalizer is dependent on the channel profile, the modulation scheme, the encoder constraint length and the size of the interleaver. In this work the encoder constraint length and the size of the interleaver are fixed. For channel coding a rate $\frac{1}{2}$ recursive systematic convolutional code with memory $m_c = 2$ is used.

Parameter	Value
S_R	20MHz
α	0.5
N_F	8dB
P_T	0dBm
G_T	0dB
G_R	0dB
f_c	2.4GHz
λ	0.125
n	4

Table 3.1: Transmission Parameter

The constraint length $L = 4$, generator polynomial $G = [7, 5]$ and the Block length of the code is 4096.

Figure 3.3 shows the BER results comparing the performance of Proposed turbo equalization algorithms with Conventional methods using 8PSK modulation. Proposed Turbo equalizer has 2dB gain over the conventional Decision feedback equalizer and 6dB gain over linear equalizer. Figure 3.4, shows the performance of the BER as a function of signal to noise ratio (SNR) for code using BPSK, QPSK, 8PSK, and 16QAM modulation, using Proakis Channel B in [53] and decoded with MAP algorithm [64].

These performance curves are important, as they represent an upper bound on performance for the iterative Equalization receiver. If we take a target of 10^{-4}, then to achieve this target BPSK mode required 5dB, QPSK 5.5dB, 8PSK 7.5dB, 16QAM 8.3dB respectively shown in Figure 3.4. As the modulation order increases, the iterative gain increases and more data are transmitted with reasonable complexity.

Figure 3.5 shows the daterate achieved for 8PSK and 16QAM modulation scheme for the proposed turbo equalizer and the conventional method. Maximum data rate for 16QAM is 19.22Mbits/s for proposed method and 13.53Mbits/s for conventional method. Also for 8PSK, Maximum data rate for is 9.55 for proposed method and 5.97 for conventional method in Mbits/s respectively. With Iterative equalization the bit rate is increased even further by introducing higher order modulation such as 16QAM.

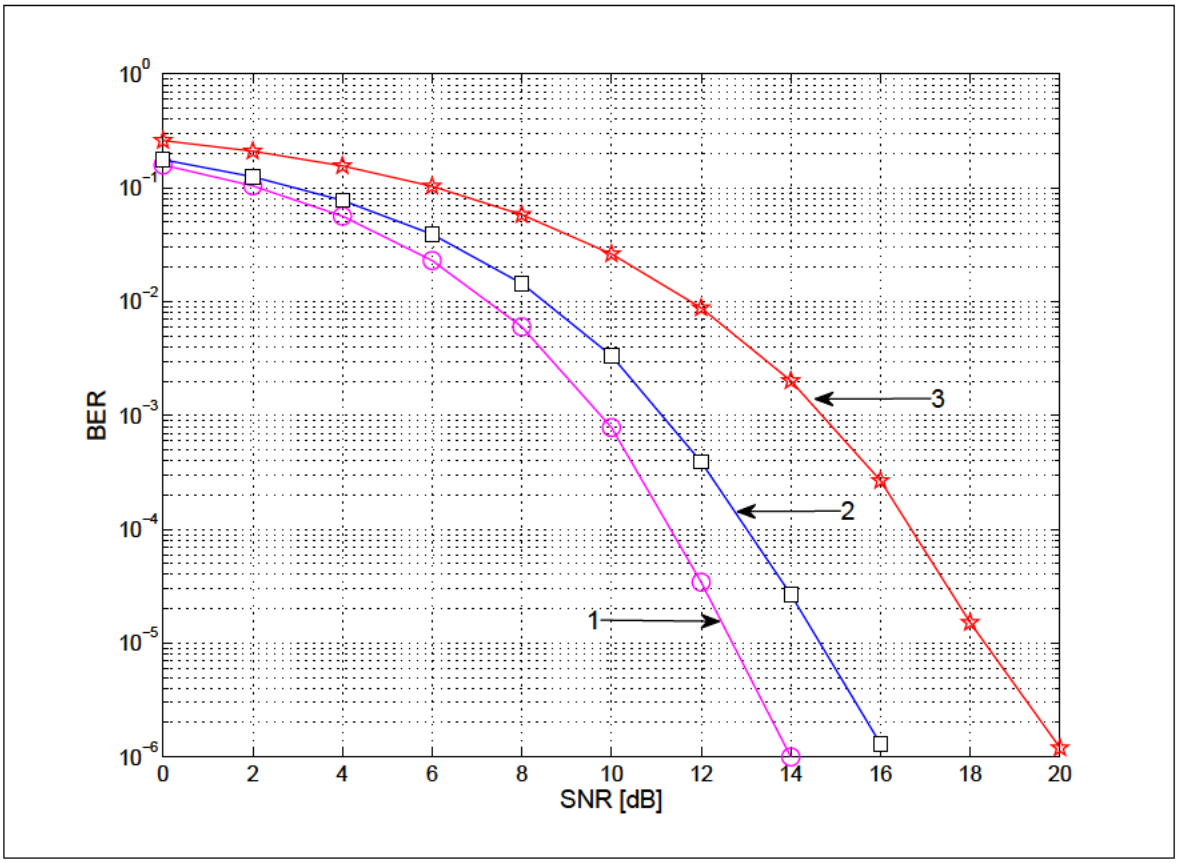

Figure 3.3: BER results comparing the performance of Proposed turbo equalization algorithms with Conventional methods using 8PSK modulation.

1. Proposed Turbo equalizer

2. Conventional Decision feedback Equalizer

3. Conventional Linear Equalizer

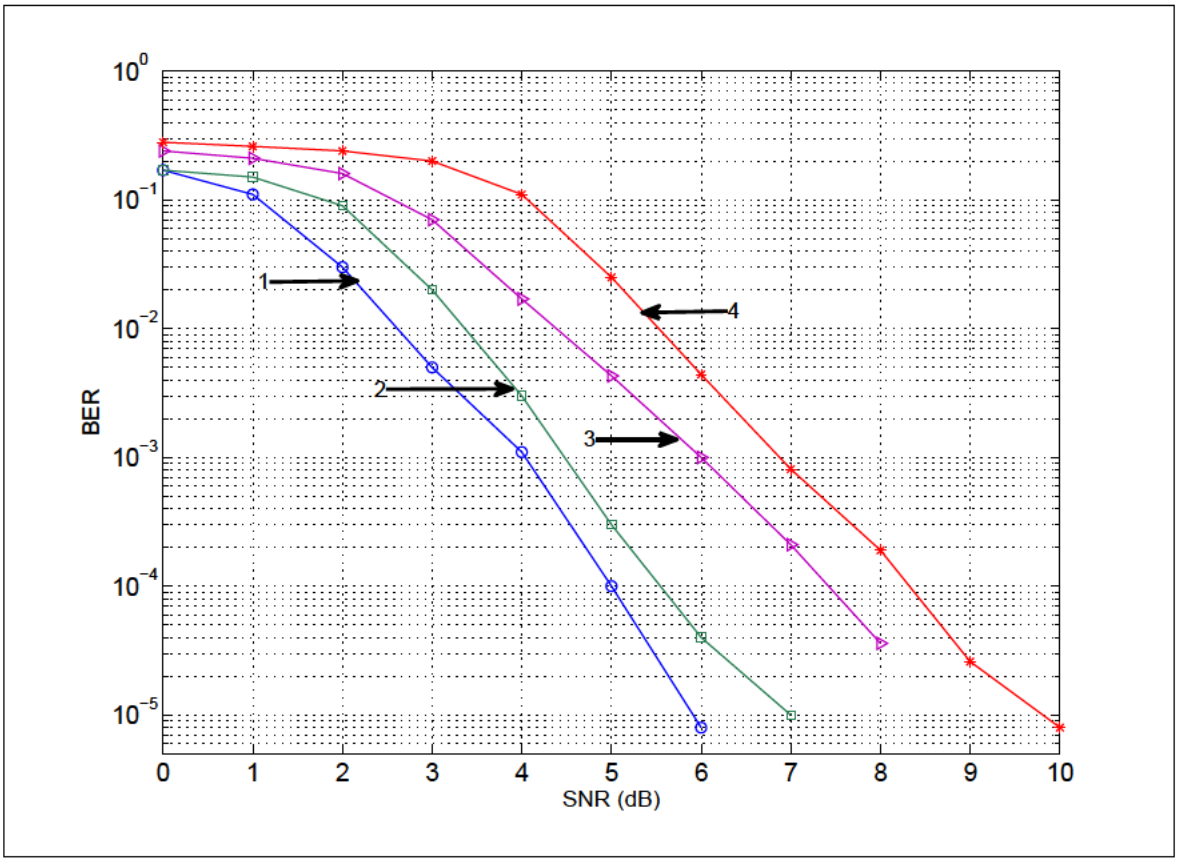

Figure 3.4: Figure 4 BER using BPSK, QPSK, 8PSK, and 16QAM modulation as a function of SNR.

1. BPSK for Proposed Turbo equalizer
2. QPSK for Proposed Turbo equalizer
3. 8PSK for Proposed Turbo equalizer
4. 16QAM for Proposed Turbo equalizer

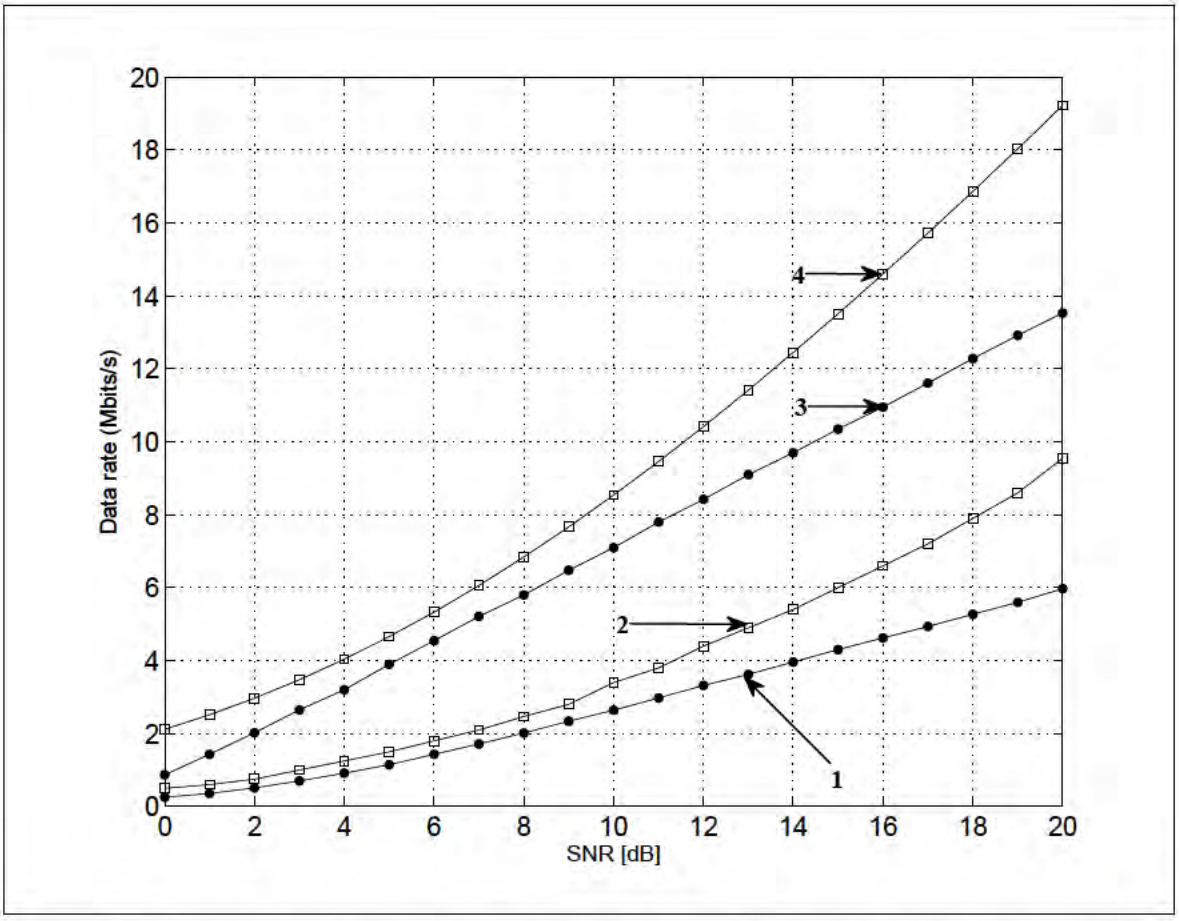

Figure 3.5: Data rate for channel B using 8PSK and 16QAM modulation as a function of SNR.

1. 8PSK for Conventional Decision feedback equalizer
2. 8PSK for Proposed Turbo equalizer
3. 16QAM for Conventional Decision feedback equalizer
4. 16QAM for Proposed Turbo equalizer

3.7 Summary

The results confirmed the suitability of using iterative equalization to increase data rate. It was also demonstrate that the iterative gain is greater for higher modulation orders. However, there is a trade off, between the iterative gain for higher modulation orders and the complexity of the receiver.

The complexity at the receiver is dominated by the complexity of the MAP equalizer. In the next chapter, a modified approach is proposed to mitigate the error propagation in the DFE algorithm when used in turbo equalization while retaining low computational complexity.

Chapter 4

Modified Iterative Decision Feedback Equalization

4.1 Introduction

In communication systems, data is transmitted over a channel with intersymbol interference (ISI). At the transmitter, the data is often protected by the addition of a controlled amount of redundancy using forward error correction or an error-correction code (ECC). It is then the task of the receiver to exploit both the structure of the transmit symbol constellation (as viewed at the output of the channel) and the structure of the code to detect and decode the transmitted data sequence. The methods that exploit the structure of the transmitted symbol constellation are referred to as equalization, whereas those that exploit the structure of the code are termed decoding [71].

A number of important advances have been made in the area of joint equalization and decoding in which traditional equalization methods and decoding methods exchange information in an iterative fashion until convergence is achieved. In its original form, turbo equalization [26] employed maximum a posteriori probability (MAP) equalization and decoding methods in such an iterative scheme.

At the receiver, the encoder and the discrete-time equivalent channel are treated as the parallel concatenation of two codes. Hence, the so-called turbo principle [72] can easily be applied. The performance of the system is improved in the fashion of exchanging the extrinsic information iteratively among the soft-input/soft-output (SISO) equalizer and SISO channel decoder until convergence is achieved. To achieve optimal equalization, symbol-by symbol maximum-a-posteriori (MAP) algorithm is used in [25] or soft Maximum-Likelihood Sequence Estimation (MLSE) detector minimizing the sequence error via maximum likelihood estimation [58, 73, 74]. In [26], the first proposed turbo equalization implements the soft output Viterbi algorithm (SOVA) exclusively for both equalization and decoding, as in [69].

Unfortunately, these optimum algorithms are not usually applicable to many practical communication systems in use today due to their high computational complexity. For large constellation size M modulation used with long discrete-time equivalent channel length L results in high computational complexity of $O(M^L)$ that is unmanageable for equalization [75]. As a consequence, an efficient reduced complexity SISO equalizer is required for sub-optimal turbo equalization, with very little performance degradation.

Due to this reason, many authors in the recent literature have investigated the low complexity SISO equalizers. In [76], Wang and Poor developed an iterative receiver structure for decoding multiuser information data in code division multiple access. The minimum mean square error (MMSE) linear equalizer (LE) implemented in turbo equalization cancels the inter-symbol interference and multi-access interference successfully. Ariyavisitakul and Li [77] proposed a joint convolutional coding and decision feedback equalizer (DFE) in an iterative equalization scheme.

The DFE uses a combination of soft decisions and tentative decisions obtained from the Viterbi decoder to cancel Inter Symbol Interference (ISI). Tuchler showed that the MMSE-based LE performs well compared with MAP equalizer while only low computational complexity is needed [78]. The equalization was extended to multilevel modulation in [71].

The effects of error propagation are observed clearly from the simulation results of [78] and [71] where the turbo equalizer does not produce significant improvement in multipath channels throughout the iterations. Besides, the gain in bit error rate (BER) offered by the conventional DFE diminished dramatically after several iterations.

This has led to the new approach proposed in this chapter. The Modified approach mitigates the error propagation in the DFE algorithm when used in turbo equalization while retaining low computational complexity. It estimates the data using the a priori information from the SISO channel decoder and also the a priori detected data from previous iteration to minimize error propagation. From the simulation results, it can be shown that the BER performance of the modified DFE algorithm provides significant improvement when compared with the conventional DFE algorithm in [71], [78] using the higher-level modulation scheme.

In this chapter our contribution is as follows:

- modified DFE algorithm provides significant improvement when compared with the conventional DFE algorithm using the higher-level modulation scheme.
- It was shown that at higher level modulation, the modified DEF has 1.6dB gain over the conventional DEF after seven iterations.

The rest of this chapter is organized as follows: Section 4.2 introduces the System

Model for the Proposed Approach. Section 4.3 presents the Iterative Equalization principle used. Section 4.4 presents the Conventional approach of Decision Feedback Equalizer. The Modified Decision Feedback Equalizer approach is in section 4.5. Simulation results for the proposed system are in Section 4.6. Finally in Section 4.7, a summary of the chapter is presented.

4.2 Proposed System Model for Modified DFE Algorithm

The system model is shown in Figure 4.1. In the transmitter side, a block of data bits ***u*** is protected by the convolutional encoder and interleaved to overcome fast fading phenomenon. The encoded bits $a = (a_0, a_1, ..a_{k-1})^T$ are modulated. The modulated symbols are denoted by $b = (b_0, b_1, \ldots b_{k-1})^T$ and transmitted over a frequency selective fading channel. In this study a block fading channel characteristics is assumed; hence the channel is time-invariant during one transmission burst. Thermal noise at the receiver is modelled as additive white Gaussian noise (AWGN). The received signal **d** that is sampled at the symbol rate can be given by the equation

$$\mathbf{d} = \mathbf{Ah} + \mathbf{w} \tag{4.1}$$

where **A** is the transmitted symbol. The channel impulse response is described by the vector $\mathbf{h} = (h_0, h_1 \ldots h_L)^T$, which consists of symbol spaced complex-valued channel taps. The white noise samples are denoted by **w**; the noise variance is $\sigma^2 = N_0/2$.

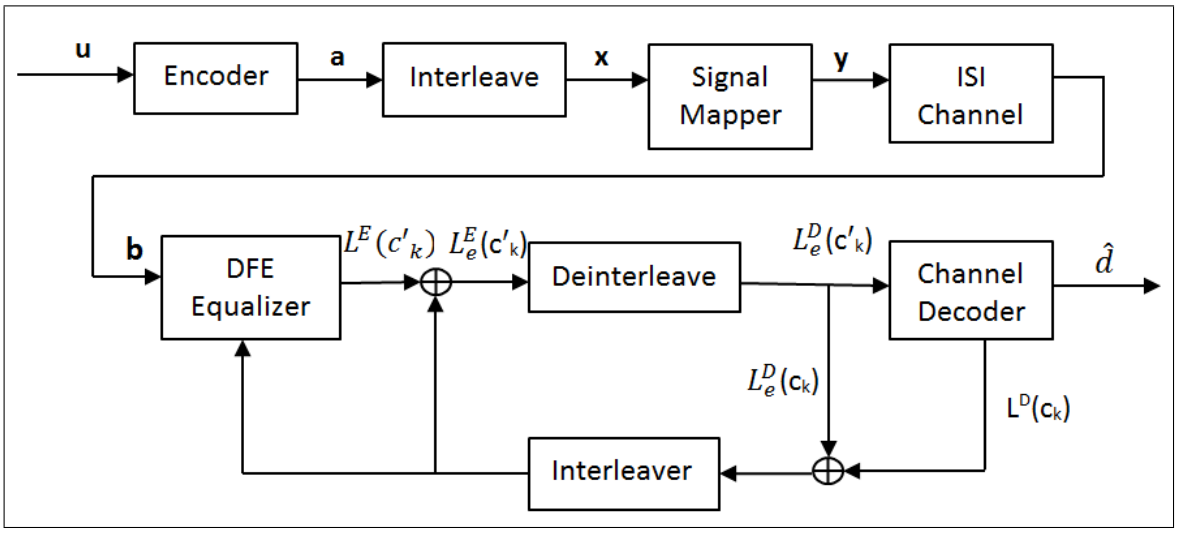

Figure 4.1: System Model for the Modified DFE.

4.3 The Iterative Equalization Principle Used

Figure 4.1, shows the turbo equalization receiver structure used in this study. Both the equalizer and the decoder employ the soft input soft output (SISO) algorithm in [25]. Soft input symbols are fed into the decoder from a sampled receive filter stream **d** and bit-wise hard decisions are produced as the final output. The equalizer provides soft outputs, information on the coded bits for the channel decoder. The soft information on the bits are usually given as a log-likelihood ratio (LLR) or L-value denoted as $L^E(c_k)$, the same method used in chapter two.

$$L^E(c_k) = \log \frac{P(c_k = +1|d)}{P(c_k = -1|d)} \tag{4.2}$$

This is the ratio between the conditional bit probabilities in the logarithmic domain. These L-values are deinterleaved and given for the channel decoder, which uses them to recover the information bits ***u***. At the first iteration round there is no feedback information from the channel decoder available, so the equalizer calculates the L-values $L^E(c_k)$ that are just based on the received samples *d* from the channel. The L-values are deinterleaved to break consecutive bits far apart and thus giving the channel decoder independent input values.

The soft values $L^E(c'_k)$ are provided for the SISO channel decoder. The decoder has to calculate new L-values $L^D(c'_k)$ for the coded bits **c**, since they are needed in the feedback branch to the equalizer. The equalizer is able to produce the L-values $L^E(c'_k)$

based on the received samples from the channel, so that information should not be repeated in the feedback. Hence, the feedback only contains the extra information that is obtained from the surrounding bits in the channel decoding. The input L-values and the obtained extra information are called intrinsic and extrinsic information. The extrinsic information from the channel decoder is given as in [26], [72] as:

$$L_e^D(c_k) = L^D(c_k) - L_e^E(c_k) \tag{4.3}$$

where $L_e^E(c_k)$ denotes the extrinsic information from the equalizer. The turbo equalization technique is based on the utilization of this extrinsic information at the next iteration round [72]. So it is passed through the interleaver to the equalizer as *a priori* information on the bit reliabilities. By exploiting this side information in the detection, more reliable decisions are achieved. Also in the extrinsic information for the equalizer output is $L_e^E(c_k)$ in [79] is extracted from the output as follows

$$L_e^E(c_k) = L^E(c_k) - L_e^D(c_k) \tag{4.4}$$

This equalizer information is again used in the SISO decoder to produce new soft outputs and furthermore, the new extrinsic information according to (4.3). The number of iterations may depend on the processing power available or the achieved performance improvement. At the final stage, there is no need for the SISO decoder, since only hard decisions on the information bits are needed.

The Turbo equalization receiver is able to improve the performance, but at the cost of higher complexity. The main burden is the complex SISO decoder, especially due to the coding schemes that are based on the constraint length of 5. Also, as the equalization and decoding are performed several times, the receiver complexity grows respectively.

4.4 Conventional Decision Feedback Equalizer

The modulated signals that are transmitted according to the relationship (4.1) and (4.2) can be seen as the a posteriori probability for each data and is given as:

$$Pr\langle x_m = +1|d_m\rangle = \frac{Pr\langle d_m|X_m^{+1}\rangle Pr(x_m = +1)}{Pr\langle d_m|X_m^{x}\rangle Pr(x_m = x)} \tag{4.5}$$

such that $x \in \{-1, +1\}$

$$X_m^{+1} = [x_0 \quad x_1 \cdots \quad x_{m-1} \quad +1] \tag{4.6}$$

$$Pr\langle d_m|X_m^{+1}\rangle\rangle = \frac{1}{\sqrt{2\pi\sigma^2}} \exp\left[-\frac{1}{2\sigma^2}|d_m - u_0 - \sum_{l-1}^{L-1} u_l x_{m-l}|^2\right] \tag{4.7}$$

where the x_i is the estimated hard feedback symbols. Substituting (4.5) and (4.7) into (4.2), the a posteriori LLR of the coded bits is given as

$$\bigwedge(x_m) = \underbrace{\ln \frac{\exp\left[-\frac{1}{2\sigma^2}|d_m - u_0(+1) - \sum_{l-1}^{L-1} u_l x_{m-l}|^2\right]}{\exp\left[-\frac{1}{2\sigma^2}|d_m - u_0(-1) - \sum_{l-1}^{L-1} u_l x_{m-l}|^2\right]}} + \underbrace{\ln \frac{P(x_i = +1)}{P(x_i = -1)}} \tag{4.8}$$

A similar a posteriori LLR can be found in [45]. The hard decided coded bits can be estimated and fed back to the equalizer for the next symbol estimation. Assuming that all the feedback symbols are estimated correctly, the cancellation of ISI interference results in better BER performance. The extrinsic LLR $L_E(x_m)$, the first term of (4.8), is interleaved and delivered to the channel decoder as the a priori information.

The performance of the conventional MMSE DFE is poor in turbo equalization due to the residual interference in the presence of the severely multipath channels and incorrect symbols are being fed back during equalization. In [77], [71], it has been shown that MMSE DFE is not an effective equalizer and it has only small improvement throughout the iterations when compared with an MMSE LE.

4.5 Proposed Modified Decision Feedback Equalizer

The modified DFE algorithm for the iterative receiver improves BER performance over an ISI channel. The key idea is increasing the reliability of the extrinsic LLR by computing an additional parameter. Let us define x_m^k as the n^{th} symbol estimated at k^{th} iteration from the equalizer. In the first iteration of turbo equalization, the a posteriori LLR is calculated

based on Equation (4.8) and there is no a priori LLR available from the channel decoder. Starting from the second iteration, a new a posteriori probability of the code bit is defined as follows:

$$Pr\langle x_m^k = +1 | d_m, d_{m+1}\rangle \triangleq \frac{Pr\langle d_m, d_{m+1} | x_{m+1}^{k+1}, X_m^{+1}\rangle Pr(x_m^k = +1)}{\sum x Pr\langle d_m, d_{m+1} | x_{m+1}^{k+1}, X_m^{+1}\rangle Pr(x_m^k = x)} \tag{4.9}$$

$x \in \{-1, +1\}$, where, k=2, 3, . . . , denotes the number of iteration and x_m^k is the code bit estimated in k^{th} iteration. $Pr(x_m^k = -1 | d_m, d_{m+1})$ shows that the received samples are independent. The probability of received samples d_m and d_{m+1} at k^{th} iteration is obtained using (4.7) and can be written as

$$Pr\langle (d_m, d_{m+1} | x_{m+1}^{k+1}, X_m^{+1}\rangle = \frac{1}{\sqrt{2\pi\sigma^2}} \exp\left[-\frac{1}{2\sigma^2} q_0(x_m = +1) + q_1(x_m = +1)\right] \tag{4.10}$$

where $q_0(x_m = x) = |r_m - u_0.x - \sum_{l-1}^{L-1} u_l x_{m-l}^k|^2$

$q_0(x_m = x) = \left| r_{m=1} - u_0.x - \left(u_0 x_{m+1}^{k-1} - \sum_{l-1}^{L-1} u_l x_{m-l}^k\right)\right|^2$

The modified a posteriori LLR is

$$L(x_m^k) = \ln \frac{Pr\langle x_m^k = +1 | d_m, d_{m+1}\rangle}{Pr\langle x_m k = -1 | d_m, d_{m+1}\rangle} \tag{4.11}$$

Substituting (4.10) into (4.9) the modified a posteriori LLR of code bit at k^{th} iteration is given as:

$$L(x_m^k) = \underbrace{\ln \frac{\exp\left[-\frac{1}{2\sigma^2} q_0(x_m = +1) + q_1(x_m = +1)\right]}{\exp\left[-\frac{1}{2\sigma^2} q_0(x_m = +1) + q_1(x_m = -1)\right]}} + \underbrace{\frac{Pr(x_m^k = +1)}{Pr(x_m^k = -1)}} \tag{4.12}$$

Comparing equations (4.8) and (4.11) , it can be seen that the modified algorithm considered the additional parameter. The conventional DFE discards the estimated symbol set *x* at the end of process. On the other hand, the modified DFE algorithm not only has the estimated set of symbols (x_m^k) that are fed back to the equalizer for ISI cancellation, it also keeps the data in memory for the estimation in the next iteration *(k+1)*.

Hence, the modified algorithm treats the detected symbol *x* from the last iteration as another set of a priori information besides $L(x_m)$ that is delivered from the channel decoder. For the a higher constellation modulation scheme, the estimation is based on the complex number symbols $S_i \in S$. Hence the LLR calculation of the code bits is denoted as $R_m^S i \triangleq [r_0 \quad r_1 \quad ...r_{m-1} \quad S_i]$, $S_i^{+1} \triangleq S_i \in S : z_{ij} = +1$

where $R_m^S i$ is the estimated feedback sequence and S_i^{+1} consist of a set of symbols. The modified a posteriori probability of code bits for higher modulation systems is given in (4.12) as:

$$Pr(x_{m,j}(k)) = 1|a_m, a_{m+1}) \triangleq \frac{\sum s_j \in S_j^{+1} Pr(d_m, d_{m+1}|x_{m+1}^{k-1}, R_m^S i) Pr(x_{m,j}^k = +1)}{\sum s_j \in S_j^{+1} Pr(d_m, d_{m+1}|x_{m+1}^{k-1}, R_m^S i) Pr(x_{m,j}^k = x)} \tag{4.13}$$

The complexity of the modified algorithm is higher than the conventional DFE in [25], but still has lower complexity when compared with optimum equalizers [58, 73, 74].

4.6 Simulation Results for the Modified Decision Feedback Equalizer

The simulation results compare the proposed method with the existing algorithm. The performance of the decoder has been evaluated by simulations. The ISI channel considered has the impulse response given by $h = [0.227 \quad 0.46 \quad 0.688 \quad 0.46 \quad 0.227]^T$. The channel code rate is $\frac{1}{2}$ RSC with the generator polynomial [37, 21] in octal form, separated by a random interleaver of length 4096. The soft output Viterbi algorithm [80] has been used in the SISO decoder. The results are obtained for 8PSK, 16QAM and 64QAM modulation schemes.

In the 8PSK system shown in Figure 4.2, the conventional DFE has BER of 3.0×10^{-4} at 5dB after seven iterations. It has only 1.3dB gain compared with the BER after second iteration. The modified DFE algorithm achieved 2.6dB gain after second iteration. Figure 3 shows that at the BER of 6.4×10^{-5}, at 9dB after seven iterations, the modified DFE achieved 1.3dB gain over the conventional DFE algorithm. It can also be seen that

in Figure 4.3, at higher level of modulation, the modified DEF has 1.6dB gain over the conventional DEF after seven iterations.

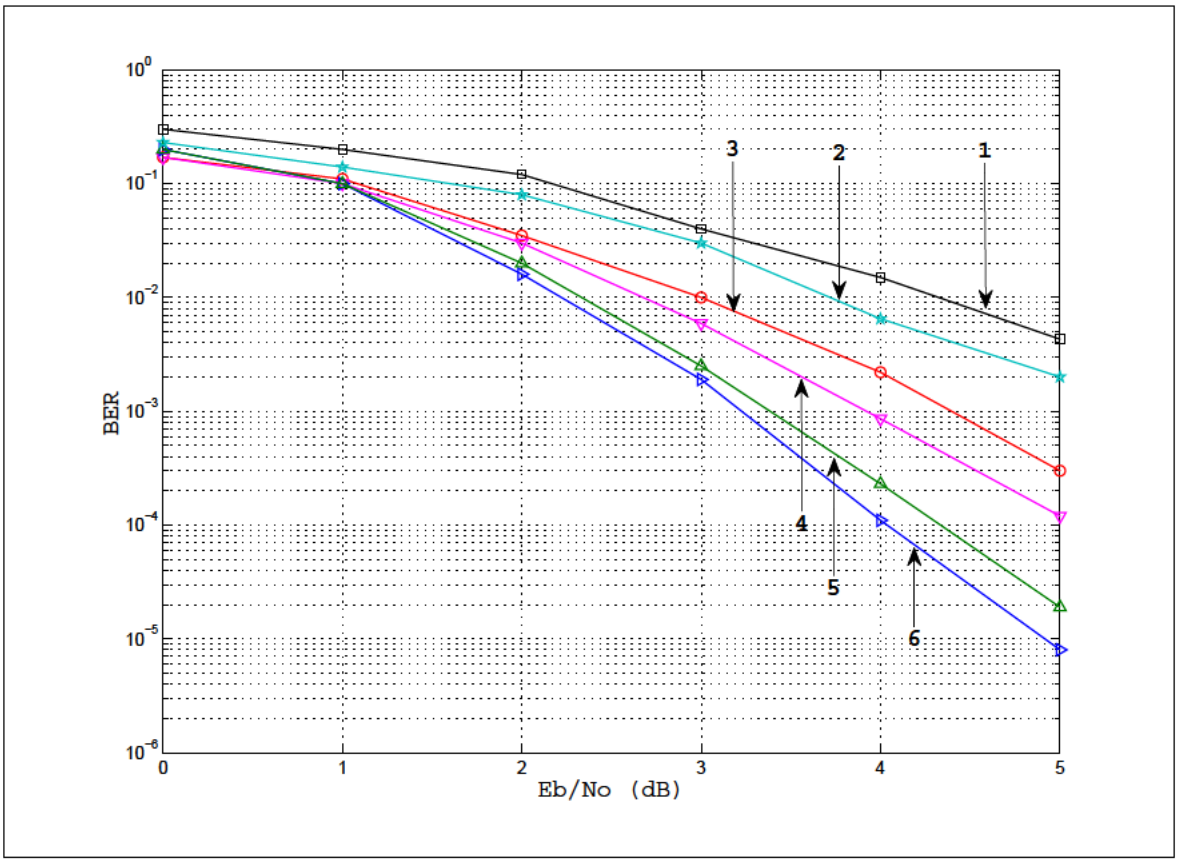

Figure 4.2: BER performance of Proposed and conventional DFE in 8PSK modulation.

1. Conventional DFE after 2 Iterations
2. Conventional DFE after 5 Iterations
3. Conventional DFE after 7 Iterations
4. Proposed DFE 2 after Iterations
5. Proposed DFE 5 after Iteration
6. Proposed DFE 7 after Iterations

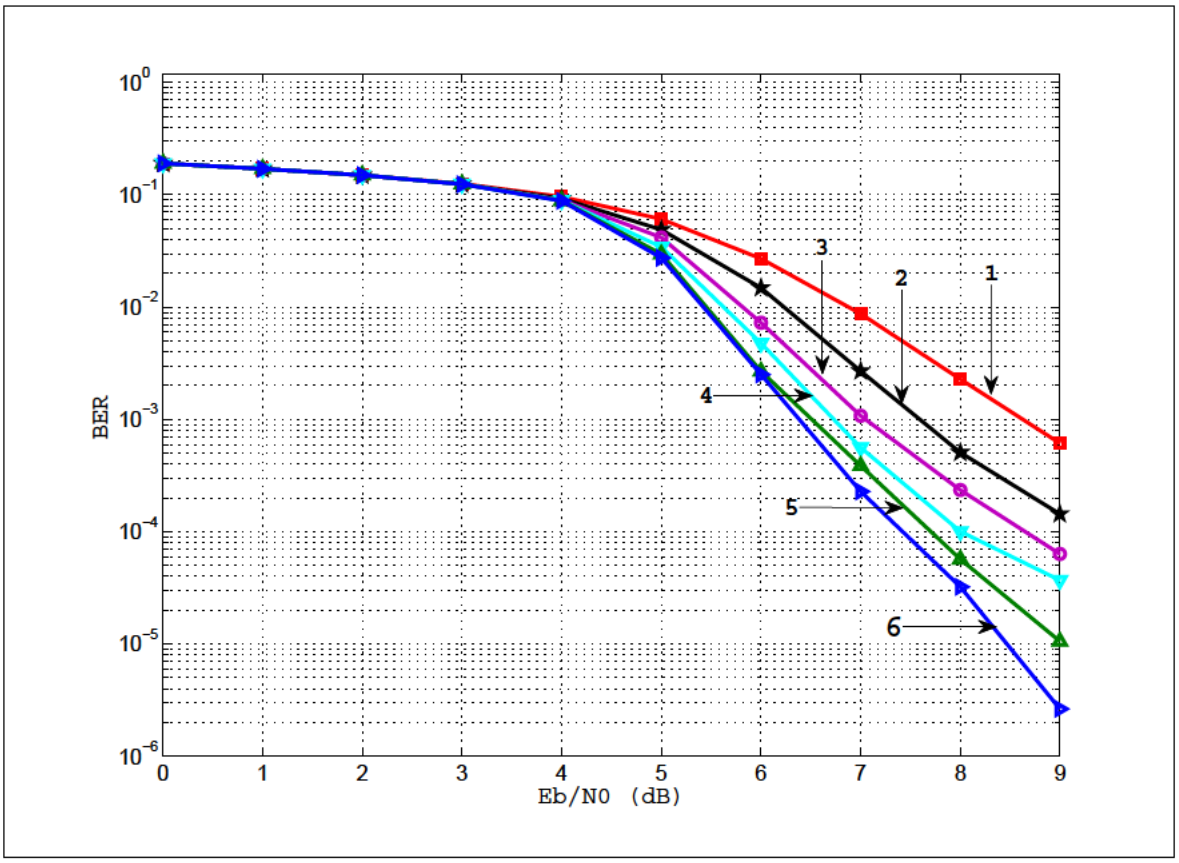

Figure 4.3: BER performance of Proposed and conventional DFE in 16QAM modulation.

1. Conventional DFE after 2 Iterations
2. Conventional DFE after 5 Iterations
3. Conventional DFE after 7 Iterations
4. Proposed DFE 2 after Iterations
5. Proposed DFE 5 after Iteration
6. Proposed DFE 7 after Iterations

4.7 Summary

The Modified Decision Feedback equalizer (DFE) was shown to have superior performance compared with the conventional DFE in [76] and [78] even at higher level of modulation scheme. The modified method improves the BER performance by computing an additional parameter using the feedback symbols from previous iteration and combine it with a priori information. After each iteration, the detected symbols are saved as a priori data for the next iteration. In the next the chapter, the iterative decoding with imperfect MMSE decision feedback equalizer using different modulation schemes is investigated.

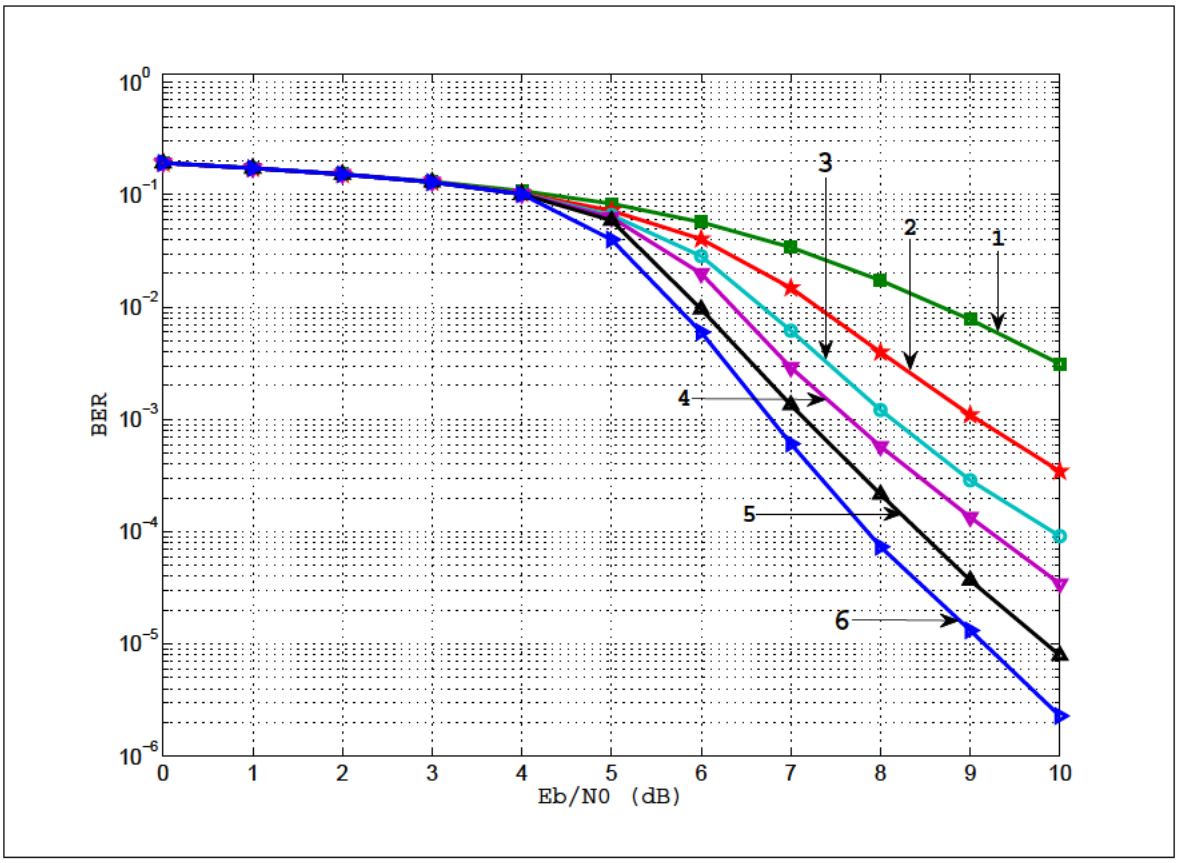

Figure 4.4: BER performance of Proposed and conventional DFE in 64QAM modulation.

1. Conventional DFE after 2 Iterations
2. Conventional DFE after 5 Iterations
3. Conventional DFE after 7 Iterations
4. Proposed DFE 2 after Iterations
5. Proposed DFE 5 after Iteration
6. Proposed DFE 7 after Iterations

Chapter 5

Imperfect Iterative MMSE DFE for Communication Networks

5.1 Introduction

Turbo equalization is a technique that combines channel equalization and coding in an iterative detection scheme. It was originally proposed in [63] and named turbo equalization due to its similarity to previously proposed turbo codes [81]. The discrete-coefficient channel model is a finite-state machine that can be described by a state diagram and a corresponding trellis diagram. The turbo equalizer in [63] combines Maximum Likelihood (ML) or trellis-based equalization and ML channel code decoding in a serial concatenated scheme in order to improve the Bit Error Rate (BER) performance at the receiver side.

The scheme proposed in [63] suffers from high computational complexity since the computational complexity of the ML based equalizer grows exponentially with the number of discrete channel coefficients and becomes very high for long channels. An alternative low complexity scheme, employs low complexity equalizers (filters) instead of the ML equalization. The first low-complexity turbo equalizer was proposed in [82], where ML equalization has been replaced by a low complexity adaptive Least Means Square (LMS) Interference Canceller. A Minimum Mean Square Error (MMSE) Linear Equalizer (LE) for turbo equalization has been introduced in [78, 83].

Although this scheme has been shown to achieve excellent BER performance, the computational complexity is still dramatically high, requiring one matrix inversion per each transmitted bit per one turbo iteration. However, the problem of the high complexity has been solved in the same work [83] by employing an approximate solution with certain degradation in the SNR-BER performance. A low-complexity turbo equalization scheme has been analyzed in [84]. All low-complexity turbo equalization schemes presented in [78, 82–85] are structurally equivalent with the only difference being in the way how the filter coefficients are determined.

However in this chapter, Iterative decoding with imperfect MMSE decision feedback equalizer using different modulation scheme is investigated. It is assumed that at low signal to noise ratio, the decision feedback equalizer propagates error which makes the feedback imperfect. The conventional method assumed a perfect feedback. In [78] using Iterative equalization and decoding, the performance of MMSE LE was better than MMSE DFE.

The performance degradation was due to not taking into account the feedback errors. This work took into consideration the imperfect feedback error due to error propagation. It was assumed that soft outputs from channel decoder are independent identically distributed Gaussian random variables with known mean and variance. The Imperfect MMSE DFE using different modulation outperforms other turbo equalization algorithms of similar computational complexity in terms of bit-error rate. The achieved improvement is up to 3dB for severe frequency-selective channels [27].

In this chapter the contributions are as follows:

- The Imperfect MMSE DFE coefficients are obtained without assuming perfect feedback. The derived turbo equalizer reduces the computational complexity compared to the schemes proposed in [78, 82, 83].
- Finding the probability density function (pdf) of soft decision feedback symbols assuming that soft outputs from the SISO channel decoder are independent identically distributed (i.i.d.) Gaussian random variables.
- Results show that for time-invariant communication channels that exhibit severe ISI with different modulation schemes, the Imperfect MMSE DFE outperforms the Exact MMSE LE in [78, 82].

The rest of this chapter is organized as follows: Section 5.2 introduced the System Model for Iterative decoding with Imperfect MMSE DFE, Section 5.3 analysed the Proposed MMSE DFE with Imperfect feedback. In Section 5.4 results for the Proposed MMSE DFE with Imperfect feedback were carried out. Finally in Section 5.5, a summary of the chapter is presented. The work presented in this chapter is published in [27].

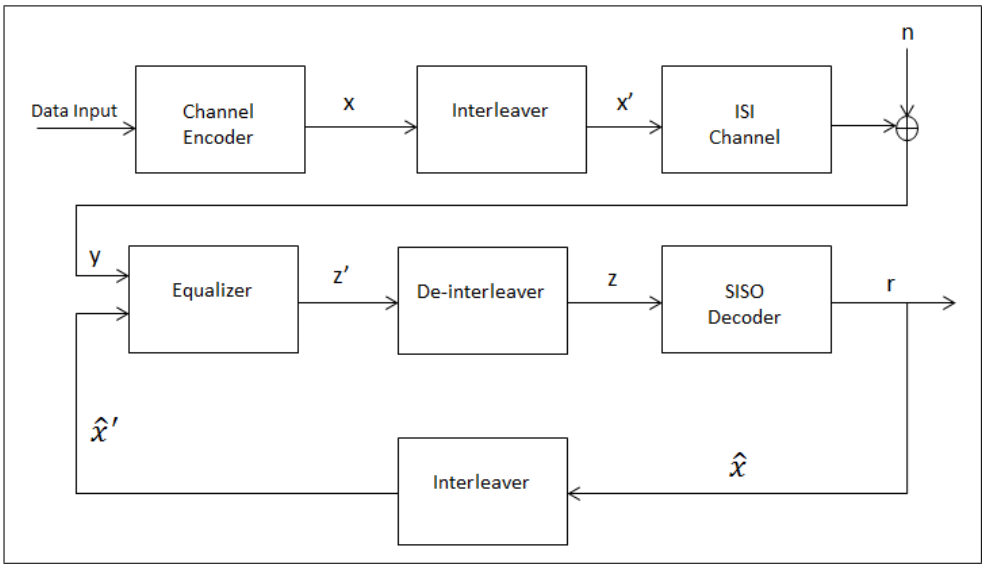

Figure 5.1: System Model for Iterative decoding with Imperfect MMSE DFE.

5.2 System Model for Iterative decoding with Imperfect MMSE DFE

The block diagram of the system model is shown in Figure 5.1. The binary information bits are encoded with Recursive Systematic Convolutional (RSC) channel encoder and code rate 1/2. The interleaved coded bits are modulated using different modulated scheme and the symbols are transmitted through the ISI channel. At the receiver, the received sequence $\mathbf{r}_k$ at the time instant k is given by

$$\mathbf{r}_k = \mathbf{H}\mathbf{x}_k + \mathbf{n}_k \tag{5.1}$$

where $\mathbf{H}$ is the Toeplitz channel impulse response matrix, $\mathbf{x}_k$ is the input vector of transmitted symbols. $\mathbf{n}_k$ is the vector of Additive White Gaussian Noise (AWGN) samples with covariance matrix $\sigma_{\mathbf{n}}^2\mathbf{I}$. The received sequence is equalized, deinterleaved, and decoded using the SISO decoder. The decoder finds soft outputs as log-probability ratios (LPRs) defined in [45] as:

$$\bigwedge(x_k)^{(n)} = \log \frac{p(x_k = 1|\mathbf{z}^n)}{p(x_k = 0|\mathbf{z}^n}, \tag{5.2}$$

where z is the soft outputs from the decoder. Once the Likelihood Probability Ratio (LPRs) are calculated, the expectations used at the following iteration are obtained as [63]

$$\hat{x}_k^n = \tanh \frac{\bigwedge^{(n)}(x_k)}{2} \tag{5.3}$$

To simplify Equation (5.3), *x* and *L* are used to replace $\hat{x}_k^n$ and $\bigwedge^{(n)}(x_k)$ respectively.

$$x = \tanh \frac{L}{2} \tag{5.4}$$

L is assumed to comply with gaussian probability distribution with mean and variance $\bar{L}$ and $\sigma^2_{L(n)}$ as referenced in [86]. The pdf of *x* can be represented as

$$f_x(x) = \frac{f_{L_1}}{|g'(L_1)|} + ... + \frac{f_{L_n}}{|g'(L_n)|} + ... \tag{5.5}$$

as in [87]. where L_n are the roots of the equation, $x = g(L)$, $g'(L)$ is the derivatives of $g(L)$, and f_L is the gaussian pdf of L. From equation (5.4) the only real root is

$$L_1 = \log \frac{1+x}{1-x} \tag{5.6}$$

and

$$g'(L) = \frac{d}{dL}[\tanh \frac{L}{2}] = \frac{2e^L}{(1+e^L)^2} \tag{5.7}$$

For long sequences, the LPRs at the output of the SISO decoders can be regarded as Gaussian random variables [86] and the Gaussian assumption about LPRs, the pdf of the soft decision feedback signal at iteration can be found. From equation (5.5) and taking into consideration (5.6) and (5.7), the pdf the random variable is given as

$$p(\hat{x}_k^{(n)} x_{k+1}) = \sqrt{\frac{2}{\pi\sigma^2_{L(n)}}} \frac{1}{1-(\hat{x}_k^{(n)})^2} \times \exp\left(-\frac{\left(log\left(\frac{1+x_k^{(n)}}{1-x_k^{(n)}}\right) - \bar{L}^{(n)} \right)^2}{2\sigma^2_{L(n)}} \right) \tag{5.8}$$

given that the coded symbol, x_k = +1, where $\bar{L}^{(n)}$ and $\sigma^2_{L(n)}$ are the mean value and the variance of LPRs at iteration.

5.3 Proposed MMSE DFE with Imperfect Feedback

The DFE consists of two linear filters, namely, feed-forward filter (FFF) and feedback filter (FBF). In previous work on the turbo DFE [88], the MMSE criterion has been considered as the optimization criterion in determining the equalizer coefficients. Based on the conventional perfect decision feedback assumption, a general expression for both MMSE DFE and MMSE IC coefficients can be written as

$$\mathbf{c} = \mathbf{W}_U^{-1}\mathbf{R}_k \tag{5.9}$$

$$\mathbf{s} = \mathbf{L}_D^H \mathbf{c} \tag{5.10}$$

where **c** and **s** are FFF and FBF coefficients, respectively, and is the k^{th} column of the channel matrix **L** related to the currently detected symbol. $\mathbf{W}_U$ and $\mathbf{L}_D$ are derived as follows. The received sequence is given as

$$\mathbf{r} = \mathbf{L}_U x + \mathbf{L}_D \mathbf{x} + \mathbf{n} \tag{5.11}$$

where $\mathbf{L}_U$ and $\mathbf{L}_D$ are the undecided and decided symbols respectively. The matrix $\mathbf{L}_D$ is obtained as $\mathbf{L}_D = \mathbf{L} - \mathbf{L}_U$, the error at the equalizer output is

$$e_k = x_k - (\mathbf{c}^L \mathbf{r} - \mathbf{s}^L \hat{x}) \tag{5.12}$$

substituting (5.11) into (5.12)

$$e_k = x_k - (\mathbf{c}^L \mathbf{L}_U \mathbf{x} + \mathbf{c}^L \mathbf{L}_D x + \mathbf{c}^L n + \mathbf{s}^L x - \mathbf{s}^L \mathbf{n}_b) \tag{5.13}$$

where $\mathbf{n}_b$ is the decision feedback error samples vector. The minimum square error is

$$\varepsilon = E[|e_k|^2] = \sigma_x^2 + \mathbf{c}^L \mathbf{W}_R \mathbf{c} + \mathbf{c}^L \mathbf{R}_D \mathbf{c} - 2\mathbf{c}^L \mathbf{L}_D \mathbf{s} + \mathbf{s}^L \mathbf{W}_b \mathbf{b} - 2\mathbf{c}^L \mathbf{R}_k \tag{5.14}$$

where $\mathbf{W}_U = \mathbf{L}_U \mathbf{L}_U^H + \sigma_n^2 I_L$, $\mathbf{W}_D = \mathbf{L}_D \mathbf{L}_D^H$, σ_x^2 is the average power of the received symbols, and can be normalised to 1 without the loss of generality. If the feedback errors are assumed to be independent identically distributed (i.i.d) random variables with variance σ_b^2, $\mathbf{W}_b = (1 + \sigma_b^2 \mathbf{I}_k)$, where $\mathbf{I}_k$ is the identity matrix.

Finding the gradients and set them to 0 results to

$$\nabla_c \varepsilon = \frac{\partial \varepsilon}{\partial c} = 2\mathbf{W}_R \mathbf{c} + 2\mathbf{W}_D c - 2\mathbf{L}_D b - 2\mathbf{h}_k = 0 \tag{5.15}$$

$$\nabla_{\mathbf{s}} \varepsilon = \partial \varepsilon \partial \mathbf{s} = 2\mathbf{W}_b b - 2\mathbf{L}_D^H \mathbf{c} = 0 \tag{5.16}$$

For low SNRs, the feedback error cannot be neglected, and a new solution that takes into account the error propagation is found as

$$\mathbf{c}^{(n)} = \left(\mathbf{W}_U + \frac{\sigma_{s(n)}^2}{1 + \sigma_{s(n)}^2} \mathbf{W}_D \right) \tag{5.17}$$

and

$$\mathbf{s}^{(n)} = \left(1 + \sigma^2_{s(n)}\right)^{-1} \mathbf{L}^L_D \mathbf{c} \tag{5.18}$$

where $\sigma^2_{s(n)}$ is the variance of the feedback error at iteration. The error is defined as the difference between correct and estimated symbols, hence , $e^{(n)}_k$ = x_k - $\hat{x}^{(n)}_k$. The FFF/FBF coefficients are recalculated once per each turbo iteration, which is in contrast to [78], where the coefficients are recalculated with every coded bit at each iteration of the second central moment using the pdf in (5.8), which yields

$$\sigma^2_{b(n)} = \int_{-1}^{1} (1 - \hat{x}^{(n)}_k)^2 p(\hat{x}^{(n)}_k | x_k = +1) d\hat{x}^{(n)}_k \tag{5.19}$$

simplify futher to

$$\sigma^2_{b(n)} \quad = \quad \sqrt{\frac{2}{\pi\sigma^2_{L(n)}}} \int_{-1}^{1} \frac{1 - \hat{x}^{(n)}_k}{1 + \hat{x}^{(n)}_k} \quad \times \quad \exp\left(- \frac{\left(log\left(\frac{1+x^{(n)}_k}{1-x^{(n)}_k} \right) - \bar{L}^{(n)} \right)^2}{2\sigma^2_{L(n)}} \right) \tag{5.20}$$

Here we estimate the error variance over the whole frame while typically symbol-wise estimates are used. The FFF at all iterations is fed by the received sequence r_k. The output of the DFE at iteration can be represented as

$$z\prime^{(n)}_k = (\mathbf{c}^{(n)})^{\mathbf{L}} \mathbf{r}_k - (\mathbf{s}^{(n)})^{\mathbf{L}} \hat{\mathbf{x}}^{(n)}_k \tag{5.21}$$

At the first iteration, the DFE is implemented and is calculated using (5.9) and (5.10), and $\hat{x}^{(1)}_k$ is a vector containing past hard decisions taken directly from the output of the DFE. At higher iterations (n $>$ 1), and $\mathbf{c}^{(n)}$ and $\mathbf{s}^{(n)}$ are calculated using (5.17) and (5.20). $\bar{x}^{(n))}_k$ and is a vector containing expectations from the previous iteration (n - 1) according to (5.7). Equations (5.17) and (5.18) represent MMSE solution when the feedback error is modeled according to (5.20). It is the property of the MMSE solution [87, 89, 90] that is unique and that makes all other values for the FFF and FBF coefficients different from MMSE ones.

Consequently, the conventional MMSE DFE with the coefficients obtained according to (5.9) and (5.10) (assuming perfect feedback) produces a MSE that is always $\varepsilon \geq \varepsilon$MMSE, and the equality holds if and only if $\sigma^2_{s(n)}$ = 0.

5.4 Simulation Results for Proposed MMSE DFE with Imperfect feedback

The simulation results show improvement with the Imperfect MMSE DFE. The ISI channel considered here has the channel impulse response of $h = [0.04, -0.05, 0.07, -0.21, -0.5, 0.72, 0.36, 0, 0.21, 0.03, 0.07]^T$ in [53], Generator polynomial is [7, 5]. The results are obtained from an 8 state recursive systematic convolutional channel code. Coded bits are modulated using BPSK, QPSK, and 8PSK. The FFF taps is N = 10, while FBF is 6 taps long at first iteration and 15 at higher iterations.

The encoded bits are interleaved by random interleaver of size L = 4096 bits. The Soft output Viterbi algorithm (SOVA) [45] has been used in the SISO decoder. Figure 5.2 shows the BER performance for proposed Imperfect DFE, the Exact MMSE LE used in [82] and the conventional DFE MMSE algorithm for BPSK modulation. The proposed scheme has 0.4dB gain over the Exact MMSE LE and 3dB over conventional DFE. In Figure 5.3 Imperfect MMSE DFE gains 0.7dB for QPSK Modulation. At 8PSK modulation, the proposed method gains 1dB over Exact MMSE LE shown in Figure 5.4. As the symbol rate increases, the Imperfect DFE seems to perform better.

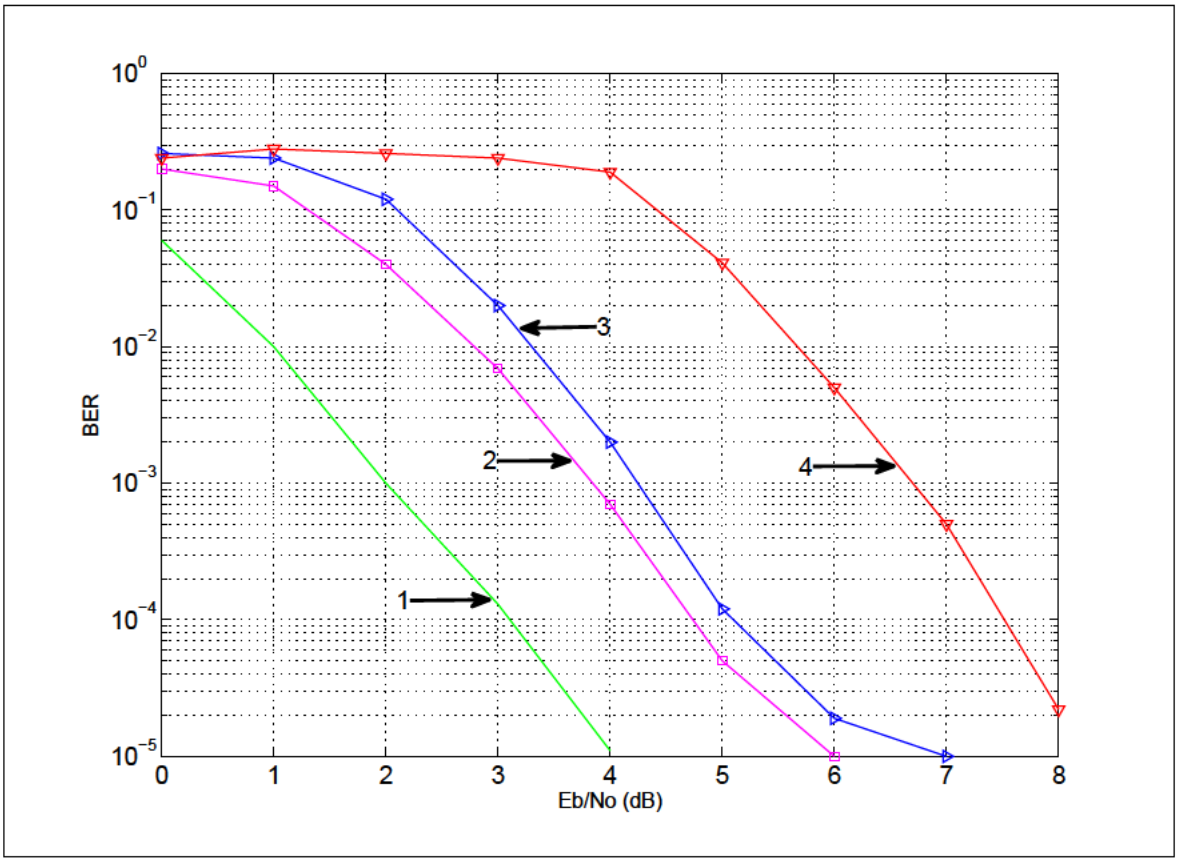

Figure 5.2: BER comparisons for different MMSE turbo equalization algorithms for BPSK.

1. No ISI
2. Proposed Imperfect MMSE DFE
3. Exact MMSE LE used in [82]
4. MMSE DFE (Conventional)

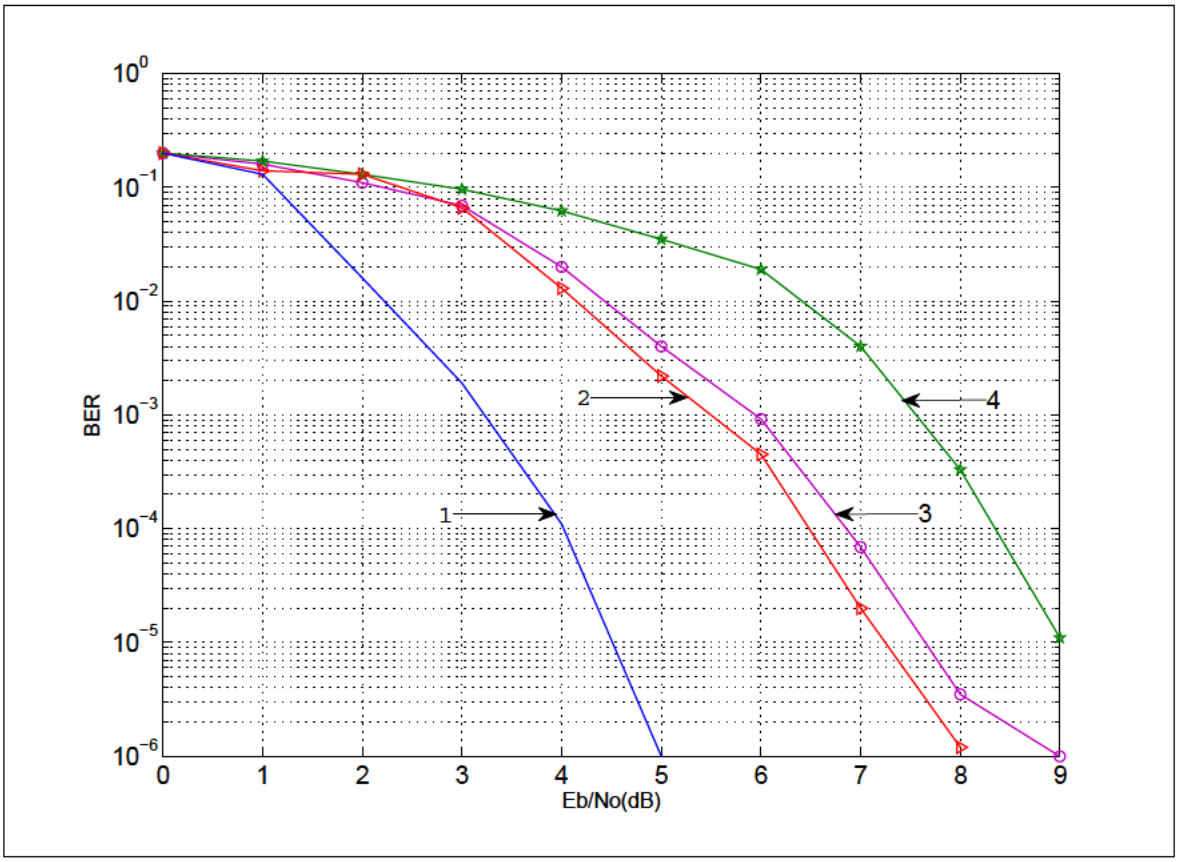

Figure 5.3: BER comparisons for different MMSE turbo equalization algorithms for QPSK.

1. No ISI
2. Proposed Imperfect MMSE DFE
3. Exact MMSE LE used in [82]
4. MMSE DFE (Conventional)

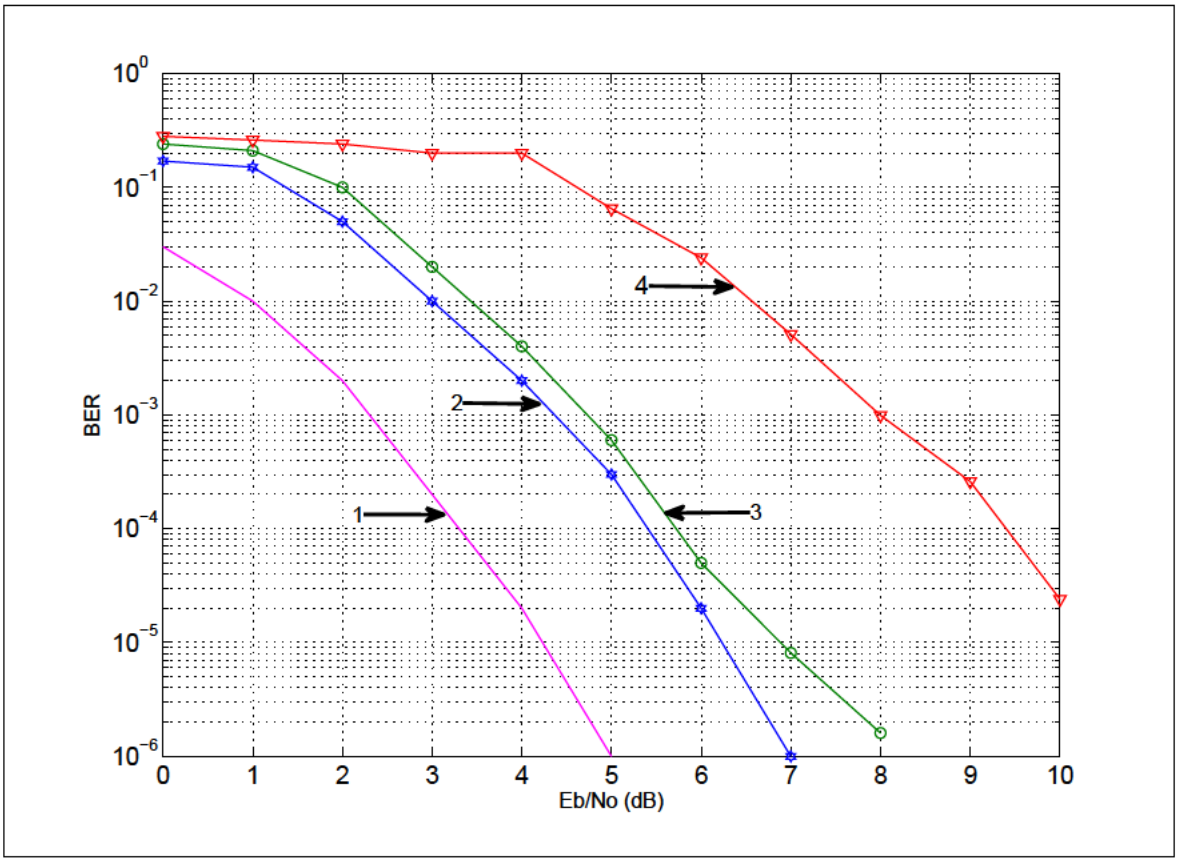

Figure 5.4: BER comparisons for different MMSE turbo equalization algorithms for 8PSK.

1. No ISI

2. Proposed Imperfect MMSE DFE

3. Exact MMSE LE used in [82]

4. MMSE DFE (Conventional)

5.5 Summary

This chapter analyzed the performance of Imperfect MMSE DFE with different modulation schemes. The Imperfect algorithm does not use the conventional assumption of a perfect feedback but takes into account the feedback error propagation. The obtained simulation results for different modulation schemes in the presence of severe interference achieved better BER performance in comparison to the Exact MMSE LE and the conventional MMSE DFE.

At lower signal to noise ratio Decision feedback equalizer performs poorly when compared to linear equalization because of the feedback errors. Next chapter examined a prefiltering method where an All-pass Filter is employed at the receiver before equalization to create a minimum phase overall impulse response.

Chapter 6

Enhanced Equalization for Mobile Communication Systems

6.1 Introduction

Mobile communications systems suffer from multipath propagation and fading which cause ISI and decrease system performance. In high-rate digital transmission over dispersive channels, the received signal is impaired by intersymbol interference (ISI) and additive noise. Equalization at the receiver side is necessary in order to obtain reliable estimates of the transmitted symbols. It is well known, that the optimum equalization algorithm is given by maximum- likelihood sequence detection (MLSD) [73], which can be realized in a recursive manner using the Viterbi algorithm (VA).

However, for channels with large delay spread, long impulse responses, and transmission using nonbinary signal alphabets, a very high complexity may result for the VA, and suboptimum schemes have to be considered for a practical implementation. Potential candidates are decision feedback equalization (DFE), delayed decision feedback sequence estimation (DDFSE) [91], reduced state sequence estimation (RSSE) [92], the M-algorithm [93], and various members of the family of sequential decoding algorithms like the Fano algorithm or the stack algorithm [93].

The Decision feedback equalizer (DFE) is an important component in many digital communication receivers and is used to suppress ISI caused by dispersive propagation channels [94, 95], as well as reject in-band interference [96–99]. The DFE incorporates a feedforward filter that operates on the received signal to suppress precursor ISI, with a feedback filter that operates on previously detected channel symbols to suppress postcursor ISI. The DFE generally outperforms the traditional linear equalizer, particularly if the channel has deep spectral nulls in its response [96]. However, degradation in DFE performance occurs when incorrectly detected symbols are fed through the feedback filter. Then instead of mitigating ISI from the cursor sample, the DFE enhances ISI.

Error propagation may cause bursts of decision errors and a corresponding increase in the average probability of bit and symbol error. Moreover, the bursty nature of DFE errors has implications for error correction coding and interleaver depth that may be incorporated into the receiver design [100–107]. Also, high-order modulation formats may be more susceptible than low-order formats.

Therefore, a need exists to quantify DFE performance in the presence of decision

error feedback and to mitigate the effects of error propagation. Various techniques for mitigating error propagation have also been proposed. Large taps in the feedback filter of an equalizer designed using the minimum mean-square-error (MSE) criterion because significant self-generated ISI if decision errors are made [108].

Due to highly dispersive channels, ISI is a common problem in telecommunication systems, such as terrestrial television broadcasting, digital data communication systems, and cellular mobile communication systems [109]. The main reasons for the ISI are of high-speed transmission and multipath fading. In such systems, the channel impulse response can span tens or even hundreds of symbol periods [26], [110].

The conventional approach to turbo equalization uses a soft-input soft output (SISO) equalizer based on the forward–backward algorithm of Bahl, Cocke, Jelinek, and Raviv (BCJR) [25], but the computational complexity of this algorithm increases exponentially with the channel memory. This has motivated the development of reduced-complexity alternatives to the BCJR equalizer, such as the soft interference cancellers proposed in [63, 78, 88, 111–113]. These structures use a linear filter to equalize the received sequence.

A prefiltering method is considered in this work where an All-pass Filter is employed at the receiver before equalization to create a minimum phase overall impulse response. In the presence of ISI, the All-pass Filter concentrates the maximum symbol energy in the correct sampling instances and subsequently cancel the non causal precursor ISI by replacing the samples and channel by their minimum phase equivalent [30]. The use of All-pass Filtering is beneficial to the performance of a communication receiver that operates in a dispersive multipath propagation environment and thereby improves capacity.

Secondly, a low complexity soft feedback Equalizer Interference canceller (SFEIC) is proposed based on filtering and cancellation of residual ISI. However, unlike the interference cancellers of [31, 63, 78, 88, 111–113], the SFEIC uses a structure similar to a decision-feedback equalizer (DFE), combining the equalizer outputs and a priori information to form more reliable estimates of the residual postcursor ISI.

As in [78, 111–113], the equalizer coefficients are computed so as to minimize the MSE between the equalizer output and the transmitted symbol. However, the coefficients

of the minimum-MSE (MMSE) structures in [78, 111–113] have to be computed for every symbol, even when the channel is static, resulting in a per-symbol complexity that is quadratic in the length of the equalizer.

The proposed Soft Feedback Equalizer Interference Canceller (SFEIC) combines the equalizer outputs and a priori information to form more reliable estimates that perform successive interference cancellation. The receiver performs soft output decisions, achieved by a soft-input soft-output (SISO) detector and a SISO channel decoders, through an iterative process [31].The results presented shows that the proposed SFEIC BER perform well compared with MAP equalizer and outperform the conventional MMSE decision feedback equalizer.

The main contribution in this chapter is summarized as follows:

- The capacity of the dispersive multipath propagation channel was enhanced by using a prefilter at the receiver before equalization.
- The proposed low complexity soft feedback Equalizer Interference canceller (SFEIC) that combines the equalizer outputs and a priori information to form more reliable estimates and perform successive interference cancellation.

The rest of this chapter is organized as follows: System Model for Enhanced Equalization is shown in Section 6.2. The proposed method using All-pass Filter is described in Section 6.3. Performance results for the proposed Enhanced Equalization are in Section 6.4, Section 6.5 describes the Channel Model for Interference Cancellation Using Iterative Equalization. The proposed Soft-Feedback Interference Canceller Algorithm is analysed in section 6.6. Simulation Results for Interference Cancellation Using Iterative Equalization is in Section 6.7. Finally in Section 6.8, a summary of the chapter is presented. The work presented in this chapter has been published in [30, 31].

6.2 Proposed System Model for Enhanced Equalization

Figure 6.1 shows the discrete-time equivalent baseband transmission model used in this work. A sequence of binary source symbols **u** is fed in and protected by a convolutional

encoder. Interleaved to overcome fast fading, the encoded symbols are modulated over a frequency selective fading channel. In order to facilitate calculations, it is assumed that the channel is time-invariant and the receiver has perfect knowledge of the channel impulse response (CIR). The coefficients of the overall impulse response are given by $h = [h[0] \quad h[1]\ldots h[qh-1]]^T$. The received signal sample at times *kT* in the output of the receiver is given by

$$\mathbf{r}[k] = \sum_{v=0}^{qh} \mathbf{h}[v]\mathbf{a}[k-v] + \mathbf{n}[k] \tag{6.1}$$

where $h[v]$ denotes the discrete-time overall impulse response of the filter, channel and received input filter $h[v]$ is assumed to be causal and finite order *qh*. The FIR transfer function *P(z)* is given by

$$\mathbf{r}[k] = \sum_{v=0}^{qh} \mathbf{h}[v]z^{-v} \tag{6.2}$$

n[k] is the discrete-time white Gaussian noise with power spectral density N_0. Any phase compensation is done by the All-pass Filter. The All-pass Filtering does not change the channel length or the channel energy. The estimated bits are produced by channel decoding.

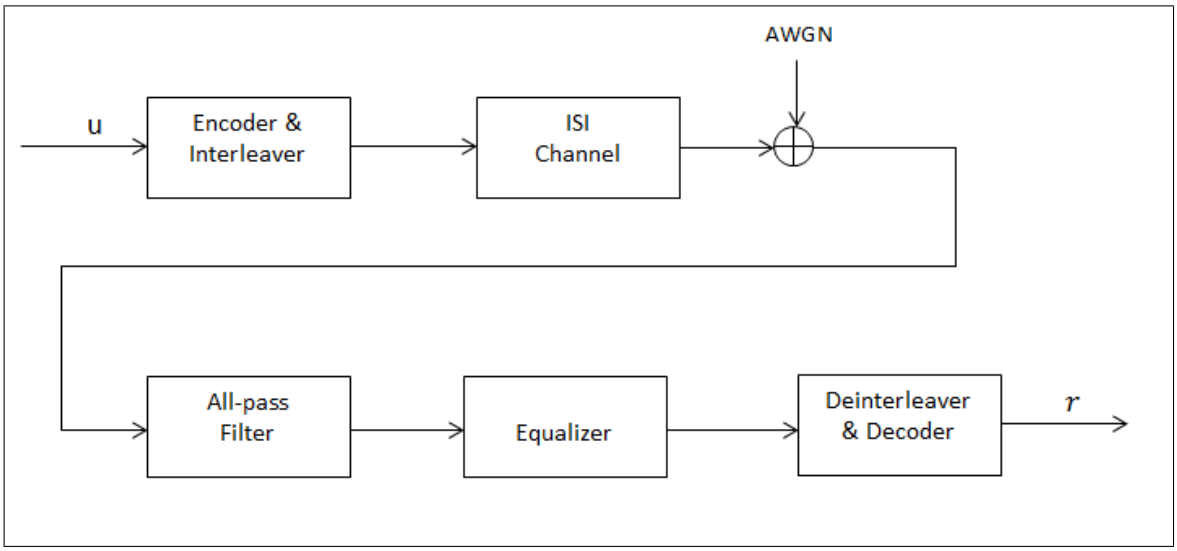

Figure 6.1: System Model for Enhanced Equalization

6.3 Proposed Method using All-pass Filter

In order to obtain high performance, the All-pass Filter transforms the CIR to their minimum-phase equivalent which has their energy concentrated in the leading taps essential for Equalization. Therefore, a discrete- time prefilter, which is an All-pass Filter, is introduced in front of equalization in order to transform the channel impulse response (CIR) into its minimum-phase equivalent. For a practical implementation, a finite impulse response (FIR) approximation is of interest and minimum mean-squared error (MMSE) LE feedforward filter is suited. However in general the transfer function P(z) is a mixed phase transfer function. The ideal All-pass Filter generating the minimum phase equivalent of *P(z)* which is denoted by G(z). Thus

$$P\min(z) = G(z).P(z) = \sum_{v=0}^{qh} h\min[v]z^{-v} \tag{6.3}$$

$$P\min(z).P^*\min(1/z^*) = P(z).P^*(1/z^*) \tag{6.4}$$

$$G(z) = \frac{Pmin(z)}{P(z)} \tag{6.5}$$

Equation(6.5) defines an allpass transfer function. $P\min(z)$ can be calculated by spectral factorization, rooting and prediction error filter. For the computation of All-pass Filter, equation (6.5) is equivalent to:

$$\frac{P\min(z)}{P(z)} = \frac{P^*(1/z^*)}{P^*\min(1/z^*)} \tag{6.6}$$

comparing equation(6.5) and (6.6). It is observed that allpass transfer function for transformation of the channel into its minimum phase equivalent is equal to

$$G(z) = \frac{P^*(1/z^*)}{P^* \min(1/z^*)} \tag{6.7}$$

It can be seen that in equations (6.7) the All-pass Filter consist of a matched filter, matched to the discrete time channel impulse response, and a second part $\frac{1}{P^* \min(1/z^*)}$. By approximating the second part, the allpole transfer function $A_2(z)$ by an FIR filter $F_2(z)$.

$$F_2(z) \approx c\frac{1}{P^* \min(1/z^*)} \tag{6.8}$$

where constant c$\neq$ 0.

$$F_2(z) = A^*(1/z^*) \tag{6.9}$$

However, the transfer function for G(z) is proposed to be:

$$A(z) = 1 - S(z) \tag{6.10}$$

where S(z) is the prediction filter denoted as:

$$1 - S(z) = 1 - \sum_{v=1}^{qp} p[v]z^{-v} \tag{6.11}$$

is the prediction error filter of the order *qp* for a random process with power spectral density. The prediction filter S(z) is designed for minimization of the output power of the error filter. The optimum coefficients for minimization of the power of the error filter are given by the solution of Yule-walker equation [114].

$$\Phi s = \psi \tag{6.12}$$

where Φ is the autocorrelation of the sequence

$$\Phi = \begin{bmatrix} \psi[0] & \psi[-1] & \cdots & \psi[-(qp-1)] \\ \psi[1] & \psi[0] & \cdots & \psi[-(qp-2)] \\ \vdots & \vdots & \ddots & \vdots \\ \psi[(qp-1)] & \psi[(qp-2)] & \cdots & \psi[0] \end{bmatrix} \tag{6.13}$$

$$\mathbf{s} = [s[1] \quad s[2] \quad ... \quad s[qp]]^T \tag{6.14}$$

where **s** is the coefficient vector of the predictive filter.

$$\psi = [\psi[1] \quad \psi[2] \quad ... \quad \psi[qp]]^T \tag{6.15}$$

$$\psi[k] = h[k] * h^*[-v] \tag{6.16}$$

where $(.)^T$ and * denote transposition and convolution respectively. The computational complexity of the proposed method is moderate, because equation (6.12) can be solved by Levinson Derbin algorithm [114]. So the allpass prefilter looks like the following:

$$G(z) = z^{(qh+qp)}.P^*(1/z^*).(1 - S^*(1/z^*) \tag{6.17}$$

where *qh* is the length of the channel impulse response.

6.4 Simulation Results for Enhanced Equalization for Mobile Communication Systems

In this section the performance of the proposed system based on different equalizers is compared. For channel coding a rate ½ recursive systematic convolutional code with memory 5 and with octal generator polynomials [23, 35] is used. The performance is evaluated for transmission over a time invariant worst case channel of h[n] = 0.227[n] + 0.46[n-1] + 0.688[n-2] + 0.46[n-3] + 0.227[n-4] from [53] for 8PSK, 16QAM and 64QAM modulation schemes.

It was assumed that the channel parameters are known to the receiver, and that the error control decoder is implemented using the BCJR algorithm. Before transmission the coded bits were interleaved by a random interleaver for size L= 2048bits. Figure 6.2 shows the performance gain of the proposed algorithm in term of BER at 10^{-4} for the 8PSK modulation scheme.

Prefiltering technique has an advantage of about 0.5dB over the conventional DFE. While retaining approximately the same complexity, a gain of about 0.7dB compared to the DFE algorithm is observed in Figure 6.3. With All-pass Filtering, fast convergence is observed for all considered modulation schemes. In Figure 6.4, there is a significant

improvement of 1.4dB gain over DFE mainly because of error propagation by the feedback loop as the symbol rate increases. Prefiltering techniques can improve equalizer performance.

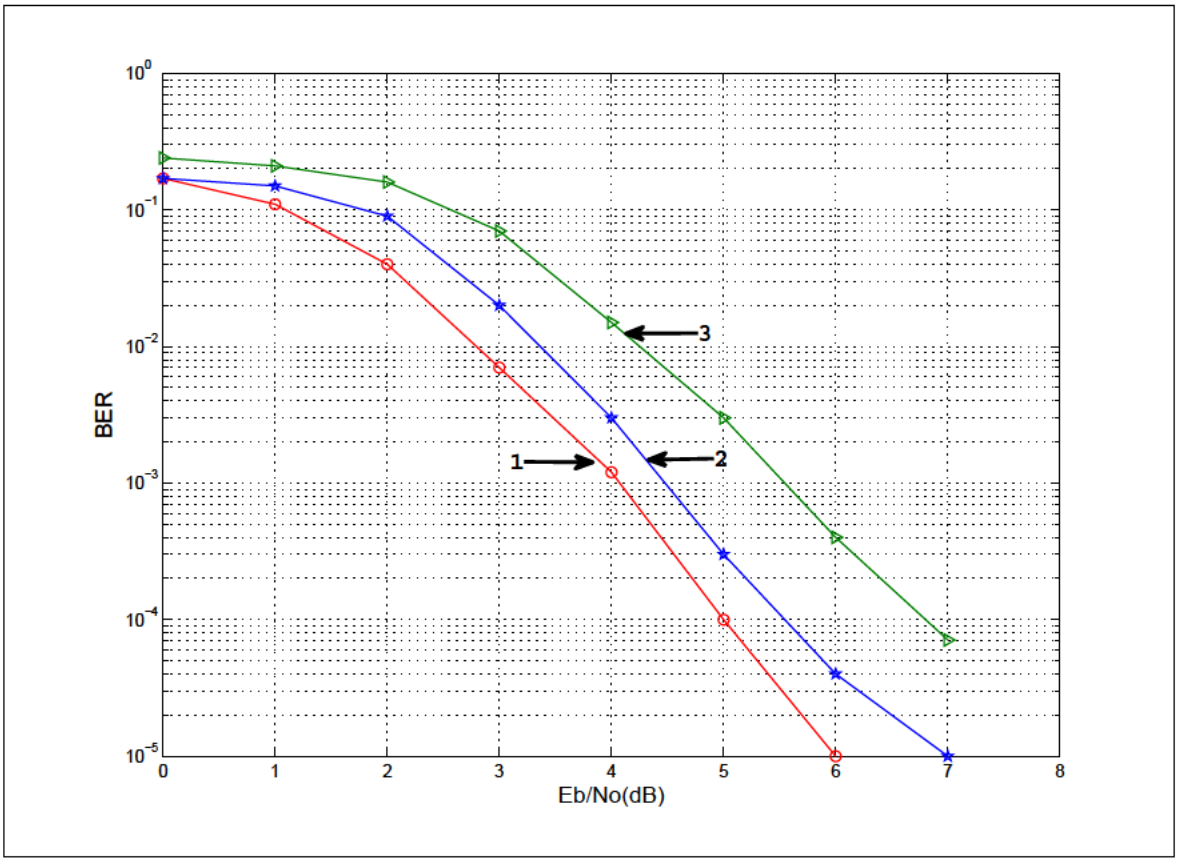

Figure 6.2: BER comparisons for different equalization algorithms for for 8PSK.

1. Using Proposed Allpass filter
2. Conventional DFE
3. Conventional Linear Equalizer

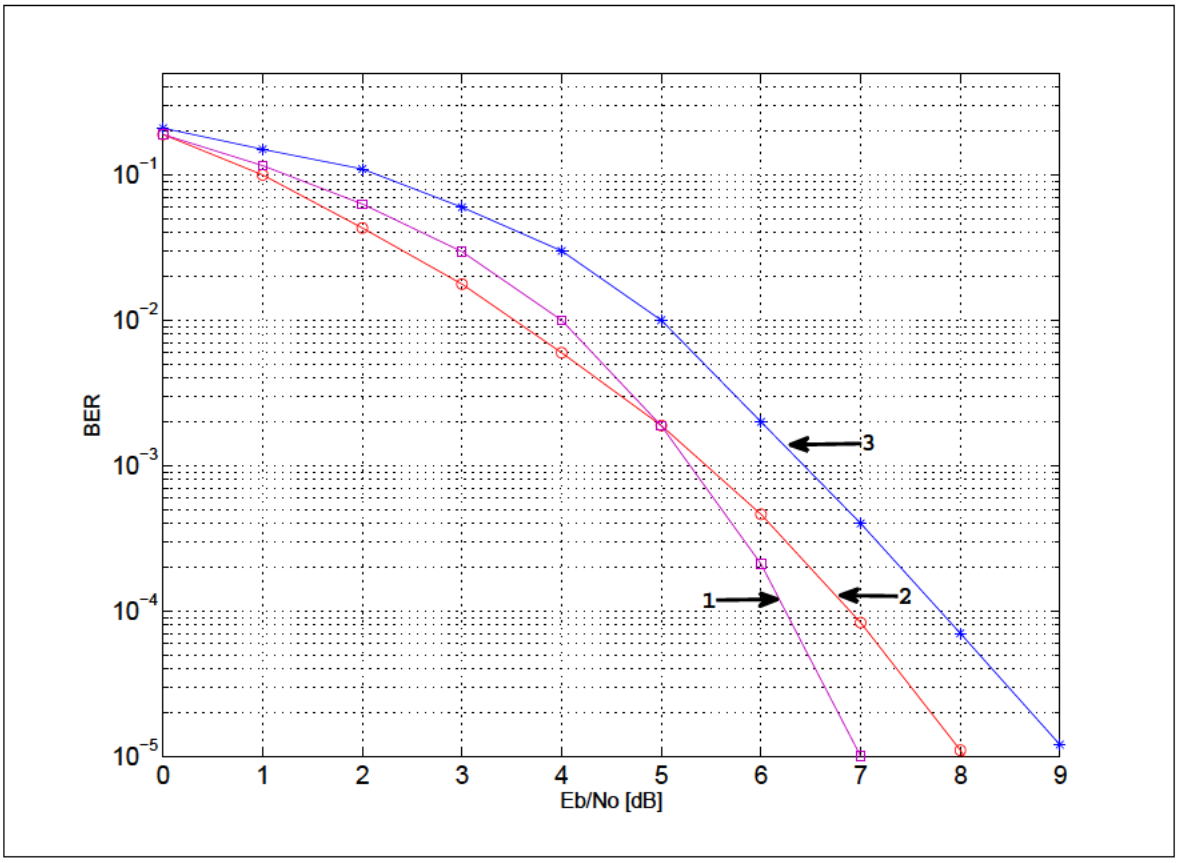

Figure 6.3: BER comparisons for different equalization algorithms for 16QAM.

1. Using Proposed Allpass filter
2. Conventional DFE
3. Conventional Linear Equalizer

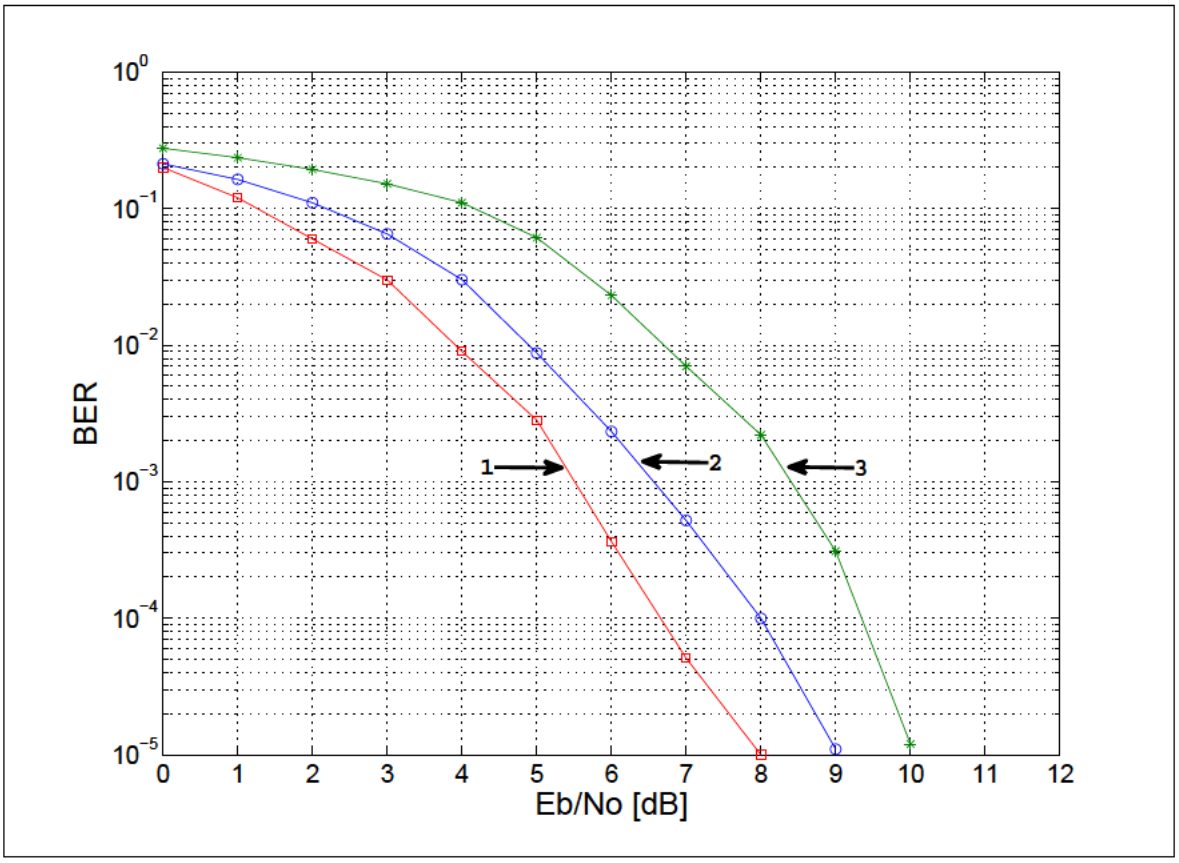

Figure 6.4: BER comparisons for different equalization algorithms for 64QAM.

1. Using Proposed Allpass filter
2. Conventional DFE
3. Conventional Linear Equalizer

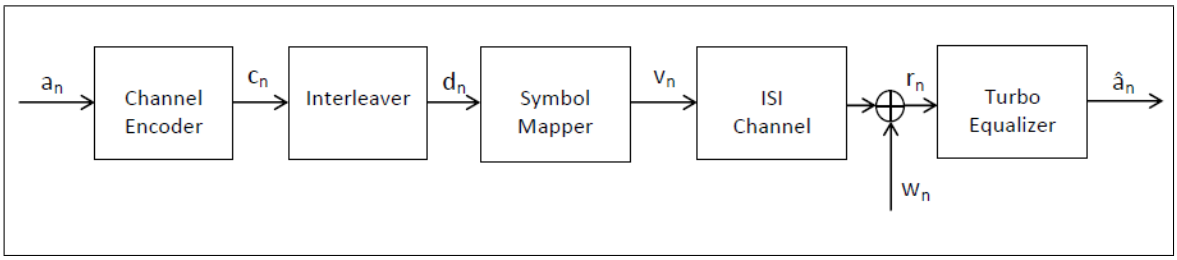

Figure 6.5: Channel model for Interference Cancellation Using Iterative Equalization

6.5 Interference Cancellation using Iterative Equalization for Communication Networks.

6.5.1 Channel Model for Interference Cancellation using Iterative Equalization.

The channel model for this system is depicted in Figure 6.5. The transmission of the sequence of interleaved coded symbols v_n through a channel whose output is given by

$$\mathbf{r}_n = \sum_{l=0}^{K} \mathbf{h}_l \mathbf{v}_{n-1} + \mathbf{w}_n \tag{6.18}$$

The channel model can be written as: $\mathbf{r}[n] = \mathbf{h}_l \mathbf{v}[n] + \mathbf{w}[n]$, where $\boldsymbol{h}$ is the channel impulse response and the channel response is given as:

$$\begin{bmatrix} h[K_2] & \cdots & h[-K_1] & \cdots & 0 \\ 0 & h[K_2] & \cdots & h[-K_1] & 0 \\ & & \vdots & & \\ 0 & \cdots & h[K_2] & \cdots & h[-K_1] \end{bmatrix} \tag{6.19}$$

and the signal vectors are given as

$\mathbf{r}[n] = [r[n–N_1 \ldots r[n] \ldots r[n+N_2]]^T$,

$\mathbf{v}[n] = [v[n-N_1–K_2] \ldots v[n] \ldots [v[n–N_2–K_1]]^T$,

$\mathbf{w}[n] = [w[n–N_1] \ldots w[n] \ldots w[n+N_2]]^T$.

where h_1 is the channel impulse response with channel ISI length K, and $\mathbf{w}_n$ is additive white Gaussian noise with variance σ^2. The modulation scheme used is quadrature phase-shift keying (QPSK) and 8PSK. As a result of the interleaving, the priors generated

by the equalizer can be assumed to be independent of those generated by the other equalizer for a certain number of iterations. Both the equalizer and the decoder employ the optimal symbol by symbol Maximum A-Posteriori (MAP) soft input soft output (SISO) algorithm [25, 71, 76].

Soft input symbols are fed into the decoder from a sampled receive filter stream r_n and hard decisions are produced as the last output. It is possible to equalize and decode in an iterative manner that is similar to turbo decoding. The equalizer provides soft outputs reliability information on the coded bits for the channel decoder. The soft information on the bit c_k is usually given as a log-likelihood ratio (LLR) same method used in chapter two.

$$LLR(c_k) = log\frac{P(ck = +1|r)}{P(ck = -1|r)} \tag{6.20}$$

This is the ratio between the conditional bit probabilities in the logarithmic domain. These LLR values are deinterleaved and given for the channel decoder, which uses them to recover the information bits $\mathbf{a}_n$ shown in Figure 6.5.

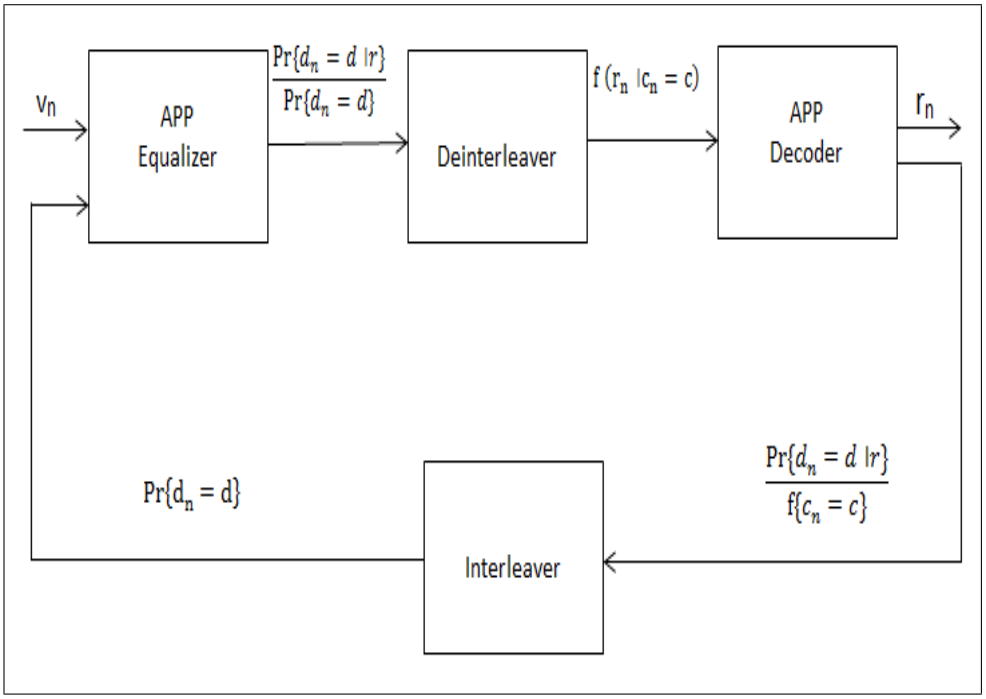

Figure 6.6: The Iterative Structure for Interference Cancellation Using Iterative Equalization

6.6 The Soft-Feedback Equalizer Interference Canceller Algorithm.

Figure 6.5 shows the block diagram of the proposed SFEIC. The received sequence $\mathbf{r}_n$ and prior probability of each transmitted bits are filtered by the linear filter whose output contain residual ISI. The equalizer estimates and uses the a priori information for of the interfering symbols, previous equalizer outputs to cancel the residual ISI. To perfectly cancel the interference, the energy of the transmitted signal $\mathbf{v}_n$ given in (6.18) is received in $K+1$ sample as $r_n, r_{n+1}, ……..., r_{n+K}$, $r_n = h_0 v_n + h_1 v_{n-1} + w_n$, $r_{n+1} = h_0 v_{n+1} + h_1 v_n + w_{n+1}$, collect all the energy for v_n into a single sample as:

$$x_n = \sum_{k=0}^{K} h_k^* r_{n+k} \tag{6.21}$$

$x_n = v_n + h_0^* h_1 v_{n-1} + h_0^* h_1 v_{n+1} + h_0^* h_1 w_n + h_0^* h_1 w_{n+1}$

Thus

$$x_n = v_n + \sum_{k=1}^{K} q_k^* v_{n+k} + \sum_{k=1}^{K} q_k^* v_{n-k} + w_n' \tag{6.22}$$

where $q_k = \sum_{l=k}^{K} f_l h_{l-k}^*$ and
$w_n' = \sum_{k=0}^{L} h_k^* w_{n+k} x_n$, is been interfered by $v_{n-K}, ….., v_{n-1}, v_{n+1}, …., v_{n+L}$ if all $v_m | m \neq n$ are known then ISI can removed from x_n. let

$$z_n = x_n + \sum_{k=1}^{K} q_k^* v_{n+k} + \sum_{k=1}^{K} q_k^* v_{n-k} + w_n' \tag{6.23}$$

$$z_n = v_n + w_n' \tag{6.24}$$

where w_n' is colored Gaussian noise with variance N_0. Interference cancellation (IC) requires the knowledge of $v_{n-K}, ….., v_{n-1}$ and $v_{n+1}, …., v_{n+K}$.$v_{n+1}, …., v_{n+K}$ correspond to the future decisions. A feedback equalizer can be used for $v_{n-K}, ….., v_{n-1}$ to cancel the interference in $\mathbf{r}_n$. SFEIC use soft-output decoder for the convolutional codes such as the a posteriori probability (APP) algorithm to compute the code symbol $Pr\{c_n = c|r\}$, from (6.23).

Extrinsic information is passed between the equalizer and the decoder as shown in Figure 6.6. $\bar{v}_n$ is the soft symbol generated from the APP algorithm. Using recursive

updates to compute the equalizer coefficients, the complexity of the SFEIC algorithm can be reduced to, at most, $O(K^2)$ where K is the length of the channel, while MAP detection are exponential in the channel length. In addition, the complexity of the MMSE equalizers employed in the SFEIC algorithm does not increase with higher order symbol constellations, while the complexity of MAP detection grows with the size of the symbol constellation.

6.7 Simulation Results for Interference Cancellation using Iterative Equalization.

The simulation results compare the proposed method with some of already exiting algorithms, the information data were coded a ½ rate recursive systematic convolutional code encoder with parity generator polynomials [23, 35] expressed in octal form. Turbo equalizer performance was evaluated for QPSK and 8PSK signalling schemes with several discrete equivalent channel responses. Before transmission, the coded bits were interleaved by a random interleaver of size N = 4096 bits.

The MMSE filter parameters were set to $M_1 = 12$ and $M_2 = 9$. Three time-invariant ISI channels in [53] were used given as

$\mathbf{H}_A = [0.04, -0.05, 0.07, -0.21, -0.5, 0.72, 0.36, 0, 0.21, 0.03, 0.07]^T$,

$\mathbf{H}_B = [0.407, 0.815, 0.407]^T$, and

$\mathbf{H}_C = [0.227, 0.46, 0.688, 0.46, 0.227]^T$.

The BER of an iterative equalizer depends upon the channel profile, modulation scheme, the encoder constraint length and also the size of the interleaver. Figure 6.7 demonstrates the effect of changing the channel delay spread with fixed modulation scheme with the proposed algorithm. Figure 6.7 shows the performance of the three channels in comparison for a channel with no ISI.

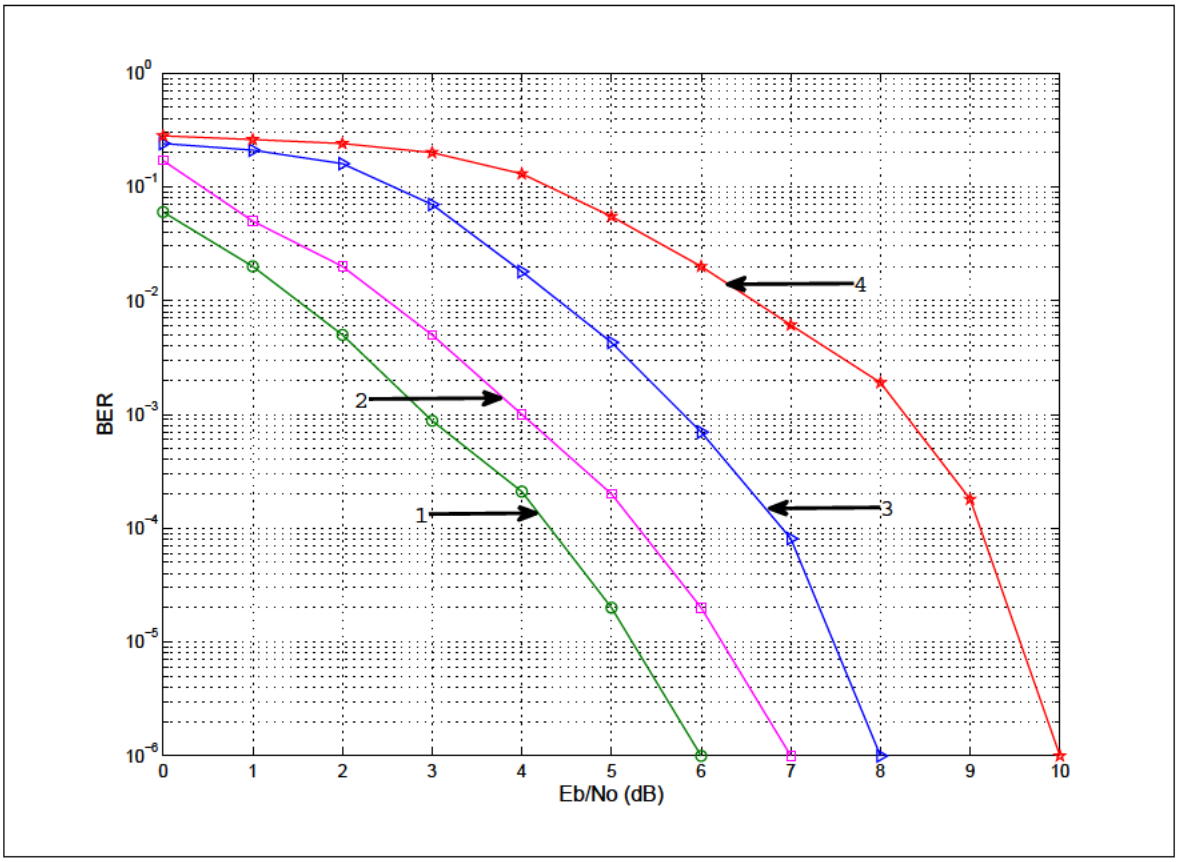

Figure 6.7: BER performance for Proakis Channel A, B and C using QPSK Modulation.

1. No ISI
2. Proakis Channel A used in [53]
3. Proakis Channel B used in [53]
4. Proakis Channel C used in [53]

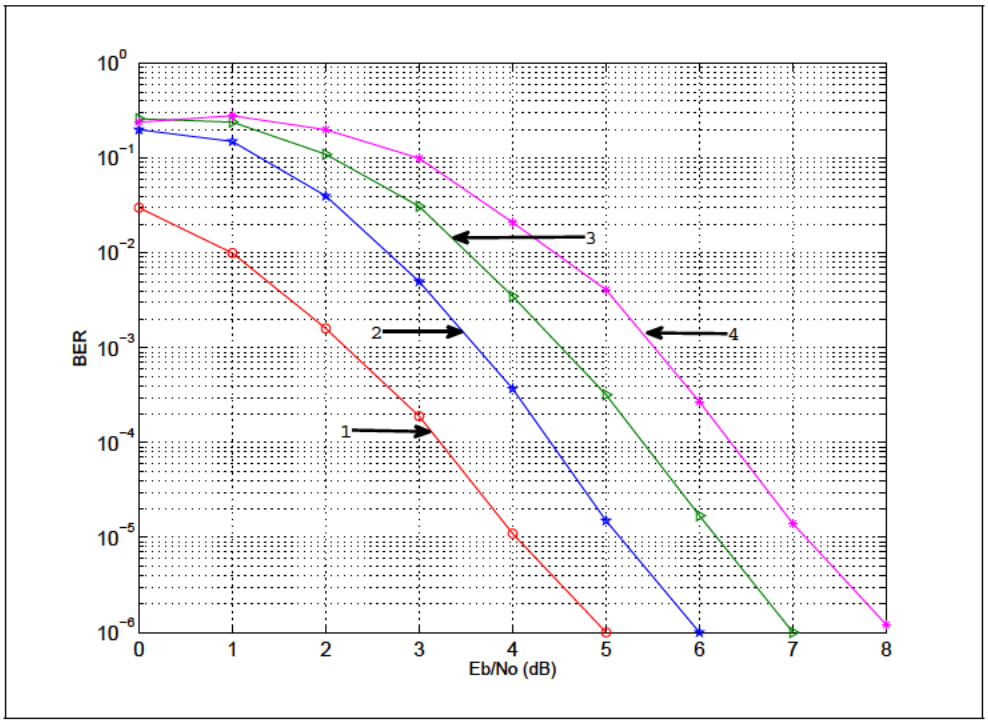

Figure 6.8: BER results comparing the performance of various turbo equalization algorithms using QPSK modulation.

1. No ISI
2. MAP Detector
3. Proposed SFEIC System using Proakis Channel A in [53]
4. Conventional MMSE DFE

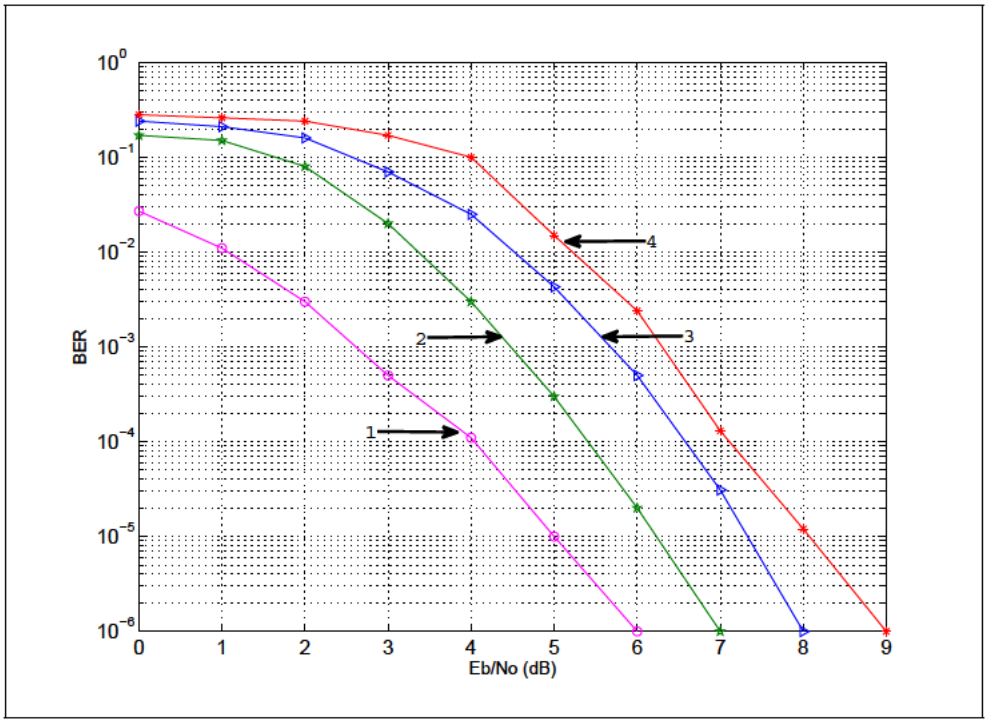

Figure 6.9: BER results comparing the performance of various turbo equalization algorithms using 8PSK modulation.

1. No ISI

2. MAP Detector

3. Proposed SFEIC System using Proakis Channel A in [53]

4. Conventional MMSE DFE

For BER target at 10^{-5}, Channel A is a good channel with only mild ISI, 1dB away from the No ISI bound, Channel B has medium ISI, 2.5dB and channel C has the worst and severe ISI, about 4.2dB from the bound. The performance of the proposed algorithm, MAP and conventional MMSE DFE are summarized in Figure 6.8 and Figure 6.9 using Prokis Channel A delay spread. At BER 10^{-5} in Figure 6.8, the SEFIC performs significantly better than the MMSE DFE for low SNR.

The SFEIC achieves 0.8dB gain over MMSE DFE equalizer and 1.0dB away from the maximum-likelihood decoding which have exponential complexity. For 8PSK modulation in Figure 6.9, it achieves better BER performance delivering it SNR gain of 0.6dB relative to MMSE DFE and 1.1dB from MAP. These results indicate that SFEIC algorithm may provide a practical means for obtaining significant performance gains for variety of

communication applications.

6.8 Summary

The results demonstrated that incorporating an All-pass Filter before equalization in the receiver is an effective method of controlling error propagation. The structure of the All-pass Filtering by using the Yule-Walker equations to calculate the channel impulse response and the prediction error with less computational complexity is analyzed. It turns out that a discrete time prefitering which creates a minimum phase impulse response is a favourable tradeoff between performance and complexity.

The SFEIC approach yields a comfortable gain compared to the conventional MMSE DFE equalization and decoding. It is shown that SFEIC is suitable for low complexity Turbo equalization using higher order signal standard. Compared with the existing method, the proposed method achieves considerable performance improvement without increasing complexity. The next chapter is about Minimization of Channel Impulse Noise using Digital Smear Desmear filter.

Chapter 7

Minimization of Channel Impulse Noise using Digital Smear Filter

7.1 Introduction

The objective at the receiving end of a data link is to be able to distinguish the noise from the signal energy by some detection process. In many data transmission systems, amplitude detection at the receiver is used. If the noise introduced into the channel is impulsive in nature, hence, has high amplitude for a short duration, it will mask the detection process unless the noise amplitude is reduced significantly before detection by some means [115].

The performance evaluation of communication systems has traditionally relied on the assumption of an additive Gaussian noise channel. However, in numerous circumstances this assumption is not always justifiable and the communication medium can be more accurately modelled by heavy-tailed, non-Gaussian distributions. One process which is not adequately described in terms of the Gaussian assumption is the process that generates impulsive noise bursts.

For example, noise experienced on radio channels typically comprises infrequent, high amplitude pulses associated with either man-made or natural sources, superimposed on a more homogeneous (Gaussian) background. Consequently, the presence of impulsive noise is a major source of performance degradation when discrete-time, linear detection schemes such as the matched filter are used; this is largely due to the existence of non-Gaussian interference being neglected in the design philosophy [116].

Impulse noise is typically characterized by high power level during a short time period and a significant lower power level during the rest of the time. There are several approaches to combat impulse noise in digital communication channels. A technique commonly used to suppress impulsive interference involves passing the received data samples through a memoryless nonlinearity.

Typical nonlinear functions are the hard-limiter and the Gaussian-tailed nonlinearity. These suppress large excursions from the wanted signal level by weighting the received data samples prior to matched filter detection. Although this approach to noise suppression is not based on any optimal criteria, it is justified in that an increased signal-to-noise ratio usually results when a suitable threshold is chosen [116].

Impulse noise can be removed by using Reed-Solomon Forward Error Correction (FEC) coding, but the disadvantage of this approach is that it requires spending some of the

transmitted data for redundancy bits, thus reducing the information rate of the transmitter. A conventional receiver reduces the effect of impulse noise by applying matched filter. A drawback of this approach is that it degrades the data rate attainable by a transmitter-receiver pair. It is possible to replace a high symbol-rate channel by multiple low symbol-rate channels, using a multi-tone approach; the overall data rate is not degraded, but the multi-tone approach will increase the complexity of the transmitter and receiver [117].

By Interleaving; the transmitter can interleave the transmitter FEC-encoded symbols over the time axis. This can improve robustness to noise impulses with durations longer than the duration of a FEC symbol. But in channel having frequent noise impulses at random times with an impulse duration significantly shorter than a FEC symbol, such an approach will have a marginal effect on the maximum rate of noise impulses that the system can tolerate. Another interleaving approach is calculating digital samples of the modulated waveform at a sample rate much higher than the symbol rate, interleaving these data samples over the time axis, transmitting the interleaved samples, and performing a corresponding de-interleaving operation in the receiver [117].

This approach can significantly improve robustness to the impulse noise, as it spreads each impulse over multiple symbols at the de-interleave output [117]. However, it may cause error propagation in case of a very high magnitude impulse; it also spreads the spectral density of the transmitted signal and therefore is not suitable for band limited modulations, such as QAM and PAM. It is more suitable for direct sequence code division multiple access (CDMA) approaches [117].

Impulsive noise consists of relatively short duration ‘on/off’ noise pulses, caused by a variety of interfering sources, channel effects or device defects, such as switching noise, interfering electromagnetic pulses, adverse communication channel environments, data packet loss, signal dropouts, physical degradation/scratch of the storage medium, clicks from computer keyboards [118].

In this chapter, a digital smear-desmear technique (SDT) based on polyphase sequences with good autocorrelation properties is described for the minimization of impulse noise. A smear filter is a device that disperses the energy contained in a wide bandwidth pulse in time while the desmear filter performs the inverse operation to the smear filter by compressing the smeared pulse in time.

These sequences are applied to the design of digital smear/desmear filters and combined with Trellis-coded modulation (TCM) codes. An intermediate set of three dependent but overdetermined criteria stemming fron the BER criterion are proposed. The purpose is to use this set of filter design criteria in [32] based on minimizing bit error rates for practical filter design. Application of these criteria guarantees the optimum performance measured by BER.

The impulse noise is modelled as a sequence of Poisson arriving delta functions with Gaussian amplitudes. With improved equalization, phase jitter tracking, timing recovery and trellis coded modulation (TCM), transmission rates achieved over band limited channels are close to the theoretical limit [119–121].

One of the main impairment on band limited channels, causing burst errors, is impulse noise (IN). In the present-day high speed modems for band limited channels there are no measures against impulse noise other than detection [115, 122, 123]. A possible counter-measure to the problem of short impulse noise (less than 10ms) is the smear-desmear technique (SDT) [115]. The SDT in [115] has been implemented in analog technology and the results were not satisfactory due to insufficient quality of analog devices.

A digital smear desmear filter technique that applies binary sequences of limited length was described in [124], [125]. The design of SDT filters in [124] is based on minimizing intersymbol interference (ISI) and maximizing filter power efficiency. In this design, losses in SNR can be significant since transmit and receive filters are not matched. Our purpose is to use the general set of filter design criteria in [32] based on minimizing bit error rates for practical filter design. As a result, another necessary requirement for minimization of the signal-to-noise ratio (SNR) loss due to mismatching filters is added to the design criteria [32] [126].

Three approaches were applied in the practical filter design. In Design 1, the smearing filters form a pair of matched filters. Filter sequences are required to have constant amplitude and good autocorrelation properties. The polyphase sequences used in this scheme possess significantly better autocorrelation properties, measured by the merit factor than the binary sequences. Design 2 is proposed for systems where very low values for ISI variance are required. Low ISI is achieved by designing the smearing filter to operate as equalizer.

The filter sequences are required to have both good autocorrelation and equalization properties. It is shown that polyphase sequences outperform known binary sequences with regard to ISI suppression and mismatching SNR loss. Design 3 can yield ISI as low as Design 2 with reduced system delays. The filter design is based on nonconstant amplitude sequences in [126], while the communication system structure is the same as in Design 2. The required filter lengths, for a specified level of ISI, are much smaller than what is used in Design 2.

The performance improvement is obtained at the cost of an additional delay in the system which can be tolerated in applications of interest. The main contribution in this chapter is summarized as follows:

- A set of filter design criteria based on minimizing the bit error probability of impulse noise using digital smear filter is analysed
- This technique also completely remove the error floor caused by the impulse noise

The chapter is organized as follows. Section 7.2 introduce the model of a digital transmission system. Section 7.3 discuss the filter criteria, Section 7.4 describes a practical filter design using SDT. Simulation results are presented in Section 7.5. Finally, a summary of the chapter is presented in Section 7.6. The work presented in this chapter is published in [32, 33].

7.2 System Transmission Model with Proposed SDT

A digital communication system with the SDT is depicted in Figure 7.1 [**?**]. A binary message sequence generated by the digital source is mapped into 16QAM trellis coded modulation signals. The modulator output symbols are then processed by the digital smear filter. In the smear filter the signal is expanded in the time domain over the filter impulse response. This results in deliberately introduced ISI. The channel is subject to AWGN and impulse noise. Ideal amplitude and phase channel characteristics as well as ideal phase tracking are assumed.

In the receiver, the desmear filter performs an inverse operation to the one in the smear filter and thus removes the ISI introduced in the transmitter. Both the smear and

desmear filtering are performed in the baseband. After processing by the desmear filter the impulse noise energy is spread out over the filter impulse response length. That results in a significant reduction of the impulse noise effect on the signal. The signal is demodulated by the Viterbi decoder.

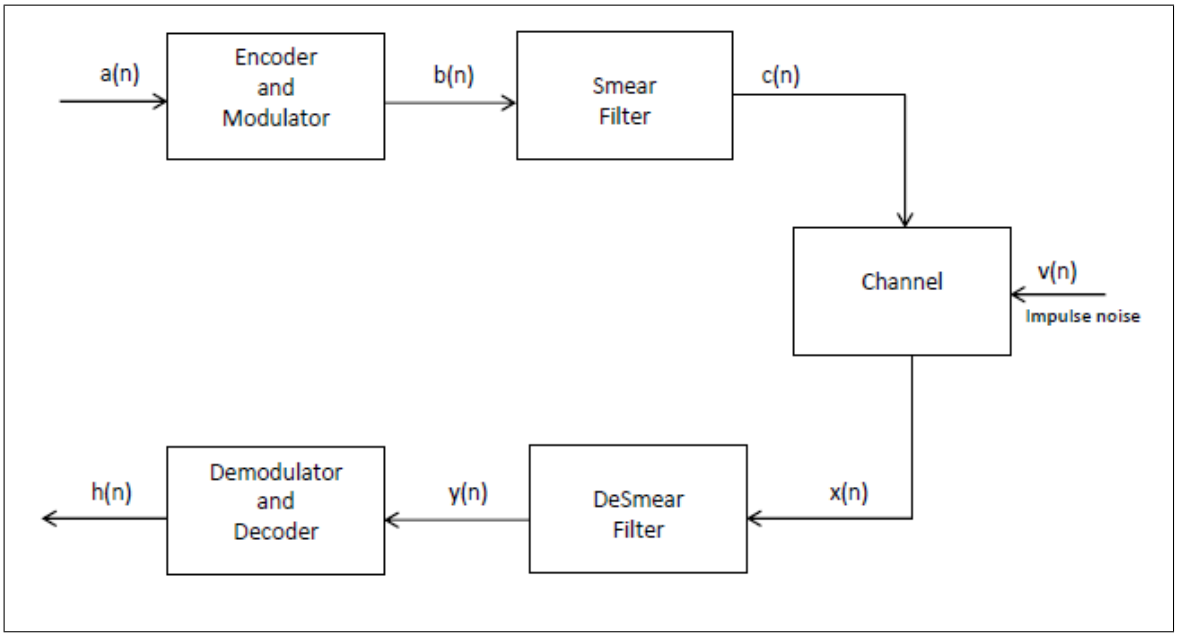

Figure 7.1: System Transmission Model with Proposed SDT

7.2.1 Transmitter Model

Let **b** = [b(0),$\cdots, b(n), \cdots$, b(m)] denote a complex symbol sequence at the output of the modulator in Figure 1. The smear filter is represented by a sequence of tap coefficients, denoted by **s** = [s(0),$\cdots, s(i), \cdots$, s(*N*)] where $s(i)$ is the *ith* tap coefficient and (*N*+1) is the number of taps. The output sequence **c** is obtained by convolving the sequence **b** and the smear filter sequence **s**. It is assumed that the filter gain denoted by A_s, is normalized to unity. That is,

$$A_s = \sum_{j=0}^{N} s(j)s^*(j) = 1 \tag{7.1}$$

where * denotes complex conjugate. The output signal c(*n*) has a gaussian distribution with a zero mean and the variance *P*.

7.2.2 Channel Model

The input symbol to the desmear filter at time *n* is given by:

$$x(n) = c(n) + v(n) + v_i(n) \tag{7.2}$$

where $v(n)$ is a sample of zero mean complex AWGN with the variance σ^2, and $v_i(n)$ is a sample of the channel impulse noise $v_i(t)$ with the variance σ_i^2. The impulse noise event times are represented by a Poisson process. The impulse noise, denoted by $v_i(t)$, can be written in the form [123]

$$v_i(t) = \sum_{k=-\infty}^{\infty} z_i(k)\delta(t - t_k) \tag{7.3}$$

where t_i represent the impulse noise event times and z_i is the impulse noise amplitudes. The Poisson random process t_i has the intensity of λ events/s and z_i is a Gaussian process with a zero mean and the variance σ_i^2 . The parameters λ and σ_i^2 are obtained from experimental data [127], [128]. Most of the symbols received are not corrupted by impulse noise. Due to the nonstationary character of impulse noise [**?**], the signal to impulse noise power ratio over one symbol interval is represented as

$$SNR_{in} = 10\log(\frac{P}{\sigma_i^2}) \tag{7.4}$$

where *P* represents the signal power. It is assumed that the average time interval between two consecutive impulse noise events of $v_i(t)$ is larger than the smear/desmear filters impulse response length consisting of *N* symbol intervals. That means that $\lambda T_s N << 1$, where T_s is the symbol interval [**?**].

7.2.3 Receiver Model

The desmear filter is represented by a coefficient sequence, denoted by d = [d(0), d(1),$\cdots$, d(N)]. To avoid a trivial solution in filter design for the desmear filter coefficient set, power constraint is included as

$$A_{sd} = \sum_{j=0}^{N} s(j)d^*(N-j) = 1 \tag{7.5}$$

where A_{sd} is the gain of the smear-desmear filter pair. The gain A_d of the desmear filter is given by

$$A_d = \sum_{j=0}^{N} d(j)d^*(j) \tag{7.6}$$

The output symbol of the desmear filter signal *y(n)* can be represented by:

$$y(n) = b(n) + b_{isi}(n) + v(n) + v_s(n) \tag{7.7}$$

where $b(n)$ is the complex symbol sequence. The total channel distortion at time *n* is given by the sum of the residual ISI, $b_{isi}(n)$, the additive white gaussian noise after the desmearing filter, $v(n)$, with a zero mean and the variance $\sigma_v^2 = A_d\sigma^2$ and the impulse noise, v_s, smeared over *N* symbol intervals. The impulse noise v_s with variance in the *(n + j)*th symbol interval is given by:

$$\sigma_s^2(n+j) = E(v_s(n+j)v_i^*(n+j)) = \sigma_i^2|d(j)|^2 \tag{7.8}$$

The residual ISI, $b_{isi}(n)$, is given by the sum of *N* independent random variables. Typically, *N* is larger than 10 and according to the central limit theorem, b_{isi} has a gaussian distribution. The sum of the three independent gaussian variables b_{isi}, v and v_i is another gaussian variable

$$e(n) = y(n) - b(n) = b_{isi}(n) + v(n) + v_s(n) \tag{7.9}$$

with the variance

$$\sigma_e^2 = E(|b_{isi}(n)|^2) + E(|v(n)|^2) + E(|v_s(n)|^2) \tag{7.10}$$

The variance σ_e^2 can be upperbounded by

$$\sigma_e^2 = \sigma_v^2 + \sigma_{isi}^2 + \sigma_s^2(n+j) \leq \sigma_v^2 + \sigma_{isi}^2 + max\,\sigma_i^2 \tag{7.11}$$

where σ_{isi}^2, the variance of the ISI and max σ_i^2 is the maximum impulse noise variance. Thus the total channel distortion can be considered as an equivalent gaussian process with the variance σ_e^2. The main objective of the system design is to minimize the bit error probability. At high signal-to-noise ratio, the bit error probability can be estimated by

$$P_b \approx \frac{N_s}{n_b} Q(\frac{d}{2\sigma_e}) \tag{7.12}$$

where N_s is the average number of the nearest neighbours in the signal set, n_b is the number of bits in a symbol and *d* is the minimum Euclidean distance in the signal set.

The ultimate performance limit of a communication system is determined by gaussian noise, the only disturbance in the channel. The performance of a real communication system with impulse noise and ISI caused by smearing filters is compared to an ideal system with AWGN only. The measure of the real system performance loss relative to the ideal system is defined as the ratio of the ideal and the real system signal-to-noise ratios given by

$$L = 10 \log_{10} \frac{\sigma_e^2}{\sigma^2} [dB] \tag{7.13}$$

Ideally, smearing filter parameters should be selected to obtain a zero performance loss. In practical filter design, the objective is to minimize the performance loss or, minimize the variance of the equivalent gaussian process σ_e^2 .

7.3 The Smearing Filter Design Criteria

The smear and desmear filters are implemented as digital filters. The initial criterion in the filter design is minimization of the performance loss given by Equation (7.13) [**?**]. Hence, the performance loss is required to be below a specified threshold T_s.

$$L_s \leq T_s \tag{7.14}$$

The performance loss directly depends on the equivalent gaussian process variance, σ_e^2. The variance σ_e^2 is given by the sum of the AWGN variance σ_v^2, the maximum smeared impulse noise variance $\max_j \sigma_s^2(N+j)$ and the residual intersymbol interference variance σ_{isi}^2 as expressed in Equation (7.11). The minimization of σ_e^2 can be done by independent minimization of each of the three components in the sum.

However, minimization of individual components can cause significant degradation of the others. For example, minimization of the residual intersymbol interference variance can cause a considerable increase in the AWGN variance due to mismatched smearing filters. Since the system performance in the absence of impulse noise is of paramount importance, the priority is given to the minimization of the AWGN variance [**?**]. The smearing filter design criteria can be summarized as follows:

Criterion I: Minimize the AWGN variance

Criterion II: Minimize the residual ISI variance

Criterion III: Minimize the impulse noise variance

7.3.1 Criterion I

In order to minimize the AWGN variance the smear and the desmear filters should satisfy the matching condition in the form of

$$s(j) = d^*(N-j) \qquad j = 0, 1, 2, \cdots, N \tag{7.15}$$

or equivalently, A_d should be equal to 1. If the matching condition expressed by (7.15) cannot be satisfied, a measure of mismatching between the smear and desmear filters called the mismatching loss in [115]is used and expressed as:

$$L_m = 10 \log_{10} \frac{\sigma_v^2}{\sigma^2} = 10 \log A_{sd}\,[dB] \tag{7.16}$$

In this filter design the mismatching loss L_m, is less than a specified threshold T_m, therefore $L_m \leq T_m$. The mismatching loss is caused by an increase of the AWGN variance relative to the ideal system with matched filters. In practical filter design, the mismatching loss is smaller than 0.3dB. But mismatched loss requirement depends on the

application. The proposed scheme requirement is suitable for 64QAM application but will cause a devastating effect for 256QAM, because they are more susceptible to noise corruption than 64QAM. Hence mismatched loss has to be less than 0.3dB.

$$L_m \leq 0.3dB \tag{7.17}$$

7.3.2 Criterion II

To minimize ISI variance, the overall transfer function of the smear filter, the channel and the desmear filter should be flat. Since it is assumed that the channel does not introduce ISI, the above condition is satisfied if the convolution of sequences **s** and **d**, denoted by C(k), has values z(0) = 1, and z(k) = 0, $k \neq 0$. where convolution C(k) is defined as

$$C(k) = \sum_{j=0}^{N} s(j)d(k+N-j) \quad where \quad k = N+1, \cdots, -1, 0, 1, \cdots, N-1 \tag{7.18}$$

If condition (7.15) is satisfied then Equation(7.18) simplifies to

$$C(k) = R(k) = \sum_{j=0}^{N} d^*(j)d(k+j) \tag{7.19}$$

where *R(k)* is the autocorrelation function of the sequence **d** . Practically, a zero ISI is an unattainable objective in filter design. But, a certain amount of residual ISI after the desmearing filter is tolerated. It is measured by the variance of the residual ISI given by

$$\sigma_{isi}^2 = \sum_{k=N+1}^{N-1} |C(k)|^2 - |C(0)|^2 \tag{7.20}$$

The signal to noise ratio loss caused by the ISI is defined as

$$L_s = 10 \log \frac{\sigma^2 + \sigma_{isi}^2}{\sigma^2} \, [dB] \tag{7.21}$$

Equivalently,

$$L_s = 10 \log \left(1 + \frac{SNR}{F_2}\right) \, [dB] \tag{7.22}$$

where SNR is the signal to AWGN power ratio defined as $SNR = \frac{|C(0)|^2}{\sigma^2}$ and $F_2 = \frac{|C(0)|^2}{\sigma_{isi}^2}$ is the merit factor defined in [124].

The residual ISI is considered as an additional gaussian process introducing a certain SNR loss at the receiver. Clearly, this loss should be minimized. It should be maintained below a specified threshold T_s, thus $L_s \leq T_s$. The loss T_s of 0.3dB is considered to be acceptable. From a practical point of view it is much easier to use a quantity called normalized ISI level, denoted by L_{isi}, defined as $L_{isi} = -10 \log F_2$[dB]. In practical filter design parameter L_{isi} is more convenient. For systems employing multilevel modulation schemes we assumed that the SNR is at least as high as 20dB, to meet the requirement (7.14).

7.3.3 Criterion III

Criterion III consists of minimization of the maximum smeared impulse noise variance. To be consistent with the already established design criteria [124], merit factor defined as the ratio of the maximum impulse noise variance and the maximum smeared impulse noise variance in a single symbol interval is introduced

$$F_2 = \frac{\sigma_i^2(n)}{\sigma_s^2(n+j)} = \frac{1}{\max_j |d(j)|^2} \tag{7.23}$$

in dB $L_{F_2} = 10\, log F_2$ [dB], where σ_i^2 is the maximum impulse noise variance and $\sigma_s^2(N+j)$ is the maximum smeared impulse noise. In practical filter design it is required that

$$L_{F_2} \leq T_{F_2} = 20[dB] \tag{7.24}$$

The impulse noise variance before spreading can be as large as the signal variance [127]. That is, occasional impulse hits can reach well above the signal level. Impulse noise spreading should reduce the impulse noise variance to the level of the AWGN variance.

A further spreading is not effective [129] [130]. Since multilevel modulation systems shown in Figure 5.18 in [131] and Figure 9.17 in [132] required the minimum SNR of 20 dB.

Clearly the merit factor F_2, as defined in Equation (7.24), should be as large as possible. It shows how much the impulse noise variance in a single symbol interval has been reduced by smearing. A filter with a larger length can produce a larger merit factor F_2. It is convenient to introduce a measure for filter smearing efficiency which does not depend on filter length in [133], [134]. The power efficiency of a sequence **d**, denoted by η, is defined by

$$\eta = \frac{\sum_{j=0}^{N} |d_j|^2}{(N+1)\max_j |d_j|^2} \tag{7.25}$$

The power efficiency has its maximum value of 1, for constant amplitude sequences, while it is less than 1 for nonconstant amplitude sequences. Combining Equations (7.6), (7.24) and (7.26) the following expression for the merit factor F_2 is obtained.

$$F_2 = \frac{\eta(N+1)}{A_d} \tag{7.26}$$

In order to maximize the merit factor F_2, sequences should have the power efficiency as large as possible. For a finite desmear filter length *N*, subject to constraints (7.1) and (7.5), it has been shown in [124] that the maximum value for F_2 is bounded by N + 1, hence $F_2 \leq N+1$. The inequality is satisfied if and only if

$$|d_j|^2 = \frac{1}{N+1} \quad and \quad s(j) = d^*(N-j) \tag{7.27}$$

The optimum merit factor F_2 is achieved only when the smearing filters form a matched filter pair are represented by sequences with constant amplitude.

7.4 Practical Filter Design

The optimum values for the three filter design criteria cannot be achieved simultaneously. In Design 1, sequences with constant amplitude and good autocorrelation properties are search for. The smear/desmear filter pair consists of matched filters. This design satisfies the requirements for optimum values of Criteria I and III, as defined by Equation (7.28).

The value of Criterion II clearly depends on the autocorrelation properties of the filter sequences. The constant amplitude sequences with the best known autocorrelation

properties are polyphase sequences [130]. The smearing filter design based on these sequences achieves an improvement of 7.78 dB in merit factor F_2 relative to the design based on binary sequences for the sequence length of 200. This type of filter design based on polyphase sequences can produce filters with ISI level, L_{isi}, of -15 dB with sequence lengths of 200, while filters designed in [124] cannot achieve σ^2_{isi} less than -8 dB.

Design 2 is suitable for systems where very low values for ISI level ($\leq -30dB$) are required. The improvement in suppresion of intersymbol interference is achieved by sequence equalization. That is, the smearing filter is designed as an equalizer and therefore the smear/desmear filter pair is not matched. While the smearing filters in this design will produce low ISI (Criterion II), the mismatched filters will result in an increased AWGN variance (Criterion I) and smeared impulse noise variance (Criterion III).

Therefore, the three design criteria should be monitored and adjusted simultaneously. It should be noted that the smear/desmear filters in this design might introduce a significant system delay of several sequence lengths. Design 3 relies on sequences with nonconstant amplitude. This design approach can achieve ISI as low as in Design 2, with an additional advantage of a lower system delay.

Criteria I and II are satisfied at the expense of the filter power efficiency η. Sequences with nonconstant amplitude will result in a non-optimum value for the impulse noise variance (Equation (7.28)) for the given desmear filter length. A possible choice is Huffman sequences which have good autocorelation properties [133] or sequences presented in [135] which have both good autocorrelation properties and power efficiency.

7.4.1 Design 1

Constant amplitude polyphase sequences with good autocorrelation properties are used In Design 1. Polyphase sequences with constant amplitude, known as Frank and P1-P4 sequences in [130], have better autocorrelation properties than M-sequences. It is important to note that polyphase sequences also are resilient to carrier phase and timing instabilities. In the sequel, we will discuss the properties of these sequences with respect to SDT applications.

7.4.2 Constant Amplitude Polyphase Sequences

For a polyphase Frank sequence of length $N = L^2$, the phase of a sequence element is $\phi(k,l) = 2\pi/L(k-1)(l-1)$ and sequence elements are $d[k+L(l-1)] = \exp(j\phi(k,l))$, where $k = 1, \cdots, L, l = 1, \cdots, L$. The phases of P1 and P2 sequence elements are given by $\phi(k,l) = -\pi/L[L-(2k-1)][(k-1)L+(l-1)]$ and $\phi(k,l) = \pi/2L(L+1+2k)(l-1)$, respectively.

It is important to observe that both P1 and P2 sequences are available only for square integer lengths of [N = ...36, 49, 64, ...]. P2 sequences are further restricted to even lengths only. Odd length P2 sequences possess rather bad autocorrelation properties .

Sequences P3 and P4 are defined for any integer length. Phases of their elements are $\phi(k) = \pi/N(k-1)^2$ and $\phi(k) = \pi/4N(2k-1)^2 - \pi/4(2k-1)$ for $1 \leq k \leq N$. The most important property of constant amplitude polyphase sequences, relevant to SDT applications, is that the mainlobe to sidelobe power ratio is a monotonically increasing function of the sequence length.

This property makes them much more effective in suppressing ISI then binary sequences [124], [125]. In addition, these sequences have constant amplitude and consequently, the optimum Criterion III (7.28). The method for generating binary sequences with high F_2 involves computer search and sequence elimination, which for large values of sequence lengths become prohibitively time consuming . On the other hand, polyphase sequences are generated analytically.

7.4.3 Design 2

A distinguishing property of this design method is a very low ISI level ($L_{isi} \leq -30dB$) achieved by sequence equalization. On the other hand, mismatched filters inevitably introduce a certain level of SNR loss [135]. This SNR loss can be maintained below a specified value by choosing a proper sequence for the desmearing filter. The sequence should have both, good autocorrelation properties measured by F_2 and good equalization properties. In the sequel a simple criterion to estimate the equalization properties of a sequence is discussed.

7.4.4 Zero Forcing Sequence Equalization

For a sequence s_j, where $j = 0, 1, \cdots N$, zero forcing equalizer or inverse filter [122] is define as a digital filter with a Kronecker delta sequence response to the sequence **s**. The Z - transform of the zero forcing equalizer is given by

$$D(z) = \frac{1}{\sum_{j=0}^{N} s_j z^{-j}} \tag{7.28}$$

A necessary requirement for the filter existence is that the Z-transform, *S(z)*, does not have zeros on the unit circle [122], where *S(z)* is the Z-transform of the sequence s_j . If the sequence power is normalized to unity (Equation (6.1)), the SNR loss of the inverse filter, denoted by L_{ZF} , is given by the ratio

$$L_{ZF} = 10 \log \frac{1}{\frac{1}{2\pi} \int_{-\pi}^{\pi} |D(e^{j\omega})|^2 d\omega} \tag{7.29}$$

The quantity $D(e^{j\omega})$ can be evaluated at a closely spaced set of points by the use of fast Fourier transform, and the integral can thus be calculated to a close approximation. The L_{ZF} loss shows the difference in SNR between a zero forcing equalizer and a matched filter. This quantity is an upper bound on the SNR loss in all other equalization methods [4]. Therefore, the L_{ZF} can be used in sequence search as an indicator of their performance with respect to the equalization SNR loss. It is worth noting that the equalization performance should be evaluated by both L_{ZF} and F_2 parameters, since a good merit factor F_2 does not guarantee a low L_{ZF} loss.

7.4.5 Sequences with Good Equalization Properties

Figure 7.2 show the merit factor F_2 for binary sequences and polyphase sequence for length 200 and 300 respectively. The main lobe to side lobe power ratio has a floor for binary sequences, while it increases monotonically with the sequence length for polyphase sequences. It has been observed that this ratio is proportional to the square root of the sequence length.

Polyphase sequences with good equalization properties ($L_{ZF} \leq 1.0dB$) are presented in Table 7.1. They are characterized by sequence length *N*, the merit factor F_2 and zero forcing equalization loss L_{ZF}. Only binary sequences from [124] with both good merit factor F_2 and low L_{ZF} loss are included in Table 7.2.

Finally, a simple example is singled out to illustrate that the merit factor F_2 and the L_{ZF} loss are not closely related and that both of them have to be used in evaluating sequence equalization properties. Polyphase sequence P2 (36) has the merit factor F_2 of 15.22 which is superior to the best known binary Barker(13) sequence with F_2 of 14.083. However, the L_{ZF} loss for P2 (36) is infinite, while Barker (13) sequence has the lowest known value for L_{ZF} of 0.21 dB.

7.4.6 Evaluation of Design 2 in Communication Systems

To evaluate the performance of filters obtained by Design 2, a number of sequences have been selected from Table 1. They are used to design smearing mismatched filters in a real system where the receive filter operates as an MMS equalizer. The MMS equalization method has been chosen because it provides the best trade-off in reducing the effects of residual ISI and gaussian noise. The principle of MMS equalization can be summarized as follows. Let *u* filter pair defined by sequence $\mathbf{s} = (s(0), \cdots, s(K))$ at the transmitter and $\mathbf{d} = (d(0), \cdots, d(N))$ at the receiver.

Note that the lengths of the smear and desmear filters are in general different due to various equalization requirements for the ISI level. If the output of the smearing filter is sequence **s**, the output **c** of the desmearing filter **d** can be expressed in matrix form as **c** = **A**.**s** where **A** is a $[(N + K + 1) \times (K + 1)]$ Toeplitz matrix defined by the first row $(d(0), 0_1, \cdots 0_K)$ and first column $(d(0), \cdots d(N), 0_{N+1}, \cdots, 0_{N+K})^T$.

If a desired desmearing filter response to sequence **s** is a sequence **z** = *(z(0), z(1), ...z (N + K))* then the mean squared error between the actual filter response denoted by **c**, and the desired filter response denoted by **z**, is given by

$$\varepsilon = \sum_{j=0}^{N+K-1} |c(j) - z(j)|^2 \tag{7.30}$$

The filter sequence **s** which minimizes the mean squared error (7.31) is given by [121]

$$\mathbf{s} = (\mathbf{A}^H.\mathbf{A})^{-1}.\mathbf{A}^H.\mathbf{z} \tag{7.31}$$

where $(\cdot)^H$ denotes a transposed and conjugated matrix. Matrix $\mathbf{A}^H.\mathbf{A}$ is a $(K + 1) \times (K + 1)$ correlation matrix of sequence **s**. Note that $\mathbf{A}^H.\mathbf{A}$ is a Toeplitz matrix whose

inverse can be calculated by the Levinson-Durbin algorithm [121].

The desired desmearing filter response is define **z** as a sequence with no ISI, with elements $z(L) = 1$, and L is the largest integer $\leq (N + K)/2$ and $z(j) = 0, j \neq L$. It is important to note that though for some sequences the zero forcing equalizer Equation (7.29) might not exist, the minimum mean square approximation, defined by Equation (7.32), always exists.

The selected binary sequences were chosen to optimize the merit factor F_2 as proposed in [126]. In general, it has been observed that binary sequences have the SNR loss in MMS equalizers, L_m, close to the SNR loss for zero forcing equalizers, L_{ZF} .

7.4.7 Design 3

In the system with sequence equalization the requirements for Criteria I and II, expressed by equation (7.17) and (7.23), respectively, cannot be met simultaneously due to prohibitively large filter lengths. To improve the filter performance for practical sequence lengths, Design 3 based on equalization and non-constant amplitude sequences is proposed.

In this design approach, the filter power efficiency, η, (Equation (7.26)) was slightly sacrifice relative to its maximum value obtained in Design 2 in order to satisfy Criteria I and II. Huffman sequences [133] are nonconstant amplitude sequences with best known ISI and power efficiency properties. A thorough examination of results presented in [133] reveals that the power efficiency of Huffman sequences does not exceed 0.43. A drawback of Huffman sequences is that good power efficiency is not guaranteed and it usually ranges between 0.3 and 0.4 [134]. A proposed nonconstant amplitude sequences is used, generated by a method presented in [136–139] which are superior to Huffman sequences with regard to power efficiency. The design method can be summarized as follows.

Step 1 Choose a Frank sequence with good zero forcing equalization loss ($L_{ZF} \leq 1dB$) as an input **d** sequence in equation (7.32) in [**?**].

Step 2 Calculate a filter sequence **s** by the MMS algorithm (Equation (7.32)). It is assumed that the filter and input sequences have the same length.

Step 3 Normalize the sequence **s** to satisfy **ss*** = 1.

Step 4 Compute the ISI level, L_{isi}, and SNR loss, L_m. Test whether they satisfy conditions (7.17) and (7.23). If the answer is positive, stop the procedure, otherwise use sequence **s** as the input vector and repeat Step 2.

This method was used to generate a series of sequences that satisfy Criteria I-III. The sequence properties are illustrated in Figure 7.3 and Figure 7.4. The results are shown for two sequence lengths of 256 and 484. These lengths were selected to achieve the specified impulse noise suppression (Equation (7.25)) for the 16QAM data transmission systems. The results show that increasing the number of iterations in the sequence design procedure generally results in a lower SNR loss (Figure 7.3) and ISI level (Figure 7.4).

Criteria I-III in [**?**] were met after 16 and 20 iterations for sequence lengths of 484 and 256, respectively. The sequence parameters are listed in Table 7.3. Table 7.4 compares Design 2 and Design 3 techniques. The two design methods are compared on the basis of values for Criteria I-III. Clearly, Design 3 offers lower values for the SNR loss and for the same values of ISI and smeared impulse noise variances introduces a lower system delay.

7.5 Simulation Results Proposed SDT System

The simulation results are for coded and uncoded band limited channels data communication systems. Figures 7.5 and 7.6 show simulation results for 16QAM trellis coded modulation signals and 64QAM for uncoded systems in the presence of impulse noise (IN). Parameters of Impulse noise (IN) are: $\lambda = 10^{-3}$ events/s, $SNR_{in} = 0$[dB]. The average time interval between two consecutive impulse noise is 0.0008s. In a communication system subject to impulse noise, it is highly likely that all affected symbols will be incorrect, resulting in error bursts with the bit error rates close to 0.5.

The results indicate that the SDT offers a significant reduction in the SNR required to achieve the same bit error rate as in a system with no SDT for both coded and uncoded systems. The coding gain of the coded system is 2dB at the BER at 10^{-3}, which is almost the same as the coding gain on gaussian channels. Also, the SDT completely removes the error floor in both systems. The reason is that at high signal-to-noise ratios the decoding

is optimal but results to codewords of low weight. And with impulsive noise which is non Gaussian in nature result to error floor at high signal-to-noise ratio. In the above example for the filter impulse response of length N=256 and the power efficiency η = 0.54, the theoretical SD gain is F=22 dB. In most cases a gain of this order is sufficient to suppress the influence of impulse noise on the bit error rate.

Figures 7.7 and 7.8 show the comparison of using the proposed SDT system with other method of minimization of impulsive noise. From the simulation result, the proposed method has 0.3dB gain over using interleaver and 1.3dB gain over using Reed-Solomon coding for 16QAM. And the Proposed method also perform better for 64QAM scheme as when compared with the other methods. SDT method has 0.7dB gain over interleaving and 2.2dB gain over Reed-Solomon coding.

The draw back for Interleaver is because, Interleaving works best when dealing with long bits than when dealing with few symbols that will be affected by impulse noise. The impulse noise affects few symbols rather than the bits which can be easily corrected by SDT method. The de-interleave output may cause error propagation in case of a very high magnitude impulse; it also spreads the spectral density of the transmitted signal and therefore is not suitable for band limited modulations, such as QAM.

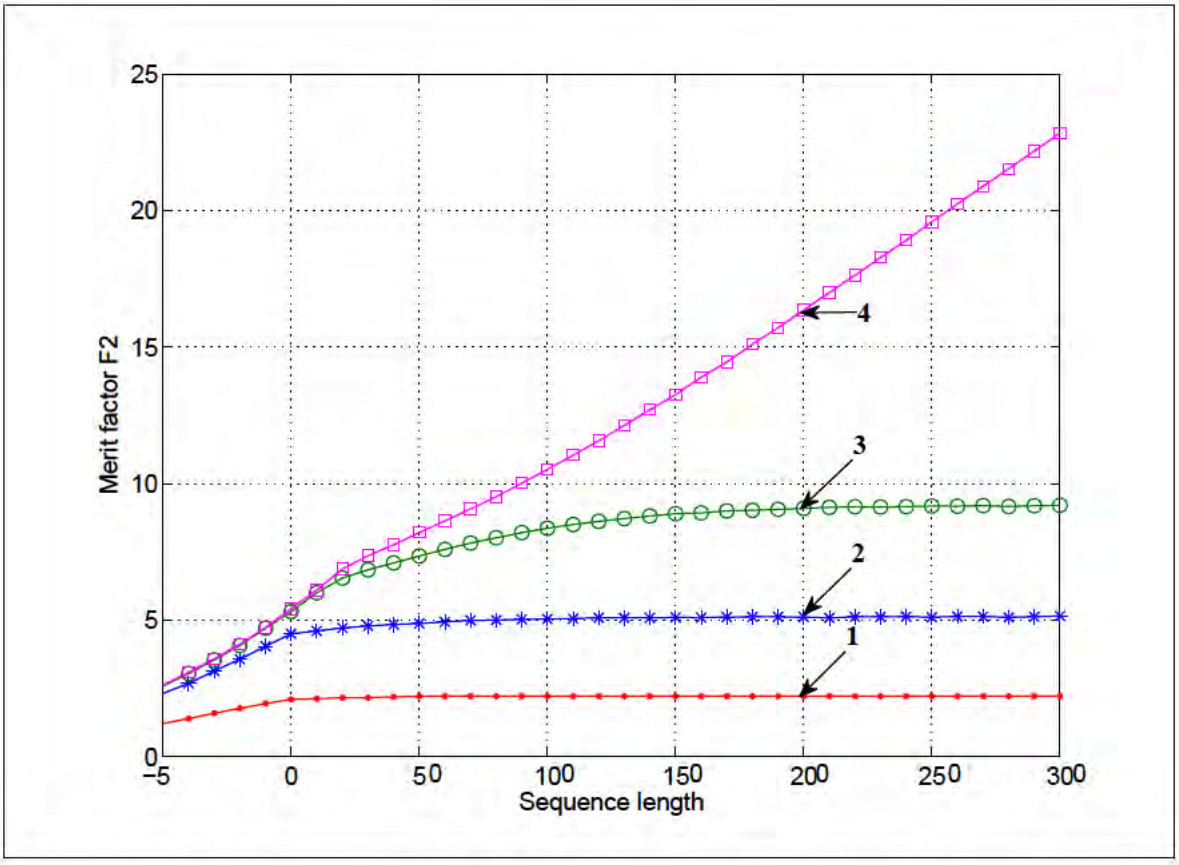

Figure 7.2: Merit factor F_2 for sequences with constant amplitude.

1. Binary sequence
2. P3 and P4 sequences
3. Frank and P1 sequence
4. P2 sequence

N	**Frank**		**P1**		**P3 and P4**	
	L_{ZF} $[dB]$	F_2	L_{ZF} $[dB]$	F_2	L_{ZF} $[dB]$	F_2
36	0.99	12.96	0.99	12.96	*	*
64	0.86	18.03	0.86	18.03	*	*
100	0.77	23.10	0.77	23.10	*	*
144	0.77	28.16	0.70	28.16	*	*
169	*	*	0.99	31.11	*	*
196	0.64	33.20	0.62	33.20	*	*
225	*	*	0.68	36.10	1.00	23.67
256	0.61	38.23	0.61	38.23	*	*
289	0.89	41.08	0.65	41.08	0.95	26.80
324	0.68	43.25	0.52	43.25	0.78	28.37
361	0.43	46.05	0.67	46.05	0.91	29.93
400	0.55	48.25	0.52	48.25	*	*

Table 7.1: Polyphase sequences with good equalization properties, where * means no value.

N	L_{ZF} $[dB]$	F_2	**N**	L_{ZF} $[dB]$	F_2	**N**	L_{ZF} $[dB]$	F_2
5	0.62	6.25	49	0.87	8.82	87	0.78	7.46
13	0.21	14.08	53	0.68	8.26	89	0.90	7.56
15	0.60	7.50	55	0.61	8.84	91	0.75	7.13
19	0.81	5.47	59	0.94	8.49	93	0.98	7.23
21	0.94	8.48	61	0.85	7.32	97	0.94	7.35
23	0.99	5.19	65	0.86	7.77	99	0.79	7.28
27	0.65	9.85	67	0.74	9.31	101	0.81	6.06
29	0.69	6.78	69	0.86	8.44	127	0.99	6.51
35	0.75	6.88	71	0.51	9.17	137	0.94	6.43
39	0.71	7.68	75	0.89	8.24	153	1.00	6.01
41	0.79	7.78	81	0.84	7.32	157	0.86	6.51
45	0.63	8.58	83	0.93	7.81	*	*	*

Table 7.2: Binary sequences obtained by limited with good equalization properties in [124], where * means no value.

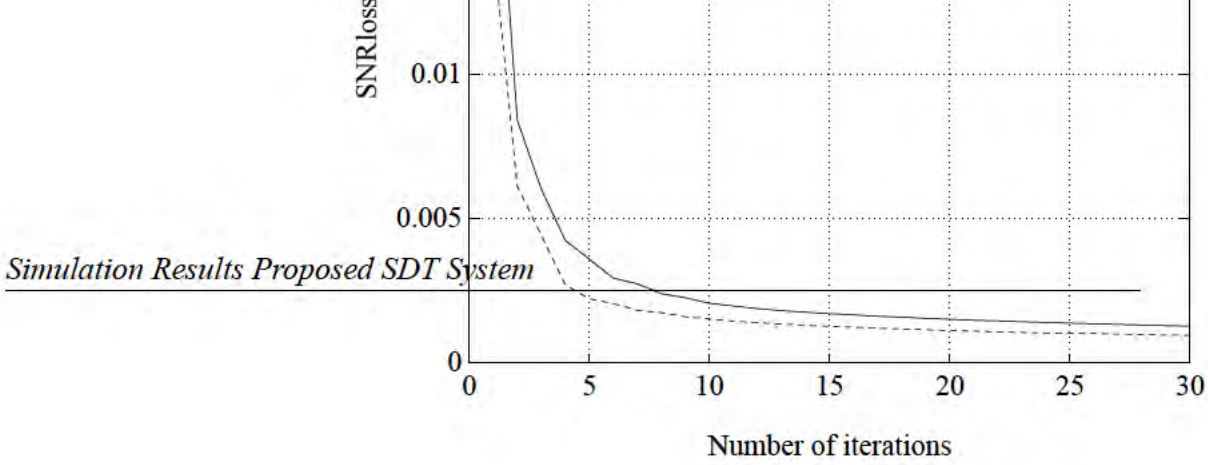

Figure 7.3: The SNR loss, *Lm* for the system employing sequences with nonconstant amplitude obtained by Design 3

Solid line: Sequence of length 256

Dash line: Sequence of length 484

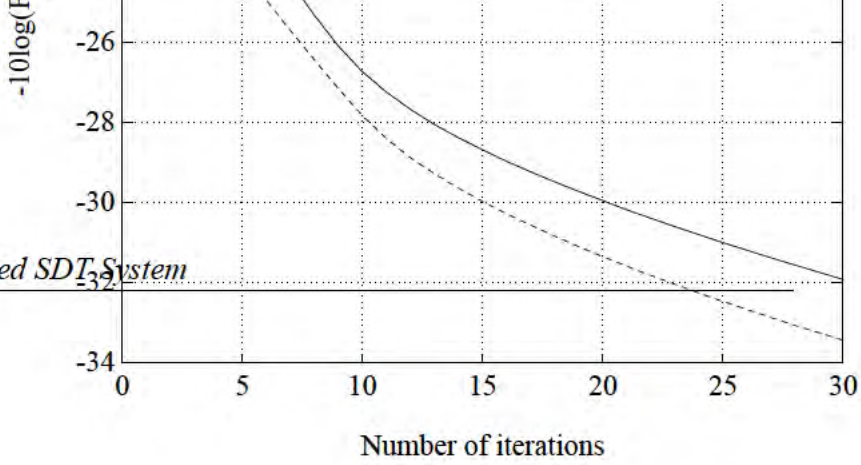

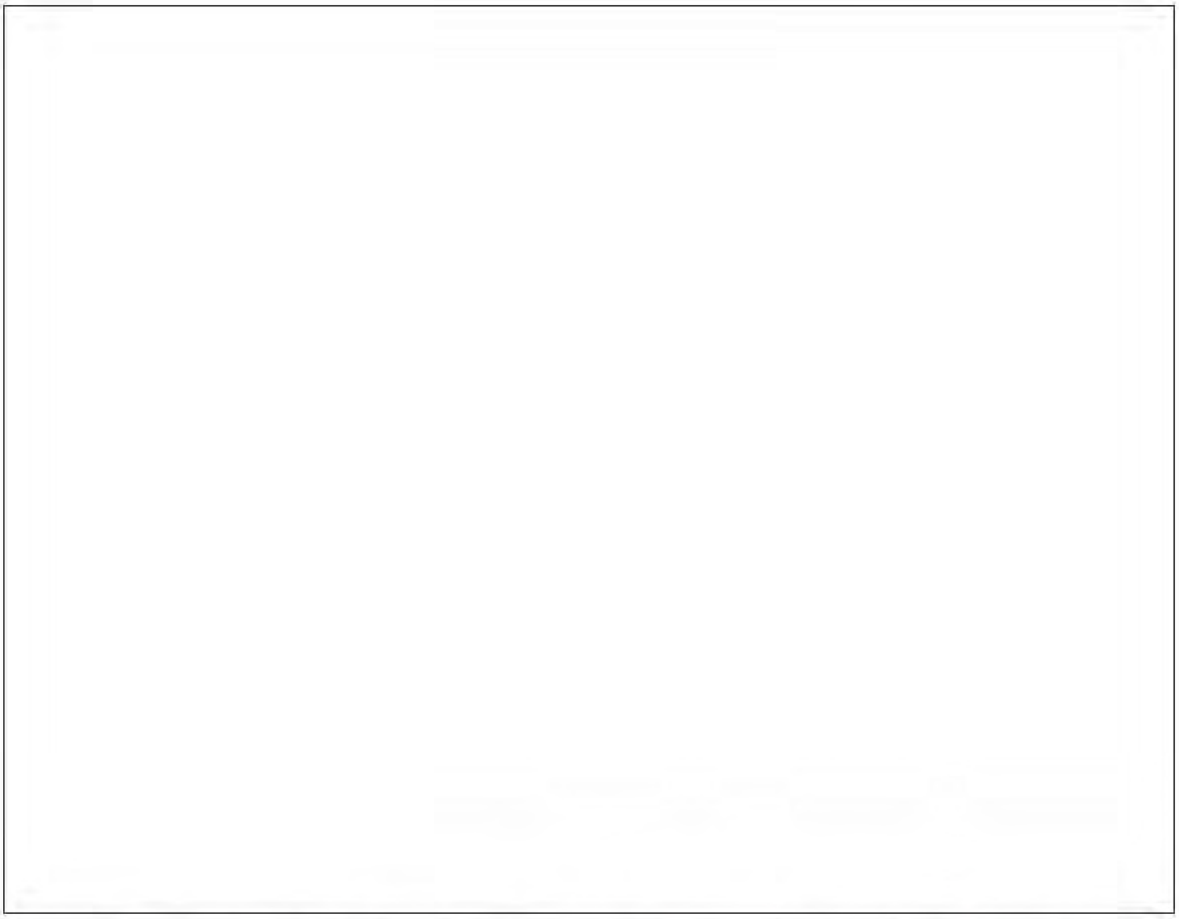

Figure 7.4: Desired level of residual ISI, L_{ISI} in terms of the number of iterations in Design 3

Solid line: Sequence of length 256

Dash line: Sequence of length 484

Filter length N+1	ISI level L_{ISI}[dB]	SNR loss L_m[dB]	Power efficiency η
256	-30.18	0.0012	0.54
484	-30.54	0.001	0.56

Table 7.3: The smearing filter parameters for the uncoded and coded systems

Design type	Seq. length	ISI level	SNR loss	IN merit factor	System delay
	N+1	L_{ISI}[dB]	L_m[dB]	F[dB]	N+K+1
Design 2	195	-30.0	2.3	20.6	2500
	196	-30.0	0.3	22.6	1500
Design 3	256	-30.18	0.0012	21.4	511
	484	-30.54	0.001	24.3	967

Table 7.4: The smearing filter design method comparison

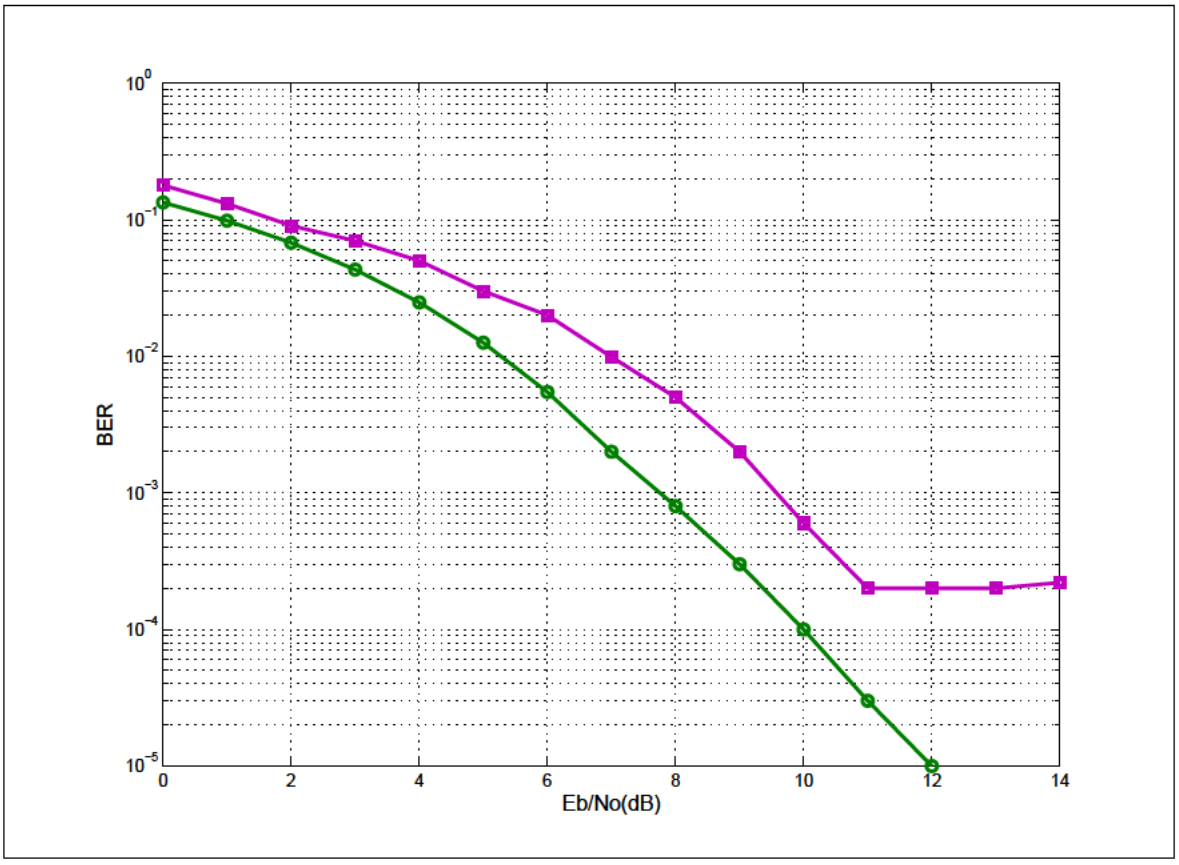

Figure 7.5: Bit error rate for coded system using 16QAM in the presence of impulse noise

1. Coded system with SDT
2. Coded system without SDT

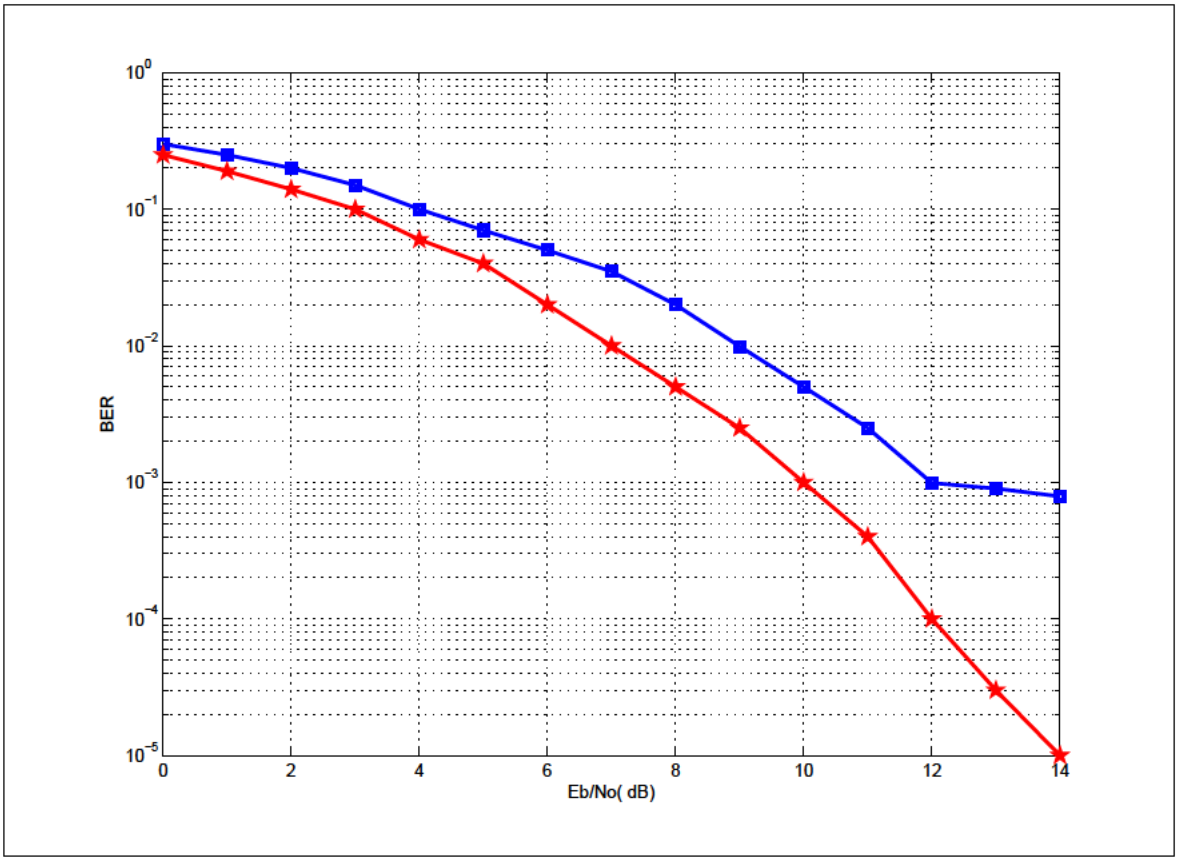

Figure 7.6: Bit error rate for uncoded system using 64QAM in the presence of impulse noise.

1. Uncoded system with SDT
2. Uncoded system without SDT

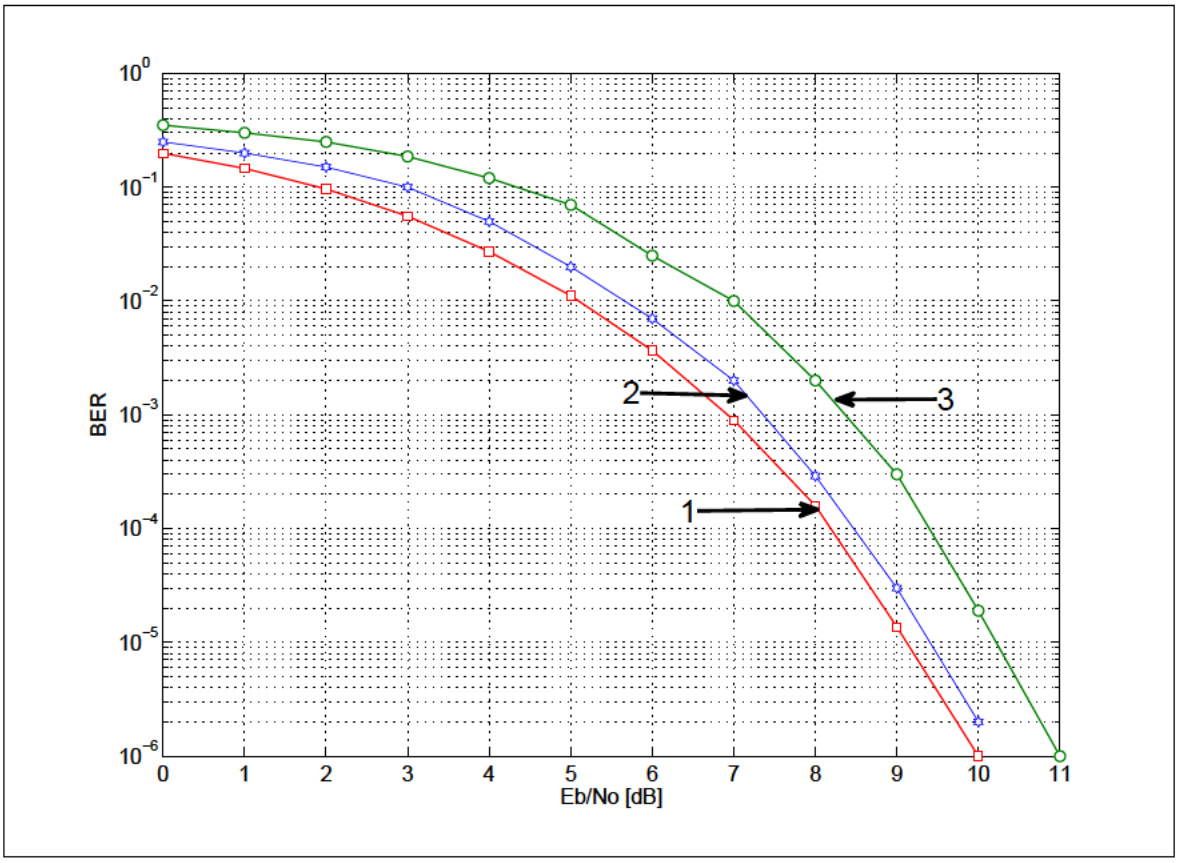

Figure 7.7: Bit error rate Comparison for Impulse noise minimization using 16QAM

1. Proposed Impulse noise minimization using SDT
2. Impulse noise minimization using Interleaver
3. Impulse noise minimization using Reed-Solomon FEC coding

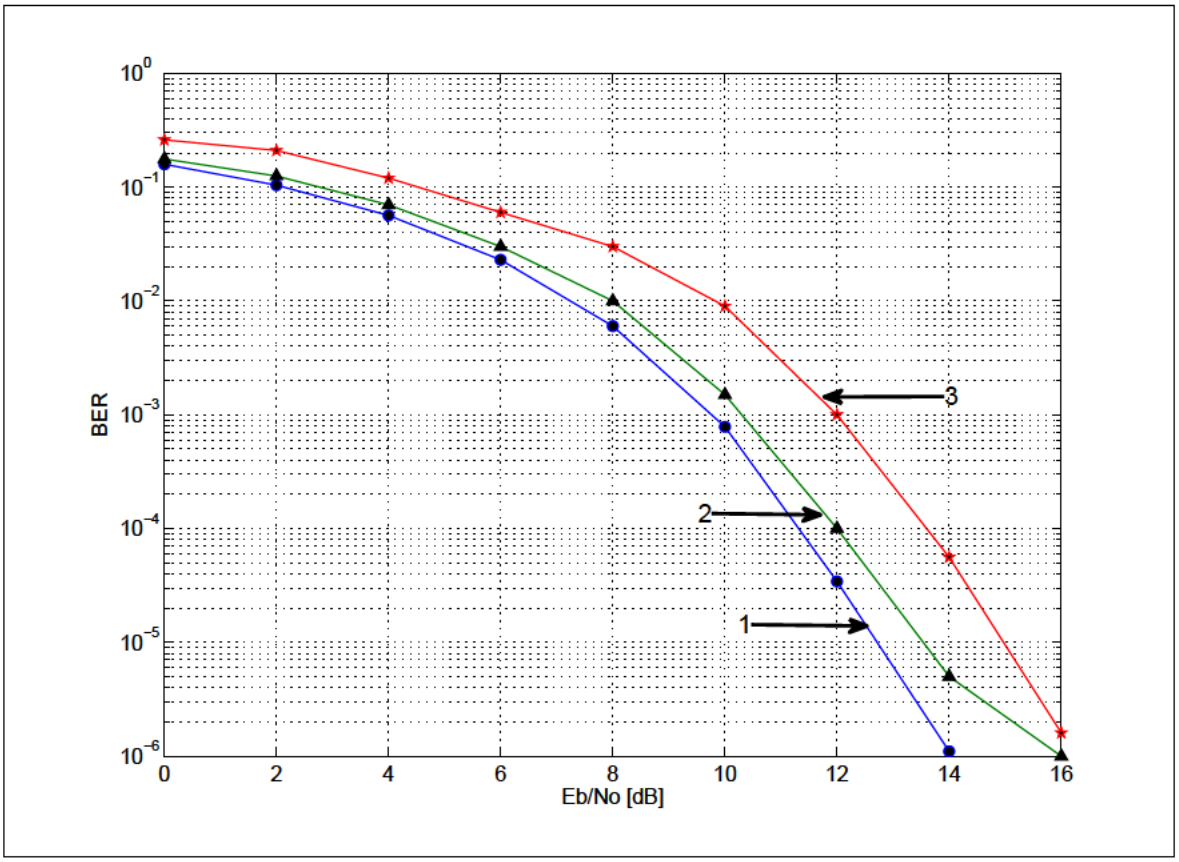

Figure 7.8: Bit error rate Comparison for Impulse noise minimization using 64QAM

1. Proposed Impulse noise minimization using SDT
2. Impulse noise minimization using Interleaver
3. Impulse noise minimization using Reed-Solomon FEC coding

7.6 Summary

The chapter presents a digital smear-desmear technique (SDT) applied to data transmission over band limited channels. The design criteria were applied to practical filter design and used in digital implementation of the SDT. Polyphase sequences that meet the design requirements were generated. The SDT is simulated and combined with Trellis-coded modulation communication systems. Simulation results shows that the SDT outperforms the system with no SDT and also perform better as when compared with other method of minimizing impulse noise. The next chapter summarizes the conclusion drawn from the preceding chapters and points toward Future Work.

Chapter 8

Conclusions and Future Work

8.1 Conclusions

This work was motivated by the desire to achieve higher data rates and reliable transmission whereby by system capacity can be increased with high quality of service. A brief summary of accomplished work is given in this chapter with an emphasis on the contributions to the subjects of Turbo equalization, and Using Turbo coded modulation in an impulsive noise environment.

The suitability of Iterative-equalization as a means of increasing date rate is investigated, where equalization and decoding are combined in an iterative process so that each operation benefits from the information delivered by the other. It was also demonstrated that the iterative gain is greater for higher modulation orders. Significant performance gains have been observed as the modulation order increases with low error rate.

A modified approach estimates the data using the a priori information from the SISO channel decoder was proposed using the a priori detected data from previous iteration to minimize error propagation. It can be shown that the BER performance of the modified DFE algorithm provides significant improvement when compared with the conventional DFE algorithm using higher-level modulation scheme.

The performance of Imperfect MMSE DFE with different modulation schemes is analyzed. The Imperfect algorithm does not use the conventional assumption of a perfect feedback but takes into account the feedback error propagation. The obtained simulation results for different modulation schemes in the presence of severe interference achieved better BER performance in comparison to the Exact MMSE LE and the conventional MMSE DFE.

The fact that incorporating an All-pass Filter before equalization in the receiver as an effective method of controlling error propagation is demonstrated. The structure of the All-pass Filtering is analyzed by using the Yule-Walker equations. It turns out that a discrete time prefitering which creates a minimum phase impulse response is a favourable trade-off between performance and complexity. A proposed SFEIC approach yields a comfortable gain compared to the conventional MMSE DFE equalization and decoding. SFEIC is suitable for low complexity Turbo equalization using higher order signal standard. Compared with the existing method, the proposed method achieves considerable

performance improvement without increasing complexity.

Finally, the implementation of a digital smear-desmear technique (SDT) applied to data transmission over band limited channels is described . The design criteria were applied to practical filter design and used in digital implementation of the SDT. Polyphase sequences that meet the design requirements were generated. The SDT is simulated and combined with Trellis-coded modulation. Results show that the SDT perform better than the system with no SDT.

8.2 Future Work

Below are some possible interesting areas for further research.

- Based on the results from this thesis, larger QAM constellation size, such as 256-QAM or 1024-QAM, and multidimensional TCM structure can be explored for even higher data rate transmission through the OFDM and UWB systems.

- Another interesting research topic involves investigating the possibility of explicitly taking advantage of a priori information in the channel estimation process. It is seen that MMSE turbo-equalizers may exhibit performance losses over severe ISI channels, especially when high-order modulations are used. The potential of MMSE equalization in the presence of a priori information has not been fully exploited yet, and that better equalizers remain to be found.

- The extension of the MMSE DFE turbo-equalization scheme to multiple-input multiple-output (MIMO) systems, where the turbo-equalizer could fully exploit the diversity offered by a rich-scattering multipath environment.

- Trellis coding with smear desmear filter technique introduced in this thesis with higher signalling in an impulsive noise environment will be a possible choice for applications with high bit rate transmission. But it would be interesting to further investigate this solution and examine in particular how it compares with using Interleaver to combat impulse noise, both from a performance and complexity point of view, in the context of broadband wireless transmissions.

- Based on the analysis of Trellis coding with smear desmear filter technique to reduce the effect of impulsive noise in band limited systems in this thesis, more evaluations of impulsive noise type can be conducted in the future for the OFDM system with robust decoding algorithms necessary in today's real communication system in which higher spectral efficiency with higher data rate transmission is highly desired.

REFERENCES

References

[1] S. B. Wicker, *Error control systems for digital communication and storage*. Prentice hall Englewood Cliffs, 1995, vol. 1.

[2] L. Shu and J. C. Daniel, *Error control coding*, 2nd ed. Prentice-hall Englewood Cliffs, 2004, vol. 123.

[3] C. S. Elwood and W. Weaver, "A mathematical theory of communication," 1948.

[4] M. Tuchler, R. Koetter, and A. Singer, "Iterative correction of isi via equalization and decoding with priors," in *Information Theory, 2000 Proceedings. IEEE International Symposium on*. IEEE, 2000, p. 100.

[5] R. Koetter, A. C. Singer, and M. Tuchler, "Turbo equalization," *IEEE Signal Processing Mag.*, vol. 21, no. 1, pp. 67–80, 2004.

[6] J. G. Proakis, M. Salehi, N. Zhou, and X. Li, *Communication systems engineering*. Prentice Hall New Jersey, 1994, vol. 94.

[7] G. J. Proakis, Manolakis, and G. Dimitris, *Digital communications*, 1995, vol. 3.

[8] G. L. Stüber, *Principles of mobile communication.*, 2nd ed. Norwell, MA: Kluwer Academic, 2001, pp. 1 – 3.

[9] A. Goldsmith, *Wireless communication.* New York, NY: Cambridge University, 2005, pp. 27 – 40.

[10] A. F. Molisch, *Wireless communication*. New York, NY: John Wiley & Sons, 2005, pp. 1 – 31.

[11] A. Goldsmith, *Wireless communications*. Cambridge university press, 2005.

[12] T. S. Rappaport *et al.*, *Wireless communications: principles and practice*. Prentice Hall PTR New Jersey, 1996, vol. 2.

[13] A. J. Goldsmith, "Design and performance of high-speed communication systems over time-varying radio channels," PhD dissertation, University of California at Berkeley, 1994.

[14] Z. Krusevac, "Model-based approach to reliable information transfer over time-varying communication channels," PhD dissertation, Australian National University, 2007.

[15] C. E. Shannon, "A mathematical theory of communication, part i," *Bell Syst. Tech. J.*, vol. 27, pp. 379 – 423, 1948.

[16] W. C. Y. Lee, "Spectrum efficiency in cellular," *IEEE Trans. Veh. Technol.*, vol. 38, pp. 69 – 75, May 1989.

[17] K. Pahlavan and A. H. Levesque, "Wireless data communication," *Proc. IEEE*, vol. 82, pp. 1398 – 1430, Sept. 1994.

[18] D. N. Hatfield, "Measures of spectral efficiency in land mobile radio," *IEEE Trans. Electromagn. Compat.*, vol. 19, no. 3, pp. 266 – 268, Aug. 1977.

[19] C. F. Ball and H. K. Ivanov, "Spectrum efficiency evaluation for different wireless technologies based on traffic modeling," in *Proc. IEEE 16th IEEE International Symposium on Personal Indoor, and Mobile Radio Communications Workshops, (PIRMC'2005)*, vol. 3, Sept. 2005, pp. 2055 – 2061.

[20] V. H. MacDonald, "The cellular concept," *Bell Syst. Tech. J.*, vol. 58, no. 1, pp. 15 – 41, Jan. 1979.

[21] G. L. Stüber, *Principles of mobile communication*, 2nd ed. Norwell, MA: Kluwer Academic, 2001, pp. 28 – 34.

[22] T. Eneh, P. Rapajic, G. Oletu, K. Anang, and L. Bello, "Adaptive mmse multiuser detection for mimo ofdm over turbo-equalization for single-carrier transmission wireless channel," in *Wireless Communications and Mobile Computing Conference (IWCMC), 2011 7th International*. IEEE, 2011, pp. 1408–1412.

[23] C. Glavieux, A. Berrou, and P. Thitimajshima, "" near shannon limit error-correcting coding and decoding: Turbo codes'," in *Proc. IEEE Int. Conf. on Communications*, 1993, pp. 1064–1070.

[24] C. Berrou and A. Glavieux, "Near optimum error correcting coding and decoding: Turbo-codes," *IEEE Trans. Commun.*, vol. 44, no. 10, pp. 1261–1271, Oct. 1996.

[25] L. Bahl, J. Cocke, F. Jelinek, and J. Raviv, "Optimal decoding of linear codes for minimizing symbol error rate (corresp.)," *IEEE Trans. Inform. Theory*, vol. 20, no. 2, pp. 284–287, 1974.

[26] C. Douillard, M. Jézéquel, C. Berrou, A. Picart, P. Didier, A. Glavieux *et al.*, "Iterative correction of intersymbol interference: Turbo-equalization," *European Transactions on Telecommunications*, vol. 6, no. 5, pp. 507–511, 2008.

[27] G. Oletu, P. Rapajic, T. Eneh, and K. Anang, "Performance of iterative decoding with imperfect mmse dfe," in *Wireless Days (WD), 2011 IFIP*. IEEE, 2011, pp. 1–3.

[28] ——, "Iterative equalization enhanced high data rate in wireless communication networks," in *Modeling and Optimization in Mobile, Ad Hoc and Wireless Networks (WiOpt), 2011 International Symposium on*. IEEE, 2011, pp. 373–373.

[29] G. Oletu, T. Eneh, P. Rapajic, and K. Anang, "Iterative equalization enhanced high data rate in wireless communication systems," *International Journal of Multimedia Technology*, vol. 2, pp. 1–4, 2012. [Online]. Available: http://www.ijmt.org

[30] G. Oletu, P. Rapajic, T. Eneh, and K. Anang, "Enhanced equalization for mobile communication systems," in *Computer Modeling and Simulation (EMS), 2011 Fifth UKSim European Symposium on*. IEEE, 2011, pp. 446–450.

[31] G. Oletu, P. Rapajic, K. Anang, and R. Wu, "Interference cancellation using iterative equalization for communication networks," in *Computer Modelling and Simulation (UKSim), 2012 UKSim 14th International Conference on*. IEEE, 2012, pp. 608–612.

[32] G. Oletu, P. Rapajic, K. Anang, R. Wu, and T. Eneh, "The smearing filter design techniques for data transmission," in *Vehicular Technology Conference (VTC Fall), 2012 IEEE*. IEEE, 2012, pp. 1–5.

[33] G. Oletu, P. Rapajic, K. Anang, and R. Wu, "Channel impulse noise minimization using digital smear and desmear filter," in *Performance Computing and Communications Conference (IPCCC), 2012 IEEE 31st International*. IEEE, 2012, pp. 456–462.

[34] C. E. Shannon, "Communication in the presence of noise," *Proceedings of the IRE*, vol. 37, no. 1, pp. 10–21, 1949.

[35] J. Woodard, T. Keller, and L. Hanzo, "Turbo-coded orthogonal frequency division multiplex transmission of 8 kbps encoded speech," 1997.

[36] P. Robertson, E. Villebrun, and P. Hoeher, "A comparison of optimal and sub-optimal map decoding algorithms operating in the log domain," in *Communications, 1995. ICC'95 Seattle,'Gateway to Globalization', 1995 IEEE International Conference on*, vol. 2. IEEE, 1995, pp. 1009–1013.

[37] J. P. Woodard and L. Hanzo, "Comparative study of turbo decoding techniques: An overview," *Vehicular Technology, IEEE Transactions on*, vol. 49, no. 6, pp. 2208–2233, 2000.

[38] C. Berrou, P. Adde, E. Angui, and S. Faudeil, "A low complexity soft-output viterbi decoder architecture," in *Communications, 1993. ICC 93. Geneva. Technical Program, Conference Record, IEEE International Conference on*, vol. 2. IEEE, 1993, pp. 737–740.

[39] S. L. Goff, A. Glavieux, and C. Berrou, "Turbo-codes and high spectral efficiency modulation," in *Communications, 1994. ICC'94, SUPERCOMM/ICC'94, Con-*

ference Record,'Serving Humanity Through Communications.'IEEE International Conference on. IEEE, 1994, pp. 645–649.

[40] U. Wachsmann and J. Huber, "Power and bandwidth efficient digital communication using turbo codes in multilevel codes," *European Transactions on Telecommunications*, vol. 6, no. 5, pp. 557–567, 2008.

[41] P. Robertson and T. Worz, "Bandwidth-efficient turbo trellis-coded modulation using punctured component codes," *IEEE J. Select. Areas Commun.*, vol. 16, no. 2, pp. 206–218, 1998.

[42] S. Benedetto and G. Montorsi, "Design of parallel concatenated convolutional codes," *IEEE Trans. Commun.*, vol. 44, no. 5, pp. 591–600, 1996.

[43] S.Benedetto and G.Montorsi, "Unveiling turbo codes: Some results on parallel concatenated coding schemes," *IEEE Trans. Inform. Theory*, vol. 42, no. 2, pp. 409–428, 1996.

[44] L.C.Perez, J.Seghers, and D. Jr, "A distance spectrum interpretation of turbo codes," *IEEE Trans. Inform. Theory*, vol. 42, no. 6, pp. 1698–1709, 1996.

[45] J. Hagenauer, E. Offer, and L. Papke, "Iterative decoding of binary block and convolutional codes," *IEEE Trans. Inform. Theory*, vol. 42, no. 2, pp. 429–445, 1996.

[46] R. Pyndiah, "Iterative decoding of product codes: Block turbo codes," in *Proceedings of the International Symposium on Turbo Codes & Related Topics*, 1997, pp. 71–79.

[47] P. Jung and M. Nasshan, "Performance evaluation of turbo codes for short frame transmission systems," *Electronics letters*, vol. 30, no. 2, pp. 111–113, 1994.

[48] P. Jung, M. Nasshan, and J. Blanz, "Application of turbo-codes to a cdma mobile radio system using joint detection and antenna diversity," in *Vehicular Technology Conference, 1994 IEEE 44th*. IEEE, 1994, pp. 770–774.

[49] A. S. Barbulescu and S. S. Pietrobon, "Interleaver design for turbo codes," *Electronics Letters*, vol. 30, no. 25, pp. 2107–2108, 1994.

[50] L. Hanzo, T. H. Liew, B. L. Yeap, and J. Wiley, *Turbo coding, turbo equalisation and space-time coding*. Wiley Online Library, 2002.

[51] B. Sklar, "A primer on turbo code concepts," *IEEE Commun. Mag.*, vol. 35, no. 12, pp. 94–102, 1997.

[52] J. D. Andersen, *A turbo tutorial*. Institut for Telekommunikation, Danmarks Tekniske Universitet, 1999.

[53] J. Proakis and M. Salehi, *Digital Communications*, ser. McGraw-Hill higher education. McGraw-Hill Companies Incorporated, 2007.

[54] C. Berrou, "The ten-year-old turbo codes are entering into service," *IEEE Commun. Mag.*, vol. 41, no. 8, pp. 110–116, 2003.

[55] T. A. Summers and S. G. Wilson, "Snr mismatch and online estimation in turbo decoding," *IEEE Trans. Commun.*, vol. 46, no. 4, pp. 421–423, 1998.

[56] P. Robertson, P. Hoeher, and E. Villebrun, "Optimal and sub-optimal maximum a posteriori algorithms suitable for turbo decoding," *European Transactions on Telecommunications*, vol. 8, no. 2, pp. 119–125, 1997.

[57] S. Benedetto, D. Divsalar, G. Montorsi, and F. Pollara, "A soft-input soft-output app module for iterative decoding of concatenated codes," *IEEE Commun. Lett.*, vol. 1, no. 1, pp. 22–24, 1997.

[58] J. Hagenauer and P. Hoeher, "A viterbi algorithm with soft-decision outputs and its applications," in *Global Telecommunications Conference, 1989, and Exhibition*. IEEE, 1989, pp. 1680–1686.

[59] J. Hagenauer, "Source-controlled channel decoding," *IEEE Trans. Commun.*, vol. 43, no. 9, pp. 2449–2457, 1995.

[60] T. K. Kanth and D. R. Prasad, "The reliability in decoding of turbo codes for wireless communications."

[61] M. Tüchler and T. Michael, "Iterative equalization using priors," 1998.

[62] X. Wang and H. V. Poor, "Turbo multiuser detection and equalization for coded cdma in multipath channels," in *Universal Personal Communications, 1998. ICUPC'98. IEEE 1998 International Conference on*, vol. 2. IEEE, 1998, pp. 1123–1127.

[63] A. Glavieux, C. Laot, and J. Labat, "Turbo equalization over a frequency selective channel," in *Proc. Int. Symp. Turbo Codes*, 1997, pp. 96–102.

[64] G. Bauch, H. Khorram, J. Hagenauer *et al.*, "Iterative equalization and decoding in mobile communications systems," *ITG FACHBERICHT*, pp. 307–312, 1997.

[65] C. Laot, A. Glavieux, and J. Labat, "Turbo equalization: adaptive equalization and channel decoding jointly optimized," *Selected Areas in Communications, IEEE Journal on*, vol. 19, no. 9, pp. 1744–1752, 2001.

[66] A. G. Lillie, A. R. Nix, P. N. Fletcher, and J. P. McGeehan, "The application of iterative equalisation to high data rate wireless personal area networks," *IEEE Trans. Consumer Electron.*, vol. 48, no. 3, pp. 743–753, 2002.

[67] R. Chang and J. Hancock, "On receiver structures for channels having memory," *IEEE Trans. Inform. Theory*, vol. 12, no. 4, pp. 463–468, 1966.

[68] Y. Li, B. Vucetic, and Y. Sato, "Optimum soft-output detection for channels with intersymbol interference," *IEEE Trans. Inform. Theory*, vol. 41, no. 3, pp. 704–713, 1995.

[69] G. Bauch and V. Franz, "A comparison of soft-in/soft-out algorithms for 'turbo detection'," in *Proc. Int. Conf. Telecomm*. Citeseer, 1998, pp. 259–263.

[70] S. Sampei, *Applications of digital wireless technologies to global wireless communications*. Prentice Hall PTR, 1997.

[71] M. Tuchler, A. C. Singer, and R. Koetter, "Minimum mean squared error equalization using a priori information," *IEEE Trans. Signal Processing*, vol. 50, no. 3, pp. 673–683, 2002.

[72] C.Berrou, A.Glavieux, and P.Thitimajshima, "Near shannon limit error-correcting coding and decoding: Turbo-codes. 1," in *Communications, 1993. ICC 93. Geneva. Technical Program, Conference Record, IEEE International Conference on*, vol. 2. IEEE, 1993, pp. 1064–1070.

[73] G. F. Jr, "Maximum-likelihood sequence estimation of digital sequences in the presence of intersymbol interference," *IEEE Trans. Inform. Theory*, vol. 18, no. 3, pp. 363–378, 1972.

[74] J. Hagenauer and L. Papke, "Decoding "turbo"-codes with the soft output viterbi algorithm (sova)," in *Information Theory, 1994. Proceedings., 1994 IEEE International Symposium on*. IEEE, 1994, p. 164.

[75] S. P. Panigrahi, S. K. Padhy, and S. K. Nayak, "An improved decision feedback equalization using a priori information," *International journal of adaptive control and signal processing*, vol. 24, no. 1, pp. 41–50, 2010.

[76] X. Wang and H. V. Poor, "Iterative (turbo) soft interference cancellation and decoding for coded cdma," *IEEE Trans. Commun.*, vol. 47, no. 7, pp. 1046–1061, 1999.

[77] S. Ariyavisitakul and Y. Li, "Joint coding and decision feedback equalization for broadband wireless channels," in *Vehicular Technology Conference, 1998. VTC 98. 48th IEEE*, vol. 3. IEEE, 1998, pp. 2256–2261.

[78] M. Tuchler, R. Koetter, and A. C. Singer, "Turbo equalization: principles and new results," *Communications, IEEE Transactions on*, vol. 50, no. 5, pp. 754–767, 2002.

[79] M. Pukkila, "Turbo equalisation for the enhanced gprs system," in *Personal, Indoor and Mobile Radio Communications, 2000. PIMRC 2000. The 11th IEEE International Symposium on*, vol. 2. IEEE, 2000, pp. 893–897.

[80] P. Strauch, C. Luschi, M. Sandell, and R. Yan, "Turbo equalization for an 8-psk modulation scheme in a mobile tdma communication system," in *Vehicular Technology Conference, 1999. VTC 1999-Fall. IEEE VTS 50th*, vol. 3. IEEE, 1999, pp. 1605–1609.

[81] Z. N. Wu and J. M. Cioffi, "Low-complexity iterative decoding with decision-aided equalization for magnetic recording channels," *IEEE J. Select. Areas Commun.*, vol. 19, no. 4, pp. 699–708, 2001.

[82] M. Tuchler and J. Hagenauer, "Linear time and frequency domain turbo equalization," in *Vehicular Technology Conference, 2001. VTC 2001 Spring. IEEE VTS 53rd*, vol. 2. IEEE, 2001, pp. 1449–1453.

[83] S. Jiang, L. Ping, H. Sun, and C. S. Leung, "Modified lmmse turbo equalization," *IEEE Commun. Lett.*, vol. 8, no. 3, pp. 174–176, 2004.

[84] V. Trajkovic and P. Rapajic, "Adaptive decision feedback turbo equalization and multiuser detection," in *Spread Spectrum Techniques and Applications, 2004 IEEE Eighth International Symposium on*. IEEE, 2004, pp. 540–544.

[85] N. Al-Dhahir and J. M. Cioffi, "Mmse decision-feedback equalizers: finite-length results," *IEEE Trans. Inform. Theory*, vol. 41, no. 4, pp. 961–975, 1995.

[86] S. T. Brink, "Convergence behavior of iteratively decoded parallel concatenated codes," *IEEE Trans. Commun.*, vol. 49, no. 10, pp. 1727–1737, 2001.

[87] A. Papoulis and S. U. Pillai, *Probability, random variables and stochastic processes with errata sheet*. McGraw-Hill Science/Engineering/Math, 2001.

[88] Z. Wu, "Turbo decision aided equalization for magnetic recording channels," *Coding and Iterative Detection for Magnetic Recording Channels*, pp. 71–102, 2000.

[89] S. Haykin, "Adaptive filter theory (ise)," 2003.

[90] V. D. Trajković, P. B. Rapajic, and R. Kennedy, "Turbo dfe algorithm with imperfect decision feedback," *IEEE Signal Processing Lett.*, vol. 12, no. 12, Dec. 2000.

[91] A. Duel-Hallen and C. Heegard, "Delayed decision-feedback sequence estimation," *IEEE Trans. Commun.*, vol. 37, no. 5, pp. 428–436, 1989.

[92] M. V. Eyuboglu and S. U. H. Qureshi, "Reduced-state sequence estimation with set partitioning and decision feedback," *IEEE Trans. Commun.*, vol. 36, no. 1, pp. 13–20, 1988.

[93] J. Anderson and S. Mohan, "Sequential coding algorithms: A survey and cost analysis," *IEEE Trans. Commun.*, vol. 32, no. 2, pp. 169–176, 1984.

[94] P. Monsen, "Adaptive equalization of the slow fading channel," *IEEE Trans. Commun.*, vol. 22, no. 8, pp. 1064–1075, 1974.

[95] S. U. H. Qureshi, "Adaptive equalization," *Proceedings of the IEEE*, vol. 73, no. 9, pp. 1349–1387, 1985.

[96] P. Monsen, "Mmse equalization of interference on fading diversity channels," *IEEE Trans. Commun.*, vol. 32, no. 1, pp. 5–12, 1984.

[97] L. Li and L. Milstein, "Rejection of cw interference in qpsk systems using decision-feedback filters," *IEEE Trans. Commun.*, vol. 31, no. 4, pp. 473–483, 1983.

[98] W. H. Gerstacker, F. Obernosterer, R. Meyer, and J. B. Huber, "An efficient method for prefilter computation for reduced-state equalization," in *Personal, Indoor and Mobile Radio Communications, 2000. PIMRC 2000. The 11th IEEE International Symposium on*, vol. 1. IEEE, 2000, pp. 604–609.

[99] ——, "On prefilter computation for reduced-state equalization," *Wireless Communications, IEEE Transactions on*, vol. 1, no. 4, pp. 793–800, 2002.

[100] K. A. Hamied and G. L. Stuber, "Performance of trellis-coded modulation for equalized multipath fading isi channels," *IEEE Trans. Veh. Technol.*, vol. 44, no. 1, pp. 50–58, 1995.

[101] D. Costello, P. Chevillat, and L. Perez, "Channel coding considerations for wireless lans," in *Information Theory. 1997. Proceedings., 1997 IEEE International Symposium on*. IEEE, 1997, p. 462.

[102] P. Monsen, "Theoretical and measured performance of a dfe modem on a fading multipath channel," *IEEE Trans. Commun.*, vol. 25, no. 10, pp. 1144–1153, 1977.

[103] R. Kennedy and B. Anderson, "Recovery times of decision feedback equalizers on noiseless channels," *IEEE Trans. Commun.*, vol. 35, no. 10, pp. 1012–1021, 1987.

[104] D. Duttweiler, J. Mazo, and D. Messerschmitt, "An upper bound on the error probability in decision-feedback equalization," *IEEE Trans. Inform. Theory*, vol. 20, no. 4, pp. 490–497, 1974.

[105] N. Beaulieu, "Bounds on recovery times of decision feedback equalizers," *IEEE Trans. Commun.*, vol. 42, no. 10, pp. 2786–2794, 1994.

[106] S. A. Altekar and N. C. Beaulieu, "Upper bounds to the error probability of decision feedback equalization," *IEEE Trans. Inform. Theory*, vol. 39, no. 1, pp. 145–156, 1993.

[107] W. W. Choy and N. C. Beaulieu, "Improved bounds for error recovery times of decision feedback equalization," *IEEE Trans. Inform. Theory*, vol. 43, no. 3, pp. 890–902, 1997.

[108] M. Reuter, J. C. Allen, J. R. Zeidler, and R. C. North, "Mitigating error propagation effects in a decision feedback equalizer," *Communications, IEEE Transactions on*, vol. 49, no. 11, pp. 2028–2041, 2001.

[109] Y. Shi and T. Chen, "2-norm-based iterative design of filterbank transceivers: a control perspective," *Journal of Control Science and Engineering*, vol. 2008, p. 1, 2008.

[110] D. Raphaeli and Y. Zarai, "Combined turbo equalization and turbo decoding," *IEEE Commun. Lett.*, vol. 2, no. 4, pp. 107–109, 1998.

[111] D. Raphaeli and A. Saguy, "Reduced complexity app for turbo equalization," in *Communications, 2002. ICC 2002. IEEE International Conference on*, vol. 3. IEEE, 2002, pp. 1940–1943.

[112] A. Dejonghe and L. Vandendorpe, "Turbo-equalization for multilevel modulation: an efficient low-complexity scheme," in *Communications, 2002. ICC 2002. IEEE International Conference on*, vol. 3. IEEE, 2002, pp. 1863–1867.

[113] J. F. Roßler, W. H. Gerstacker, A. Lampe, and J. B. Huber, "Matched-filter-and mmse-based iterative equalization with soft feedback for qpsk transmission," in

Broadband Communications, 2002. Access, Transmission, Networking. 2002 International Zurich Seminar on. IEEE, 2002, pp. 19–1.

[114] J. Makhoul, "Linear prediction: A tutorial review," *Proceedings of the IEEE*, vol. 63, no. 4, pp. 561–580, 1975.

[115] R. Wainwright, "On the potential advantage of a smearing-desmearing filter technique in overcoming impulse-noise problems in data systems," *Communications Systems, IRE Transactions on*, vol. 9, no. 4, pp. 362–366, 1961.

[116] S. Burley and M. Darnell, "Robust impulse noise suppression using adaptive wavelet de-noising," in *Acoustics, Speech, and Signal Processing, 1997. ICASSP-97., 1997 IEEE International Conference on*, vol. 5. IEEE, 1997, pp. 3417–3420.

[117] O. Shalvi, M. Segal, and Z. Reznic, "Method and apparatus for combating impulse noise in digital communications channels," November 2003.

[118] S.V.Vaseghi, *Advanced digital signal processing and noise reduction*. Wiley, 2008.

[119] G. F. Jr, R. Gallager, G. Lang, F. Longstaff, and S. Qureshi, "Efficient modulation for band-limited channels," *IEEE J. Select. Areas Commun.*, vol. 2, no. 5, pp. 632–647, 1984.

[120] J. A. C. Bingham, "Multicarrier modulation for data transmission: An idea whose time has come," *Communications Magazine, IEEE*, vol. 28, no. 5, pp. 5–14, 1990.

[121] S. L. M. Jr, "Digital spectral analysis with applications," *Englewood Cliffs, NJ, Prentice-Hall, Inc., 1987, 512 p.*, vol. 1, 1987.

[122] J. G. Proakis, *Digital communications*. McGraw-hill, 1987, vol. 1221.

[123] D.H.Sargrad and J.W.Modestino, "Errors-and-erasures coding to combat impulse noise on digital subscriber loops," *IEEE Trans. Commun.*, vol. 38, no. 8, pp. 1145–1155, 1990.

[124] G. Beenker, T.Claasen, and P. Hermens, "Binary sequences with a maximally flat amplitude spectrum," *Philips J. Res*, vol. 40, no. 5, pp. 289–304, 1985.

[125] J. Fennick, "Amplitude distributions of telephone channel noise and a model for impulse noise," *Bell Syst. Tech. J*, vol. 48, no. 10, pp. 3243–3263, 1969.

[126] G. Beenker, T. Claasen, and P. van Gerwen, "Design of smearing filters for data transmission systems," *IEEE Trans. Commun.*, vol. 33, no. 9, pp. 955–963, 1985.

[127] M.B.Carey, H.T.Chen, A.Descloux, J. Ingle, and K.I.Park, "1982/83 end office connection study: Analog voice and voiceband data transmission performance characterization of the public switched network," *AT&T Bell Laboratories technical journal*, vol. 63, no. 9, pp. 2059–2119, 1984.

[128] J.Fennick, "Understanding impulse-noise measurements," *IEEE Trans. Commun.*, vol. 20, no. 2, pp. 247–251, 1972.

[129] F. F. Kretschmer and B. Lewis, "Doppler properties of polyphase coded pulse compression waveforms," *IEEE Trans. Aerosp. Electron. Syst.*, no. 4, pp. 521–531, 1983.

[130] M. Ackroyd, "Synthesis of efficient huffman sequences," *IEEE Trans. Aerosp. Electron. Syst.*, no. 1, pp. 2–8, 1972.

[131] J.M.Wozencraft and I.M.Jacobs, "Principles of communication engineering," *New York*, p. 319, 1965.

[132] S.Haykin, *Communication systems*. John Wiley & Sons, 2008.

[133] F. K. Jr and F. Lin, "Huffman-coded pulse compression waveforms," *Naval Research Lab. Report*, vol. 1, 1985.

[134] E. Mosca, "Sidelobe reduction in phase-coded pulse compression radars (corresp.)," *IEEE Trans. Inform. Theory*, vol. 13, no. 1, pp. 131–134, 1967.

[135] P. Rapajic and A. Zejak, "Low sidelobe multilevel sequences by minimax filter," *Electronics letters*, vol. 25, no. 16, pp. 1090–1091, 1989.

[136] S. R. Al-Araji, M. A. Al-Qutayri, K. Belhaj, and N. Al-Shwawreh, "Impulsive noise reduction techniques based on rate of occurrence estimation," in *Signal Processing*

and Its Applications, 2007. ISSPA 2007. 9th International Symposium on. IEEE, 2007, pp. 1–4.

[137] D.Kai and Y.Ruliang, "New method of chaotic polyphase sequences design," *IEEE Trans. Aerosp. Electron. Syst.*, vol. 43, no. 3, pp. 1075–1084, 2007.

[138] A.Azari, S.N.Esfahani, and M.G.Roozbahani, "A new method for timing synchronization in ofdm systems based on polyphase sequences," in *Vehicular Technology Conference (VTC 2010-Spring), 2010 IEEE 71st*. IEEE, 2010, pp. 1–5.

[139] J. Pereira and H. D. Silva, "Generalized chu polyphase sequences," in *Telecommunications, 2009. ICT'09. International Conference on*. IEEE, 2009, pp. 47–52.